Geological constraints on surface-based models through development of Rapid Reservoir Modelling

Margaret Elizabeth Hoyt Pataki

Imperial College London

Department of Earth Science and Engineering

This dissertation is submitted in partial fulfilment of the requirements for the degree of Doctor of Philosophy of Imperial College London

February, 2020

Declaration of Originality

I hereby declare that this thesis, "Geological constraints on surface-based models through development of Rapid Reservoir Modelling" is entirely my own work under the supervision of Professor Gary J. Hampson and Professor Mathew D. Jackson, completed in the Department of Earth Science and Engineering at Imperial College London. All other material in this thesis has been given full acknowledgement where appropriate. This material has not been previously submitted, in whole or in part, to any other academic institution for a degree, diploma or any other qualification.

Margaret EH Pataki

Department of Earth Science and Engineering

Imperial College London

Copyright Declaration

Abstract

Surface-based geological modelling (SBM) represents all geological heterogeneity that impacts the spatial distribution of petrophysical properties using surfaces. To create surface-based models, rules are required to govern how surfaces interact such that resulting models are geologically sound. Previous studies used implicit rules or assumptions, often with the requirement that surfaces are created in stratigraphic or hierarchical order. A comprehensive set of explicit and universal rules to govern the interaction of stratigraphic surfaces has yet to be formalised.

In this thesis, seven operators are presented that define how stratigraphic surfaces interact for geological modelling such that universal geological rules are obeyed. The operators can be applied through any SBM technique and are independent of geological process, scale and setting. The operators are demonstrated using three hand-drafted examples of siliciclastic and carbonate strata, at centimetre to kilometre scales, using outcrop, seismic and conceptual input data.

These universal stratigraphic operators are then implemented in 3D in the sketch-based interface and modelling (SBIM) research prototype software Rapid Reservoir Modelling (RRM). Three case studies are presented using examples of siliciclastic and carbonate strata from different depositional environments, at multiple scales, using seismic, outcrop, and well log data to constrain and guide the sketches. The case studies demonstrate the operators and three different techniques for moving from 2D sketch to 3D model, revealing the flexibility and broad applicability of the operators for SBIM of stratigraphy.

Lastly, the stratigraphic operators are leveraged in RRM to create structural models. Test cases are a conjugate fault model and a physical model of a salt-influenced passive margin. Gaps in the applicability of stratigraphic operators for 'sketch-what-you-see' structural modelling and diagenesis are identified and future updates to RRM are recommended. RRM is the first SBIM software that allows rapid prototyping of geological reservoir models and represents a step-change for the field.

Acknowledgements

I would first like to express my gratitude to my supervisors, Gary Hampson and Matt Jackson, who would have simply been my bosses had they not suggested I do a PhD. They have been a tremendous support during my research for both my personal and scientific life. Gary I would like to thank for his geological expertise, masterful editing and shockingly speedy reviews, alongside his supreme kindness. Matt I would like to thank for his modelling expertise, knack for a turn of phrase, straightforwardness, and humour when things required it. And, to you both, thanks for hiring me!

I would also like to thank the members of the RRM Consortium, ExxonMobil, Equinor, IBM Research, Petrobras and Shell, for their funding, scientific discussions, and continuous support for publishing and presenting this research. I would like to thank the members of the RRM Research Team (Julio Daniel Machado Silva, Clarissa Coda Marques Machado Silva, Felipe de Carvalho, Mario Costa Sousa, Zhao Zhang and Sebastian Geiger) for all the hard work and long nights to get our prototype releases ready for sponsors meetings and to Team U of C in particular for not killing me when I'd send you multipage bug lists. Thank you for turning my ideas into reality.

At Imperial, huge thanks go in particular to Carl Jacquemyn and Pete Fitch, my fellow geologists in NORMS. Carl, I wouldn't have survived without your help and commiserations with RRM. Pete, I wouldn't have survived without your moral support in general. You guys are excellent humans. Elizabeth Hauke, my current boss, I would like to thank for allowing me so much flexibility to my teaching schedule that I could actually get this thesis done. So many hours of work have gone to my thesis when they should have been directed elsewhere; I am forever grateful. Sian Evans, thank you for the use of your fabulous model data. Catherine and Harry, thanks for always being there for a beer when I needed to pretend I was a kid again. And to the rest of NORMS and the post-doc-PhD cohort, thanks for the support and good times.

Personally, I want to thank Kate (Kelly) Egan and Hilary Watford for being amazing cheerleaders through a challenging time in life. Oceans and continents can't stop a good gif when it's needed. Mr. Block, thanks for introducing me to rocks in '94. To my colleagues at CVX, thanks for teaching me about the business so I knew what I wanted out of this prototype. Mom, Dad, Jon – thanks for harassing or supporting me as required. Mom, thanks so much for all your help with the kids; I couldn't have survived without it. And to Michele Paulatto, thank you for helping make the last year of the thesis fun and for being such wonderful support for me and my munchkins. Grazie mille, amore.

This thesis is dedicated to Milo James (who is older than RRM) and Juliana Louise (who is younger than RRM) to remind them that even when things are hard, just keep working, ask for help, have fun with the people you love, work some more and eventually you will get where you want to be. I love you, Schnookles and Nugget. xo Mama

Table of Contents

Declaration of Originality 2
Copyright Declaration 2
Abstract 3
Acknowledgements 4
Table of Contents 6
List of Figures and Tables 9
1 Introduction and Previous Research 12
1.1 Introduction 12
1.2 Surface-Based Modelling 14
1.3 Sketch-Based Interfaces and Modelling 17
1.4 Conventional Structural Modelling 18
1.5 Thesis Aims and Objectives 20
1.6 Thesis Structure 21
2 Operators for Interactions of Stratigraphic Surfaces for Surface-Based Modelling 23
2.1 Summary 23
2.2 Introduction 23
2.3 Operators for Interactions of Stratigraphic Surfaces 24
2.4 Geological rule framework for SBM 25
2.5 Operators that modify a new surface 28
Preserve Above - PA 28
Preserve Below - PB 28
Preserve Between - PBW 28
2.6 Operators that modify an existing surface 30
Remove Above – RA 30
Remove Above Intersection – RAI 30
Remove Below – RB 30
Remove Below Intersection - RBI 30
2.7 Hand-drafted Case Studies 32
2.8 Case Study 2A: Handspecimen-scale model of shallow-marine tidal depositional environment generated using outcrop data 33
2.9 Case Study 2B: Basin-scale model of carbonate platform depositional environment generated using seismic data 36
2.10 Case Study 2C: Reservoir-scale model of deep-marine depositional environment generated using conceptual block diagram 39
2.11 Discussion 43

2.12 Conclusions 45
3 Application of operators to 3D Sketch-based Interface and Modelling through use of Rapid Reservoir Modelling 47
3.1 Summary 47
3.2 Introduction 47
3.3 Stratigraphic Operators for SBIM 48
3.4 Creating 3D models from 2D sketches 51
3.5 Case Study 3A: Seismic-scale prototype models of deepwater channel deposits using multiple parallel cross-sections 53
3.6 Case Study 3B: Comparative outcrop-derived prototype models of lacustrine carbonates 59
3.7 Case Study 3C: Comparative well-based prototype models of fluvial point-bar sandstones 61
3.8 Discussion 65
3.9 Conclusions 69
4 Logical Operators for Sketch-based Interfaces and Modelling of Structure in Rapid Reservoir Modelling 71
4.1 Summary 71
4.2 Introduction and Previous Research 71
4.3 Operators for Interactions of Structural Surfaces Using Existing Stratigraphic Operators .. 73
4.3.1 Stratigraphic Operators: Uses and Limitations 74
4.4 Case Study 4A: Conjugate Fault Model 80
4.5 Case Study 4B: Salt-influenced Passive Margin Analogue Model 85
4.6 New operators and operations required to fully implement structure in RRM 92
4.6.1 Geological rule framework for SBM of structure 93
4.6.2 Surfaces that terminate within the model volume 94
4.6.3 Allow sketching of non-monotonic surfaces 96
4.6.4 Modify stratigraphy in an existing model with insertion of a fault plane 98
4.6.5 New operator required: Remove Between – RBW 100
4.6.6 Sketch stratigraphy onto fault surface 101
4.6.7 Checking fault throw, sense and type with visual inspection 103
4.6.8 Metadata for structural surfaces 103
4.7 Discussion 105
4.8 Conclusions 108
5 Discussion 109
5.1 Potential for Broad Use of Stratigraphic and Structural Operators 109
5.2 Future Work 112
5.3 RRM in practice 115

6 Synopsis and Conclusions 117
6.1 Synopsis 117
6.2 Conclusions 120
References 122
Appendix 1 137
Supplemental Material ..... provided electronically

List of Figures and Tables

Figure 1.1. 16

Schematic diagram showing different methods of surface ordering for SBM.

Figure 1.2. 22

Organisation chart of day to day RRM project.

Figure 2.1. 26

Fundamental geological rules for surface intersections in SBM (after Caumon et al., 2009).

Figure 2.2. 27

These figures demonstrate the intersection of two stratigraphic surfaces.

Figure 2.3. 29

Sketch illustrating the Preserve Above (PA) operator.

Figure 2.4. 29

Sketch illustrating the Preserve Below (PB) operator.

Figure 2.5. 29

Sketch illustrating the Preserve Between (PBW) operator.

Figure 2.6. 31

Sketch illustrating the Remove Above (RA) operator.

Figure 2.7. 31

Sketch illustrating the Remove Above Intersection (RAI) operator.

Figure 2.8. 32

Sketch illustrating the Remove Below (RB) operator.

Figure 2.9. 32

Sketch illustrating the Remove Below Intersection (RBI) operator.

Figure 2.10. 34

Illustration of handspecimen-scale model of heterolithic, cross-bedded sandstones (after Legler et al., 2015; Massart et al., 2016a).

Figure 2.11. 38

Illustration of basin-scale model of carbonate platform and lateral wings (after Kosa et al., 2015).

Figure 2.12. 42

Illustration of reservoir-scale model of deepwater basin-floor fan deposits, showing a completed surface-based conceptual model (K) based on a conceptual deepwater depositional cross-section (after Posamentier & Kolla, 2003; Posamentier & Walker, 2006).

Figure 3.1. 50

These figures illustrate operators applied to a new surface *n* when it intersects the existing central surface.

Figure 3.2. 51

These figures illustrate operators applied to surfaces in an existing model when a new surface *n* is inserted (dashed orange line).

Figure 3.3. 56

Illustration of steps for model construction from parallel seismic cross-sections of deepwater deposits from the Rakhine Basin, offshore Myanmar (Xu et al., 2016).

Figure 3.4. 57

Illustration of prototype model construction from parallel seismic cross-sections of deepwater deposits from the Rakhine Basin, offshore Myanmar (Xu et al., 2016).

Figure 3.5. 58

Illustration of updates to prototype model constructed from parallel seismic cross-sections of deepwater deposits from the Rakhine Basin, offshore Myanmar (Xu et al., 2016).

Figure 3.6. 61

Illustration of models representing end-member Interpretations A and B for lacustrine microbialite and grainstone carbonates from Bohacs et al. (2013).

Figure 3.7. 64

Illustration of models representing point-bar deposits in a meandering fluvial environment (after Colombera et al., 2018).

Figure 3.8. 67

Schematic figure showing a pair of plan-view river trajectories as originally sketched (A) and as rendered in RRM (B).

Figure 4.1. 75

Sketch showing a pair of gently folded stratigraphic surfaces, which are monotonic (A) and a pair of recumbently folded stratigraphic surfaces, which are non-monotonic where overturned (B).

Figure 4.2. 76

Example of fault geometries that can (A, B) and cannot (C) be modelled with the current stratigraphic operators in RRM.

Figure 4.3. 77

These figures demonstrate the different ways that models in Figure 4.2A (4.3A-C, above, Table 4.1) and Figure 4.2B (4.3D-G, below, Table 4.2) can be made using the stratigraphic operators in RRM.

Figure 4.4. 81

3D model of a conjugate fault set with offset strata (Jacquemyn, pers. comm.).

Figure 4.5. 81

This figure shows the cross-section (left) and top-view (right) of the Jacquemyn model (Figure 4.4) that was used in RRM.

Figure 4.6. 83

Four sequential steps used to sketch the conjugate fault model (cf. Figure 4.4) in RRM.

Figure 4.7. 86

Three cross-section slices from a physical model (Evans, pers. comm.) to create a 3D structural model in RRM (Figure 4.8).

Figure 4.8. 87

Six sequential steps used to sketch the analogue model (cf. Figure 4.7) in RRM.

Figure 4.9. 89

Complete cross-section through the analogue model (Evans, pers. comm.).

Figure 4.10. 95

Representations of faults that offset a stratigraphic surface and terminate within the model volume (Machado Silva pers. comm.).

Figure 4.11. 96

Fault represented by a pair of surfaces (orange) separated by a small volume.

Figure 4.12. 96

This figure shows a model that includes a fault that tips out within a region (left), which is not allowed by the stratigraphic operators in RRM.

Figure 4.13. 97

Definition of 'above' and 'below' for implementing stratigraphic operators in structurally modified settings.

Figure 4.14. 99

Potential options to accommodate insertion of a newly sketched fault into previously sketched strata.

Figure 4.15. 101

Sketch showing the proposed new operator Remove Between (RBW).

Figure 4.16. 102

Sketch showing the potential uses of sketching directly onto a fault plane.

Figure 5.1. 113

Illustration of proposed new operators applied to existing surfaces when new self-intersecting surface *n* intersects existing grey surfaces.

Table 4.1. 79

Three different paths to create model in Figure 4.2A.

Table 4.2. 79

Four different paths to create model in Figure 4.2B.

1 Introduction and Previous Research

1.1 Introduction

Capturing geological heterogeneity is a key objective when constructing numerical models of the Earth's subsurface (e.g. Kortekaas, 1985; Denver & Phillips 1990; Hamilton & Jones 1992; Hu et al., 1994; MacDonald et al., 1998; Wen et al., 1998; White and Barton, 1999; White et al., 2004; Jackson et al., 2005, 2015; Ringrose et al., 2005; Sech et al., 2009; Choi et al., 2011). Such models are used to predict the resource distribution and extraction potential of oil and gas reservoirs, geothermal reservoirs, groundwater reservoirs and ore deposits, as well as the behaviour of subsurface targets for nuclear waste or CO_2 storage (e.g. O'Sullivan et al., 2001; Juanes et al., 2006; Matthäi et al., 2007; Geiger et al., 2009; Refsgaard et al., 2012). However, the 3D geometry and spatial distribution of geological heterogeneity in the subsurface is uncertain, as boreholes sample only a small fraction of the rock volume and geophysical imaging methods lack the spatial resolution required to delineate all heterogeneities of interest (e.g. Kjønsvik et al., 1994; Jones et al., 1995; Lemon & Jones, 2003). Expert knowledge is often used to predict the likely geometry and spatial distribution of heterogeneity away from boreholes, but geological interpretations are themselves subject to uncertainty. Numerical models based on different geological interpretations can yield highly varying predictions of system behaviour (e.g. Deveugle et al., 2014).

The typical workflow for creating reservoir models begins with discretising the reservoir volume onto a grid early in the modelling process (e.g. Jackson et al., 2013). This workflow was developed in the early days of geo-modelling as a way to solve the numerical equations that are widely used by flow-simulation software (two-point flux approximation) (Jackson et al., 2013). Once commercial reservoir modelling software packages required a grid, it became the de facto way of thinking about and making models throughout the community. However, it is difficult to accurately represent reservoir heterogeneity using grid blocks of predefined size and shape (e.g. Jackson et al., 2015a, 2015b; see Section 1.2, this thesis).

Process-based forward modelling developed as means to provide understanding of the types and distributions of heterogeneity generated by a particular set of geological processes. These models are numerically based and model the geological processes that created, for example, a series of stratigraphic deposits (e.g. Cross, 1990; Merriam & Davis, 2001, Teztlaff & Priddy, 2001); the use of such models is often referred to as geological process modelling or stratigraphic forward modelling. The results of this type of model can provide a quantitative framework that extends conceptual models, help quantify uncertainty, or be used as training images for geostatistical methods (Tetzlaff et al., 2014). These process-based modelling methods are often used to understand sedimentary processes rather than as a reservoir modelling tool, because the output of process-based forward models cannot be conditioned directly to "hard" reservoir data (e.g. seismic, wells). A further technique to improve results of a grid-based approach is stratigraphic rule-based modelling (Pyrcz et al., 2015). This method is used to approximate sedimentary dynamics, similar to a stratigraphic forward model, and produce numerical descriptions of reservoir architecture and petrophysical property distribution (Pyrcz et al., 2015). The outputs of these models can be used directly as reservoir models themselves, to generate input statistics for existing reservoir models or as numerical analogues (Pyrcz et al., 2015). However, in both the case of geological process models and stratigraphic rule-based models, the results are currently designed to complement a grid-based modelling approach. In contrast, as a surface-based approach (Section 1.2, this thesis), the technique described in this thesis requires no grid.

Approaches to Computer Aided Design (CAD) and Computational Fluid Dynamics (CFD) outside of the geological modelling domain often include a significant element of prototyping: a number of simplified models are created to test different design concepts, before detailed models are created of the final agreed design (e.g. Shah et al., 2001; Cherlin et al., 2005; Arisoy & Kara, 2014). In geological modelling, analysis of different geological concepts is sometimes termed multi-deterministic scenario modelling, to differentiate it from the probabilistic modelling approaches that are used to create numerous model realisations around a single geological concept (Bentley and

Smith, 2008). However, prototyping in geological modelling is rare, in part because there are no methods or software tools that allow rapid, flexible results which can capture any geologic architecture. The focus of most previous studies has been the development of methods and tools for probabilistic modelling around a single concept (e.g. MacDonald & Aasen, 1994; Wen et al., 1998; Kupfersberger & Deutsch, 1999; Strebelle et al., 2003; Yao et al., 2004; Pyrcz et al., 2005; Strebelle, 2006).

1.2 Surface-Based Modelling

The value of using surfaces to efficiently capture aspects of geological structure and heterogeneity in reservoir models has long been recognised (e.g. Denver & Phillips 1990; Hamilton & Jones 1992; Hu et al., 1994; MacDonald et al., 1998; White and Barton, 1999; White et al., 2004). A logical extension of this recognition is provided by surface-based modelling (SBM), a geological modelling method that uses surfaces to define and bound geological domains (e.g. Deutsch et al. 2001; Pyrcz et al., 2005; Caumon et al., 2009; Zhang et al., 2009; Jackson et al., 2013). Surfaces may represent faults, joints, stratigraphic surfaces, facies boundaries, lithologic boundaries, diagenetic boundaries, and any other type of geological boundary (e.g. White and Barton, 1999; White et al., 2004; Pyrcz et al., 2005; Matthäi et al., 2007; Caumon et al., 2009; Sech et al., 2009; Geiger et al., 2009; Zhang et al., 2009; Graham et al., 2015; Massart et al., 2016a, 2016b, Jacquemyn et al., 2019). Geological domains that are bounded by surfaces can be defined without reference to an underlying grid or mesh, although a mesh may be created that conforms to the modelled surfaces when a calculation is required (Jackson et al., 2015a). The emphasis on surfaces and surface-bounded domains closely matches how geologists conceptualise and represent geological interpretations in traditional tools such as maps, cross-sections and block diagrams. The aim of SBM is not to simulate underlying geological processes (e.g. erosion), but to model their effects on preserved geometries (e.g. removal of existing surfaces) (e.g. Mallet, 2014).

Surfaces can be created through a variety of methods. For example, sketch-based interfaces and modelling (SBIM) can be used to create surfaces by drawing on a screen or tablet (e.g. Amorim et al., 2012, 2014; Natali et al., 2014a, 2014b; Jackson et al., 2015a; Section 1.3, this thesis). Non-uniform rational basis spline (NURBS) based methods use a selection of measurements to define and create parametric surfaces (e.g. Ruiu et al., 2016; Jacquemyn et al., 2019); such parametric surfaces can be created by algorithms tuned to specific depositional settings (e.g. Pyrcz et al., 2005; Sech et al., 2009). Regardless of how geological surfaces are created, a key requirement for robust and efficient application of SBM is a set of operators that govern how these surfaces interact to result in geologically consistent domains and spatial relationships.

In previous studies, SBM has been applied to stratigraphic modelling of different depositional environments, but always using implicit or specific rules to determine how surfaces interact. Model construction can follow purely stratigraphic ordering of surfaces, from oldest to youngest (e.g. Pyrcz et al., 2005), purely hierarchical ordering of surfaces, from large scale to small scale (e.g. Sech et al., 2009) or a combination of stratigraphic and hierarchical ordering (e.g. Massart et al., 2016a). Pyrcz et al. (2005) used purely stratigraphic ordering to create stochastic surface-based models of compensationally stacked turbidite lobe deposits in a deepwater fan environment. Surfaces were modelled sequentially from oldest to youngest: each new lobe deposit was inserted above previous lobe deposits and was then used to constrain the position and extent of subsequent lobe deposits, in a manner that mimicked the influence of sea-floor bathymetry on lobe-deposit stacking. The implicit assumption in this study was that surfaces do not cross. Sech et al. (2009) took a purely hierarchical approach to create a surface-based model of a wave-dominated shoreface-shelf parasequence based on a rich outcrop dataset. First, near-horizontal transgressive surfaces that defined the base and top of the parasequence were created. These transgressive surfaces defined the highest (largest scale) level of the stratigraphic hierarchy to be modelled. Second, clinoform surfaces were created within the volume defined by the transgressive surfaces; third, facies boundaries were created within each clinothem defined by the clinoform surfaces. To create the appropriate clinoform

geometry, Sech et al. (2009) projected the top parts of the clinoform surfaces upwards through the transgressive surface at the top of the parasequence and then trimmed the clinoform surfaces back to the transgressive surface, to mimic erosional truncation. Where domains bounded by clinoform surfaces and/or facies boundaries pinched out, the surfaces were manually adjusted so that they were coincident rather than crossing. In this way, Sech et al. (2009) created a model that prevented surfaces from interacting in a non-geological way. Massart et al. (2016a, 2016b) used a combined hierarchical and stratigraphic approach to surface ordering, together with stochastic surface-based algorithm methods, to model mudstone drapes in cross-bedded tidal sandstones. First, the model was split into elemental volumes defined by stratigraphically ordered surfaces representing bed boundaries. Second, the volumes were populated in a hierarchically ordered way with surfaces representing boundaries of foreset-to-toeset laminae. Third, the transmissibility of the foreset-to-toeset laminae boundaries was modified in patches to represent the presence of thin mudstone drapes. Younger bed boundaries removed pre-existing beds and foreset-to-toeset laminae boundaries to mimic erosion.

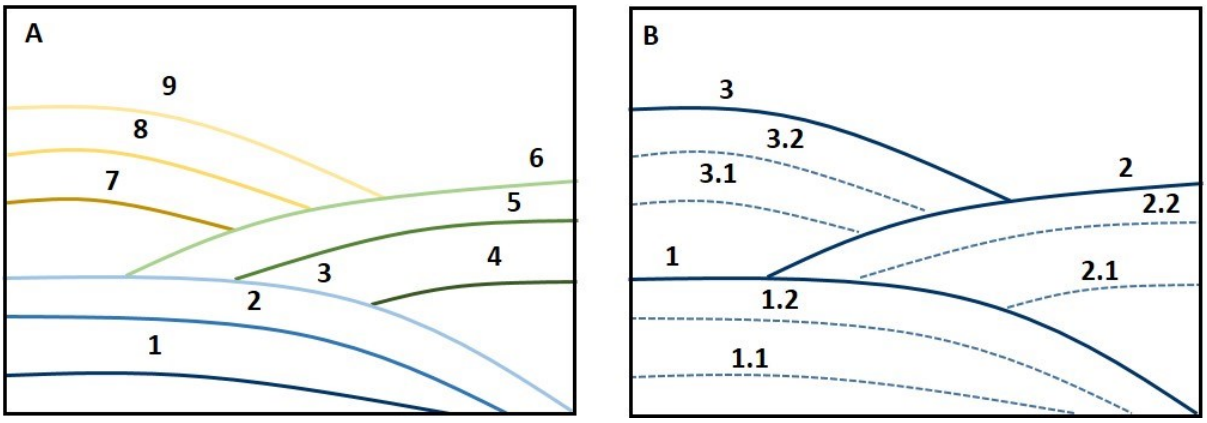

Figure 1.1. Schematic diagram showing different methods of surface ordering for SBM construction of compensationally stacked lobe deposits. A) shows a purely stratigraphic approach (e.g. Pyrcz et al., 2005) where surfaces are modelled from the base to top in depositional order (1-9). In contrast, B) shows a hierarchical approach (e.g. Sech et al., 2009) where solid surfaces (1-3) are modelled first, then internal dashed surfaces (1.1, 1.2, 2.1, 2.2, 3.1, 3.2) are modelled. A contrasting approach, where surfaces can be modelled in any order, is presented in Chapter 2.

Although the methods applied to surface intersections in these previous studies are appropriate for each individual case, they are not universally applicable. Their implementation requires the user to develop a full geological interpretation before model construction, because the surfaces are created in a sequential order that mimics their temporal stratigraphic development (Pyrcz et al., 2005; Zhang et al., 2009) or hierarchical spatial organisation (Sech et al., 2009; Graham et al., 2015; Massart et al., 2016a) (Figure 1.1). Surfaces and their interactions cannot be added, removed or edited out of the sequential order that is specified by the implementation of the rules. An approach to allow flexible and geologically appropriate surface interactions is presented in Chapter 2.

1.3 Sketch-Based Interfaces and Modelling

Sketch-Based Interface and Modelling (SBIM) is an approach for rapid model creation that is used for prototyping in CAD and CFD applications outside of the geological modelling domain (e.g. Olsen et al., 2009, 2011; Pereira et al., 2011). SBIM allows model concepts to be rapidly sketched and tested. A number of studies have also proposed the use of SBIM in geological modelling (e.g. Lidal et al., 2013; Amorim et al., 2012, 2014; Natali et al., 2014a, 2014b; Jackson et al., 2015a).These studies all involve representation of geological relationships with sketched surfaces, and by implication assume a surface-based modelling approach.

Natali et al. (2014a, 2014b) presented a SBIM methodology with application to sedimentary geology; however, their goal was to create figures or animations, particularly for teaching or discussion purposes rather than quantitative modelling of subsurface reservoirs or reservoir analogues. In their approach, the user must sketch geology in depositional order, thus requiring that a geological history be interpreted prior to sketching. This is not restrictive if the objective is to create a digitised, 3D representation of known geology, but is incompatible with using SBIM for prototyping. A prototyping SBIM tool must be flexible, allowing surfaces to be sketched in any order such that different concepts can be tested. Amorim et al. (2012) focused primarily on interpretation of horizons from three dimensional (3D) seismic data. In the examples shown, the sketched surfaces did not interact

and no rules were outlined to detail how interacting surfaces should be treated. A more recent study by Amorim et al. (2014) took a different approach to geological SBIM, starting with a blank screen and allowing the user to sketch lines, representing geological boundaries or faults, in map view. The user sketches geological symbols onto the map which are used by the program to control extrapolation of the sketched lines into 3D to form surfaces. This work is the most advanced example of SBIM for geological application; however, it is still too limited to be used for prototyping. Most significantly, in the examples shown, the sketched surfaces did not interact and no rules were outlined to detail how interacting surfaces should be treated.

Lidal et al. (2013) noted that "more research is needed to investigate whether it is possible to find one well defined toolset of sketching metaphors that is able to cover all of geological modelling." In order to create a geological SBIM framework that is robust and can be applied rapidly during sketching, operators for interaction of sketched surfaces are required. These operators should be universally applicable to all stratigraphic settings and should not require surfaces to be sketched in stratigraphic order. The operators should ensure that models contain watertight volumes bounded by geologically meaningful surfaces, such that they can be discretised for use in quantitative numerical calculations. The operators proposed in this thesis are presented in Chapter 2, with testing of their function in 3D in a SBIM software program presented in Chapter 3.

1.4 Conventional Structural Modelling

3D structural geological computer modelling is a topic that has been under investigation for over thirty years (e.g. Gjøystdal et al., 1985; Fagin, 1991; Hamilton & Jones, 1992; Mallet, 1992; Turner, 1992; Houlding, 1994; de Kemp & Sprague, 2003; Groshong, 2006; Matthäi et al, 2007; Caumon et al., 2009). Specific software packages have been designed to enable geologists to create structural models (e.g. GoCAD, Move). In conventional reservoir modelling workflows, the structural framework of a reservoir is commonly constructed prior to representing stratigraphy (e.g. Bryant & Flint, 1993). Typically this structural framework consists of stratigraphic surfaces of the top and base

reservoir, and major faults that offset these two surfaces. Top-reservoir and base-reservoir surfaces and major fault surfaces are typically derived from seismic mapping. Thus, the typical first step of a conventional reservoir model can be considered to be constructed by a form of surface-based modelling (e.g. Denver & Phillips, 1990; Hamilton & Jones, 1992), albeit one in which surface geometry may be inaccurately represented on a pillar grid of a certain resolution. Smaller-scale structures are typically not represented explicitly in conventional reservoir modelling workflows. For example, fracture networks may be investigated with numerical simulations of flow through fracture networks (e.g. Matthäi et al., 2007; Paluszny et al., 2007; Geiger & Matthäi, 2012).

Similar to the general SBM approaches presented in Section 1.2, much of structural SBM research focuses on the method of surface creation. For example, de Kemp & Sprague (2003) and Sprague and de Kemp (2005) present interpretive tools using parametric surfaces derived from Bezier curves and NURBS to capture complex fold geometries. Other approaches use triangular irregular networks to represent structural surfaces (e.g. Mallet, 1992; Ming et al., 2010). Additional research focuses on methods for combining data by using 3D geometrical methods (Fernandez et al., 2004), DEMS and maps (Dhont et al., 2005), multiple software packages (Wycisk et al., 2009) or data structuring and processing flows (Kaufman & Martin, 2008). Caumon et al. (2009) set out guidelines for 3D structural surface-based modelling. They define logical rules for building structural models, with a focus on representing faults and horizons interpreted from sparse subsurface data (Caumon et al., 2009). The rules are used to guide construction of structural models in the standard fault-then-stratigraphy pattern. Although these rules are compatible with sketch-based modelling (Caumon et al., 2009), they are not explicitly designed for this approach.

Despite the abundance of surface-based structural modelling work, very little has been done to investigate or create sketched surface-based structural models. The work of Amorim et al. (2012, 2014) and Natali et al., (2012, 2014b) are among the only published work into structural SBIM, and the approach they take differs significantly from the approach outlined in Chapter 4. Natali et al.,

(2012, 2014b) have developed methods for rapidly sketching faults and folds in 3D, but the goal of their work is visualization of geological concepts and the creation of illustrative models. They do not create 3D models for the purposes of subsurface characterisation (e.g. volumetric calculation, flow simulation), as in this thesis, but rather for the purpose of communicating geological concepts through block diagrams.

Amorim et al. (2012, 2014) share the aim of creating 3D structural models for subsurface modelling, working with seismic horizon slices (2012) and sketched geological maps (2014). The resultant models are three-dimensional in nature and faithfully represent structural relationships inherent in the input data. However, the modelled surfaces do not interact with each other, and thus no rules or operators are defined to explain how such interaction should be accommodated in three dimensions. Additionally, the authors state that strike-slip faulting cannot be represented with their approach (Amorim et al., 2014). Thus additional work is required to create sketched 3D structural surface-based models.

Chapter 4 presents a method and explores additional research required for structural SBIM, leveraging the stratigraphic operators presented in Chapter 2.

1.5 Thesis Aims and Objectives

Surface and sketch-based geological modelling lack a set of clear operators to define how geological surfaces interact in 3D. Without these defined operators, surfaces must be added sequentially according to a pre-defined order (e.g. stratigraphically or hierarchically). This thesis has four aims: (1) to define the operators required for flexible SBM of stratigraphy; (2) to implement those operators in an SBIM prototype software; (3) to demonstrate their functionality for multiple data types and geological settings; and (4) to present methods to leverage the stratigraphic operators for structural modelling.

1.6 Thesis Structure

Chapter 2 presents a set of seven universal operators for construction of stratigraphic surface-based models. In Chapter 3, these operators are implemented in 3D with a surface-based, SBIM software prototype, Rapid Reservoir Modelling (RRM). Three case studies are presented to demonstrate that the operators are applicable in multiple depositional settings (deepwater slope systems, lacustrine carbonates and fluvial point-bar deposits), to multiple data types (seismic, outcrop and wells) and with multiple methods of moving from 2D sketch to 3D model. Chapter 4 presents ways in which the stratigraphic operators as implemented in the current RRM software prototype can be leveraged to sketch structural features in models. The chapter then explores updates that are required in RRM to improve structural modelling. Chapter 5 discusses the broader applications of the operators and RRM to the geological community and presents future research directions for SBIM through RRM. The conclusions of the thesis are presented in Chapter 6. Videos of model construction in RRM are provided in Supplemental Material. Appendix 1 contains descriptions of the videos.

The research undertaken for this thesis forms part of a broad collaborative effort to develop the RRM software. My contribution was: (1) to develop and define the operators used in RRM; (2) to test and provide feedback on the various RRM software prototypes as they were released, and thus aid in software development, and (3) to construct case-study models that illustrate the operators and their implementation in RRM software. This thesis contains the first and third of my contributions, and all models presented in the thesis were generated by me. The RRM software code was written by collaborators Emilio Vital Brazil, Julio Machado Silva, Clarissa Coda Marques Machado Silva, Felipe de Carvalho and Mario Costa Sousa at the University of Calgary and Zhao Zhang and Sebastian Geiger at Heriot-Watt University, following the geological input of the author and collaborators at Imperial College London. Figure 1.2 shows an organisation chart representing day to day running of the RRM project, with the main staff, location and responsibilities shown in each box.

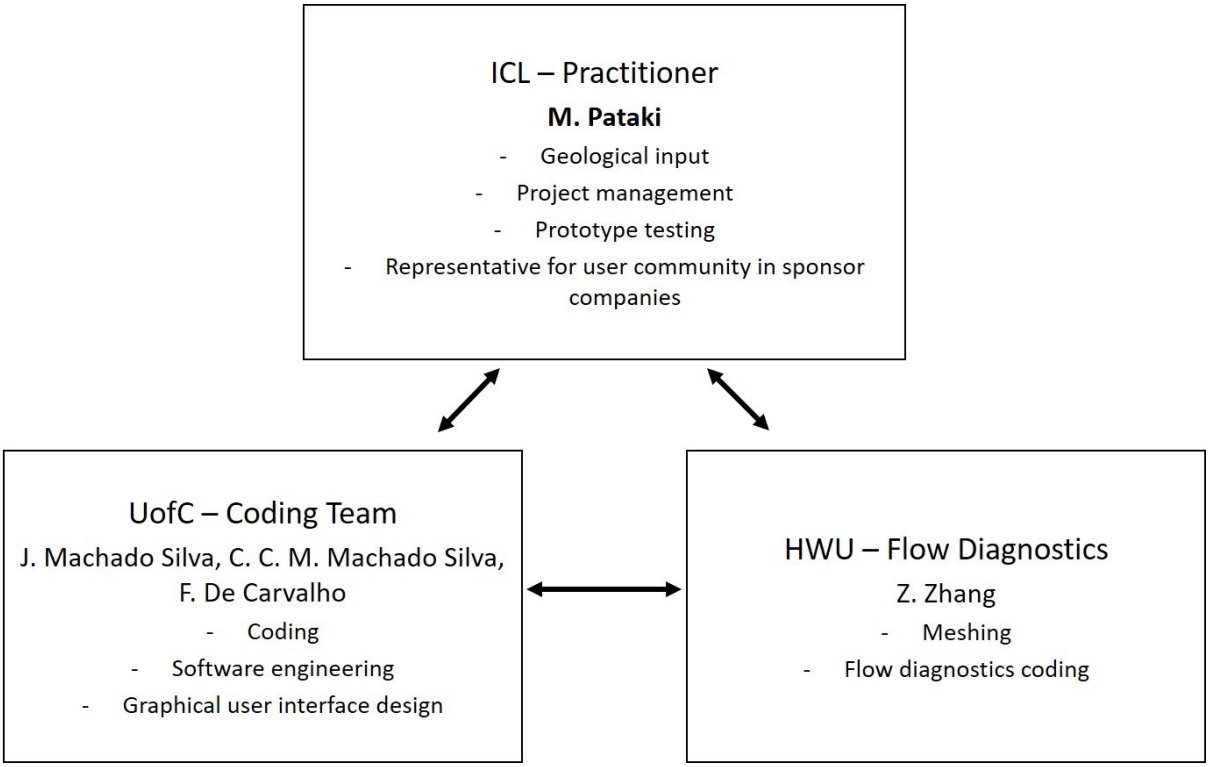

Figure 1.2. Organisation chart of day to day RRM project. Each member of the team is shown with their academic institution and main responsibilities. Groups worked collaboratively, but the project was managed and geological input, prototype testing and feedback were provided by me. All groups reported results to PIs and sponsor companies.

This thesis was written by me, after draft papers for publication that included comments and input from Imperial College London supervisors G.J. Hampson and M.D. Jackson, and Imperial College London collaborator C. Jacquemyn. I am also a co-author on five published papers written by the RRM group, for which other RRM colleagues are the lead authors (Jackson et al., 2015a; Zhang et al., 2017a; Zhang et al., 2017b; Zhang et al., 2018, Zhang et al., 2019). I presented my research at the following conferences: (1) poster presentation - AGU, San Francisco, CA, USA, December 2015; (2) oral presentation - AAPG, Calgary, AB, Canada, June 2016; (3) oral presentation - AAPG, Salt Lake City, UT, USA, May 2018; and (4) oral presentation - AAPG, San Antonio, TX, USA, May 2019.

2 Operators for Interactions of Stratigraphic Surfaces for Surface-Based Modelling

2.1 Summary

Surface-based geological modelling represents all geological heterogeneity that impacts the spatial distribution of petrophysical properties using surfaces. In order to create surface-based models, rules are required to govern how surfaces interact such that resulting models are geologically sound. Previous studies used implicit rules or assumptions, often with the requirement that surfaces are created in stratigraphic or hierarchical order. Such rules are often specific to a particular modelling method or geological setting. A comprehensive set of explicit and universal rules to govern the interaction of stratigraphic surfaces, without reference to a hierarchy (e.g. EarthVision), has yet to be formalized, despite the interaction of surfaces being integral to the definition and conceptualization of geological relationships.

In this chapter, seven operators that define how stratigraphic surfaces interact for geological modelling such that universal geological rules are obeyed are presented. The operators can be applied through any surface-based modelling technique (e.g. sketched, process-based, parametric or discretized, stochastic or deterministic) and are independent of scale, geological process and geological setting. The operators can be applied in any order, and can mimic the law of superposition, Walther's Law, sequence stratigraphy, or be used to represent facies models. Robustness and application of the operators is demonstrated using examples of siliciclastic and carbonate strata from different depositional environments, at scales from centimetres to kilometres, in two and three dimensions, and using outcrop, seismic and conceptual input data. These applications demonstrate the flexibility and broad applicability of the stratigraphic operators.

2.2 Introduction

Section 1.2 of this thesis reviewed the conventional surface-based modelling approach, where surfaces are constructed in stratigraphic or hierarchical order. In this chapter, a set of generic,

universally applicable operators are presented to define how stratigraphic surfaces can interact to produce geologically sound surface-based models. The operators can be applied on surfaces created in any order, so a full geological interpretation is not required at the outset of modelling. The operators are applicable to any depositional setting. Additionally, the operators can be implemented through any SBM framework, such as sketched, parametric or discretized, process-based, stochastic or deterministic modelling methods. Lastly, the operators are scale-independent, so the same operators apply whether modelling bed-scale or basin-scale stratigraphy.

Three case studies are presented to demonstrate the broad applicability and flexibility of our approach. The first example creates a hand specimen-scale model of rhythmically distributed mudstones in cross-bedded tidal sandstones (Legler et al., 2013, Massart et al., 2016a). The second example produces a model of carbonate platform and wing deposits based on regional seismic data (Kosa et al., 2015). The final example uses the operators to create a three-dimensional block diagram of deepwater channel deposits, based on a conceptual interpretation of seismic data (Posamentier & Kolla, 2003). These three examples demonstrate that the operators can be used at any scale, in any depositional environment and with a range of input data types.

2.3 Operators for Interactions of Stratigraphic Surfaces

First, a suite of geological rules that ensure a surface-based geological model is valid are presented. Next, the operators that define how surfaces interact such that these geological rules are obeyed are presented. The operators are designed to capture the relationships between stratigraphic surfaces that are required for model construction, but not to mimic geological processes. The operators do not require surfaces to be created in stratigraphic or hierarchical order. As in any geological modelling exercise, the operators are used most effectively when the user has a clear geological concept or scenario to be investigated (e.g. Bentley & Smith, 2008; Ringrose & Bentley, 2015).

2.4 Geological rule framework for SBM

In order to create a set of operators that apply to all types of stratigraphic surfaces for SBIM, there are three geological rules which must not be violated (Figure 2.1) (e.g. White and Barton, 1999; Jackson et al., 2005; Caumon et al., 2009):

1. Surfaces cannot cross.
2. Surfaces cannot end within a domain.
3. Surfaces can either terminate against (truncate or conform) or remove (erode), existing surfaces.

Stratigraphic surfaces are not allowed to cross, because crossing surfaces create an overlapping volume that belongs simultaneously to two geological domains (Figure 2.1A). Only one geological domain can exist in any given location. To prevent two stratigraphic surfaces from crossing, one of the surfaces is modified: it is split into sub-segments delineated by the intersection line(s) created where the surfaces cross, and the smaller surface parts are removed as necessary. The operators proposed below define which of the surfaces is split and which smaller surface parts are removed.

Each surface forms (part of) a boundary of a closed, watertight volume that defines a geological domain. Therefore, stratigraphic surfaces cannot end within a domain (”hanging surfaces”), because this would not create a closed volume (Figure 2.1B) and the same domain would exist on both sides of one surface (White and Barton, 1999). The surface ending within a domain must be cropped so that it truncates against the bounding surfaces of the domain (Figure 2.1C). The operators described below specify which of these two actions is applied. A stratigraphic surface may terminate at or remove an existing surface (Figure 2.1D, 2.1E). If these geological rules are obeyed, then the resulting model will contain only watertight volumes and will be geologically possible.

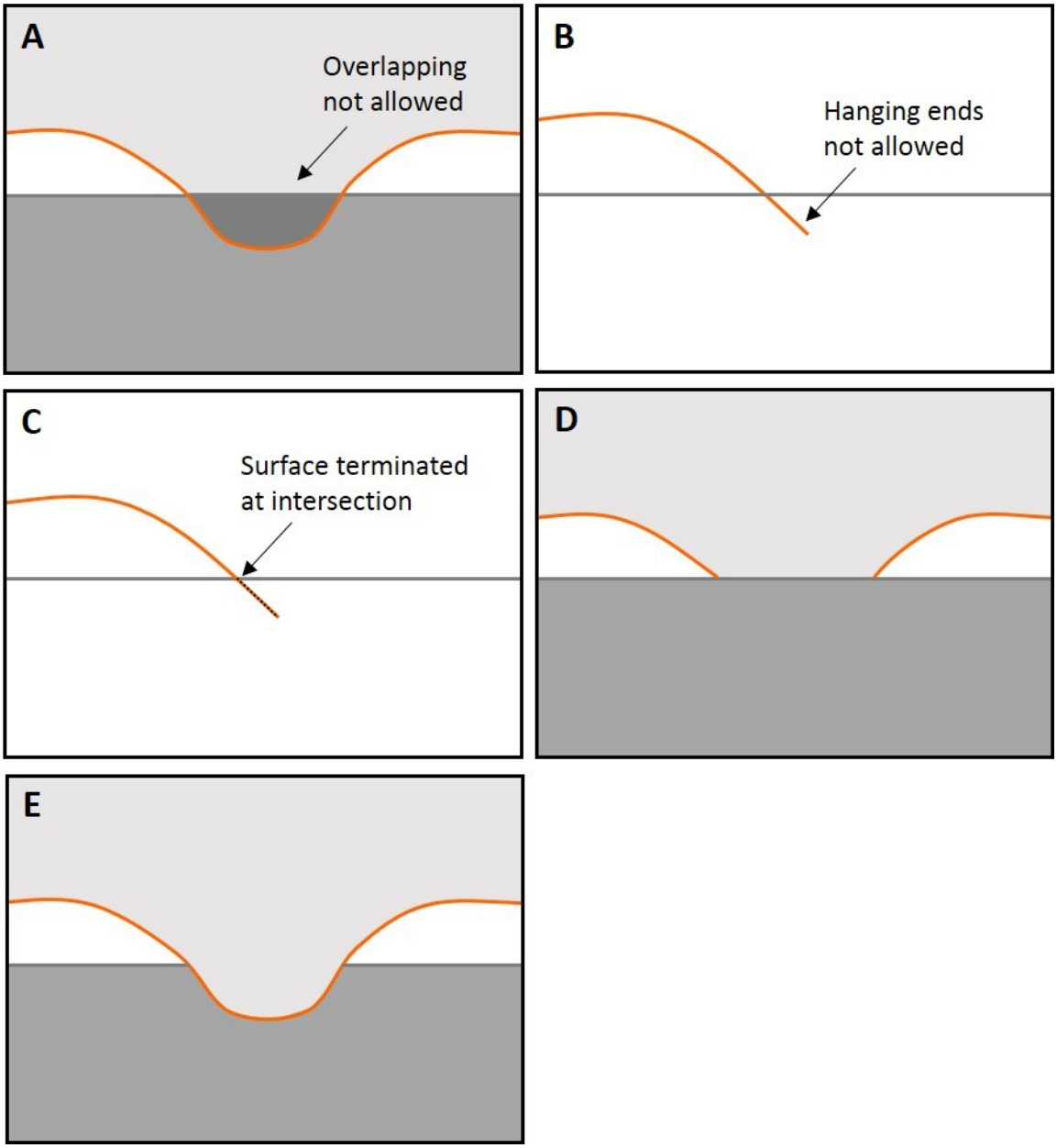

Figure 2.1. Fundamental geological rules for surface intersections in SBM (after Caumon et al., 2009). Surfaces that: (A) cross, and thus define overlapping geological domains; and (B) end within a geological domain are invalid. Surfaces that do not terminate against an existing surface (hanging surfaces, B) are cropped back to the intersection point (C). Valid surfaces may: (D) terminate at an existing surface; or (E) remove an existing surface.

In the operators presented here for stratigraphic surfaces, *above* and *below* are defined by the Cartesian coordinates (x,y,z where z represents depth) of the surfaces in question at any point. We define that z is positive upwards. Points, lines and surfaces that are *above* have higher z-values at a given (x,y) location than the reference surface; those that are *below* have lower z-values than the

reference surface (Figure 2.2). Stratigraphic surfaces are typically monotonic, such that they do not recur in a vertical column unless deformed by later folding and faulting. Representing the effects of such structural deformation is presented in Chapter 4 (this thesis). For map view, the Cartesian system could be applied to cardinal directions or model orientation.

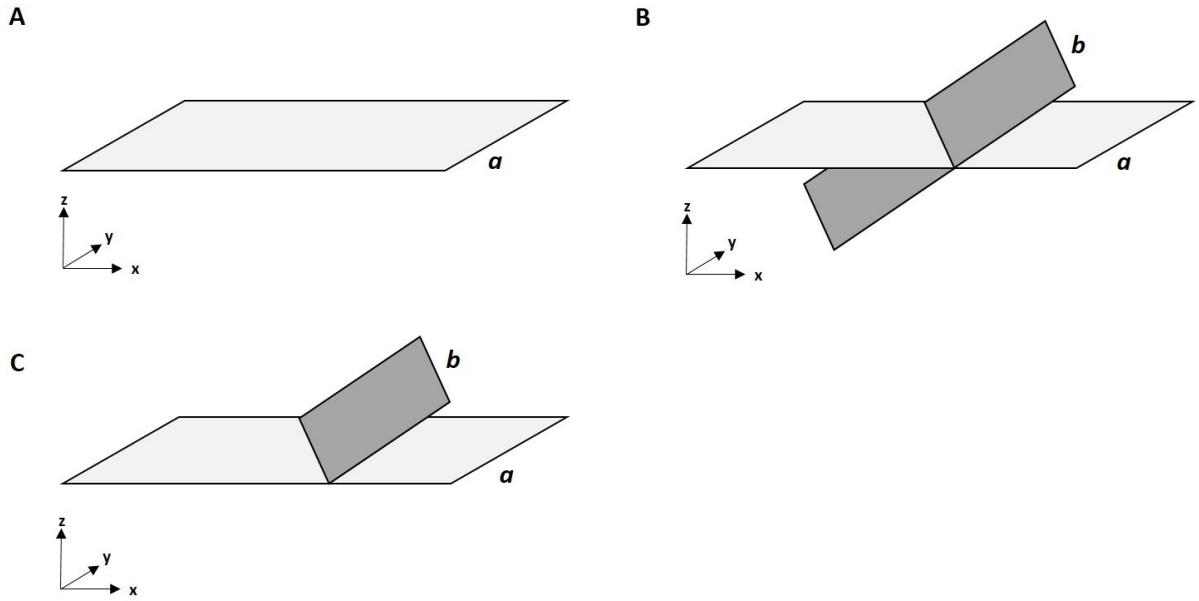

Figure 2.2. These figures demonstrate the intersection of two stratigraphic surfaces. A shows the initial model state with a horizontal surface (*a*) aligned in the x,y plane. B demonstrates the intersection of a diagonal cross-cutting surface (*b*). Intersecting surfaces are not allowed. Thus in C, only the segment of surface *b* that is above (z-positive) the reference surface *a* is preserved.

Irrespective of the method used to create new surfaces, there are two cases that must be considered: (1) a newly created surface is modified by existing surfaces; and (2) a new surface modifies existing surfaces. The operators enable the stratigraphic surfaces to interact such that the geological integrity of the model is preserved in either case. In the following descriptions, the new surface is described as *n*. No operator is required if the new surface does not intersect existing surfaces (e.g. Figure 2.1D, 2.1E). It is assumed that a model boundary exists and all surfaces terminate at this boundary.

2.5 Operators that modify a new surface

The following three operators describe how a new surface *n* is modified if it interacts with existing surfaces. For each operator an example is provided of how the operator can be used to mimic a geological process or rule, but it is not limited to those applications.

Preserve Above - PA

The Preserve Above (PA) operator is applied to existing surfaces below new surface *n*. These selected surfaces form a lower boundary for the new surface *n*. Only the part of *n* that exists above the defined surfaces is preserved (Figure 2.3). The operator PA can be used to create strata that onlap or downlap onto a surface with erosional or depositional relief.

Preserve Below - PB

The Preserve Below (PB) operator is the inverse of PA. The PB operator is applied to existing surfaces below new surface *n*. Only the part of *n* that exists below the defined surfaces is preserved (Figure 2.4). For example, the operator PB can be used to create strata that underlie an unconformity surface.

Preserve Between - PBW

The Preserve Between (PBW) operator is a combination of the operators PA and PB. The selection of two or more existing surfaces defines an area (in cross-section) or volume (in three dimensions) (Figure 2.5). Any new surface *n* cannot exist outside of the defined area or volume (i.e. will terminate at its bounding surfaces), and does not modify the bounding surfaces. Any existing surfaces that lie outside of the defined area or volume are not modified by adding a new surface *n*. For example, the operator PBW can be used to create stratigraphic surfaces within a channel fill by preserving surfaces created between the channel-fill top and base.

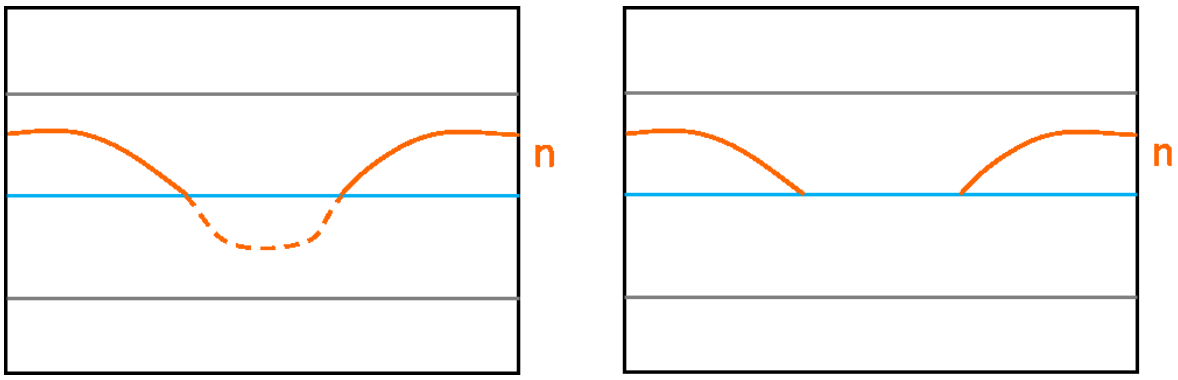

Figure 2.3. Sketch illustrating the Preserve Above (PA) operator. The blue central horizontal line is selected as the surface to PA. When the new orange line (*n*) is created (left), only the parts of *n* that lie above the existing line are preserved (right).

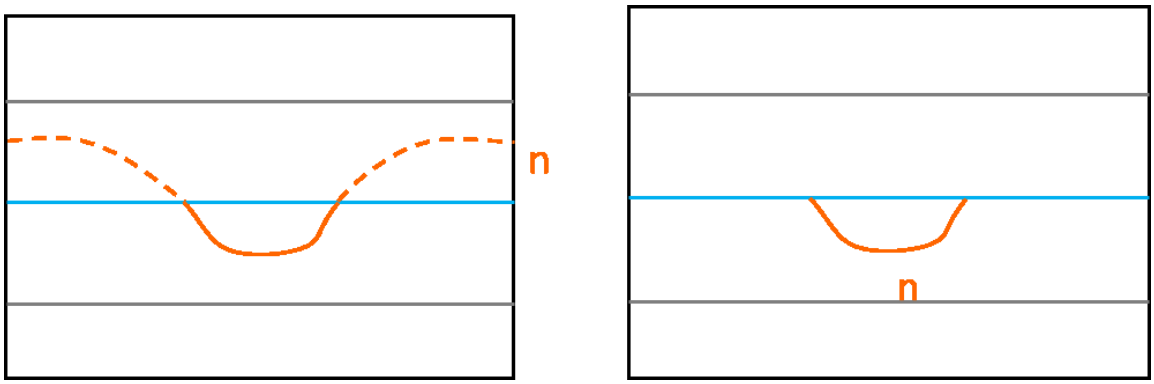

Figure 2.4. Sketch illustrating the Preserve Below (PB) operator. The blue central horizontal line is selected as the surface to PB. When the new orange line (*n*) is created (left), only the parts of *n* that lie below the existing line are preserved (right).

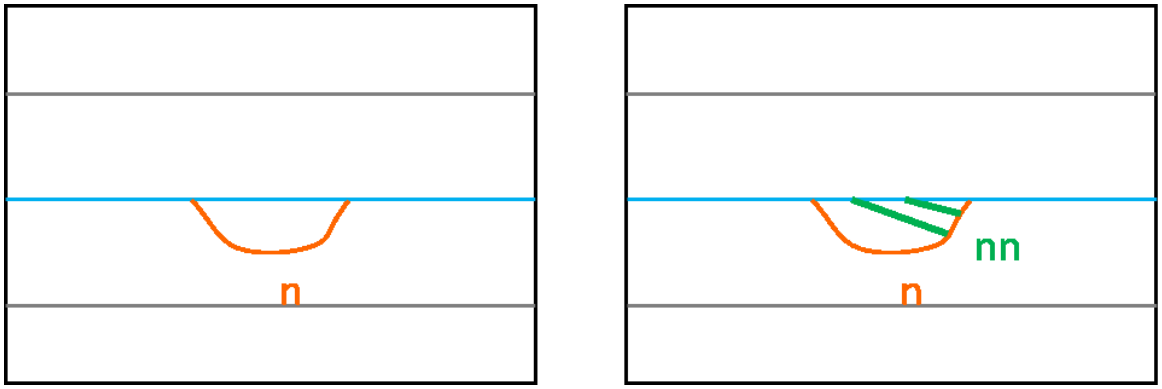

Figure 2.5. Sketch illustrating the Preserve Between (PBW) operator. The blue central horizontal line and orange line *n* are selected as the surfaces to PBW (left). When new green lines *nn* are created, they are entirely contained within the selected PBW surfaces (right).

2.6 Operators that modify an existing surface

The following four operators describe how existing surfaces are modified by a new surface *n*. For each operator an example is provided of how it can be used to mimic a geological process or rule, but it is not limited to those applications.

Remove Above – RA

The Remove Above (RA) operator specifies that any surfaces that lie above a new surface *n* will be removed, including parts of surfaces that are intersected by and lie above *n* (Figure 2.6). Any surfaces below surface *n* remain unchanged. For example, the RA operator can be used to create an erosional surface above a previously created surface(s).

Remove Above Intersection – RAI

The Remove Above Intersection (RAI) operator specifies that only the parts of surfaces which are intersected by and lie above surface *n* will be removed (Figure 2.7). Any surfaces below surface *n* remain unchanged, as do all surfaces above *n* that are not intersected by *n*. For example, the operator RAI can be used to insert an erosional channel base into a series of existing stratigraphic surfaces.

Remove Below – RB

The Remove Below (RB) operator is the opposite of RA. Any surfaces that are intersected by a new surface *n* or lie below *n* will be removed (Figure 2.8). All surfaces above *n* will remain unchanged. For example, the operator RB can be used to create a shallower interpretation of a basement contact, removing the previous interpretation.

Remove Below Intersection - RBI

The Remove Below Intersection (RBI) operator is the opposite of operator RAI. Any surfaces that are intersected by surface *n* and lie below *n* will be removed (Figure 2.9). For example, the operator RBI

can be used to insert a lateral accretion surface into a channel fill by removing previously interpreted channel-fill deposits.

In order for the RAI and RBI operators to be applied consistently, without generating hanging surface end(s) that would violate the fundamental geological rules, it is required that all existing surfaces that are truncated by removed surfaces are also removed. However, in practice the most common cases can be modelled without using operators RAI or RBI, or by using them sparingly.

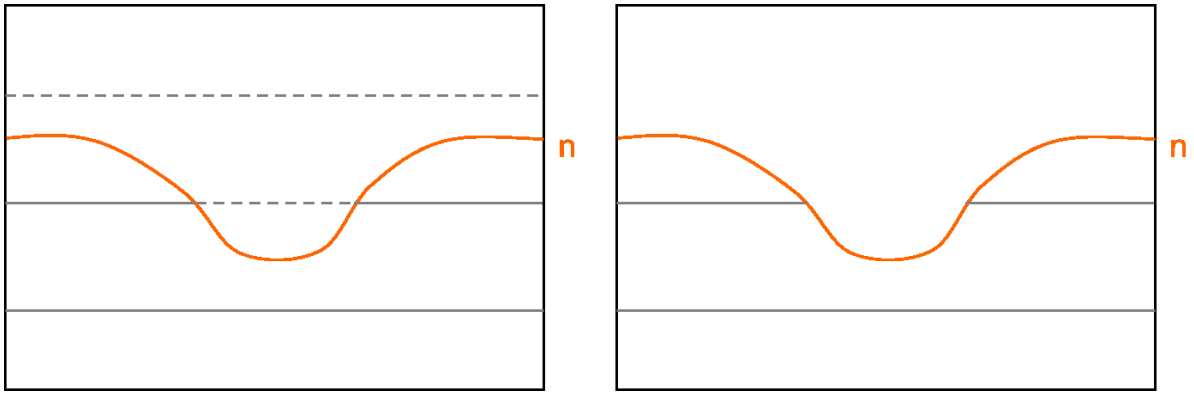

Figure 2.6. Sketch illustrating the Remove Above (RA) operator. New orange line *n* is created with RA selected. When line *n* is added (left) all existing surfaces and parts of existing surfaces above line *n* are removed (right).

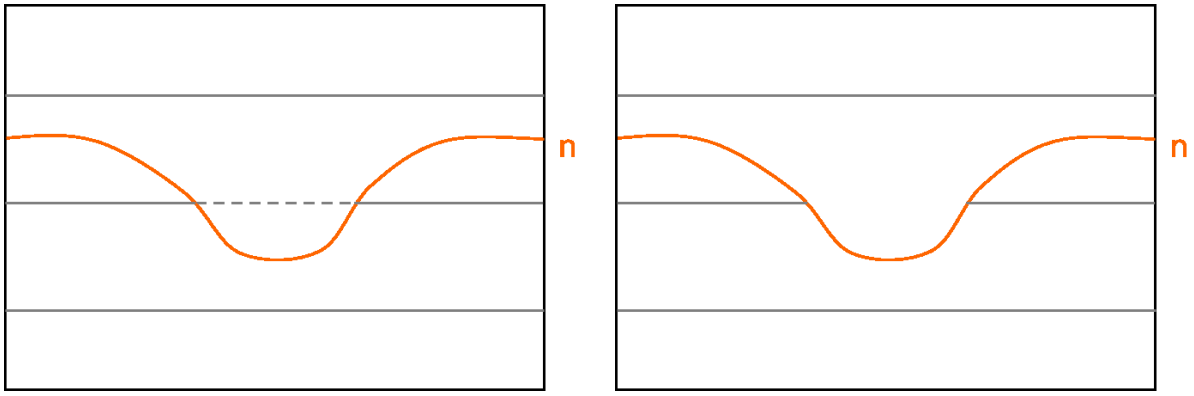

Figure 2.7. Sketch illustrating the Remove Above Intersection (RAI) operator. New orange line *n* is created with RAI selected. When line *n* is added (left) only parts of existing surfaces that are intersected by and lie above line *n* are removed (right).

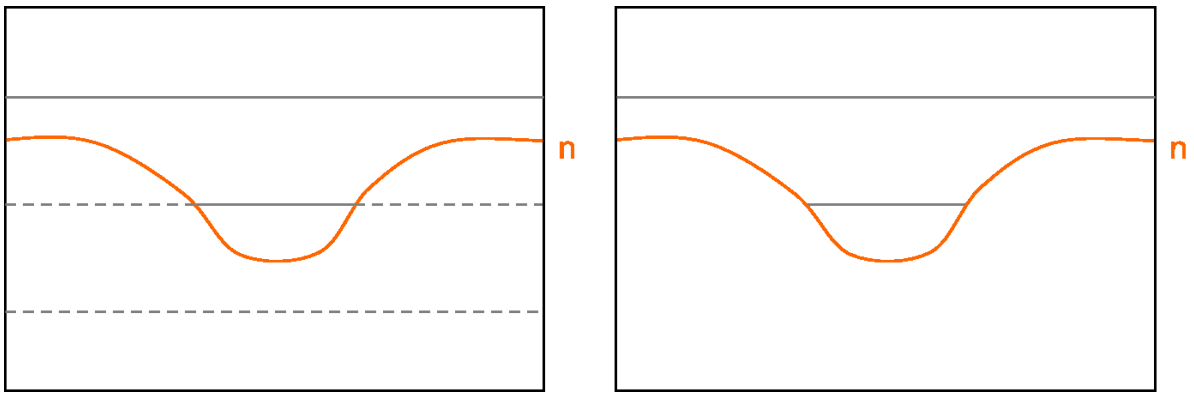

Figure 2.8. Sketch illustrating the Remove Below (RB) operator. New orange line *n* is created with RB selected. When line *n* is added (left) all existing surfaces and parts of existing surfaces below line *n* are removed (right).

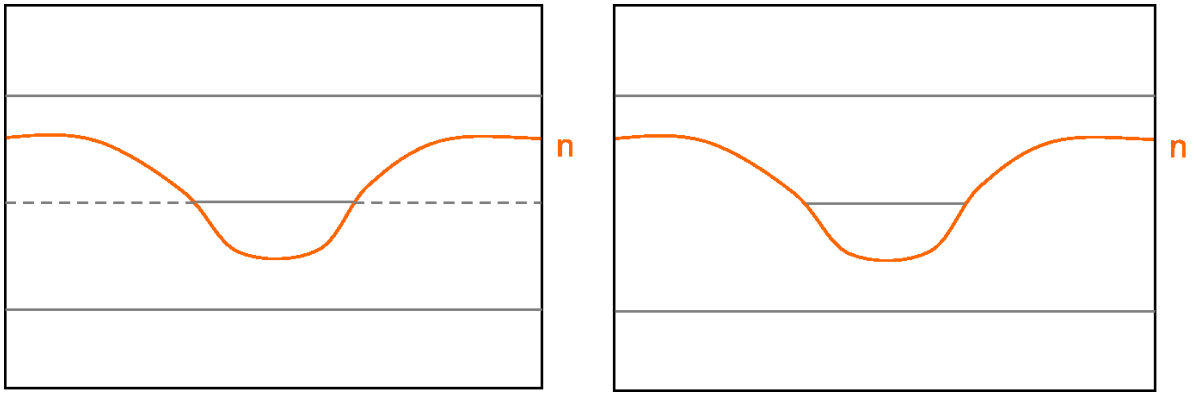

Figure 2.9. Sketch illustrating the Remove Below Intersection (RBI) operator. New orange line *n* is created with RBI selected. When line *n* is added (left) only parts of existing surfaces that are intersected by and lie below line *n* are removed (right).

2.7 Hand-drafted Case Studies

This section demonstrates application of the stratigraphic surface operators to three geological cases of different length scales and depositional environments, and using different types of input data.

Three examples are presented to illustrate the flexibility and effectiveness of the operators.

2.8 Case Study 2A: Handspecimen-scale model of shallow-marine tidal depositional environment generated using outcrop data

The following example is a handspecimen-scale model constructed from an outcrop photograph of rhythmically interbedded sandstone and mudstone laminae along foresets within a cross-bed set (tidal bundle *sensu* Boersma, 1969). The studied outcrop exposes the Eocene Dir Abu Lifa Member in the Western Desert of Egypt, and is interpreted to have formed by the migration of dunes through a distributary channel in a tide-dominated delta (Legler et al., 2013; Massart et al., 2016a). The abundance and continuity of mudstone laminae in heterolithic, cross-bedded sandstones can have a significant effect on fluid flow and effective permeability (e.g. Weber, 1986; Jackson & Muggeridge, 2000; Massart et al., 2016b). However, these small-scale heterogeneities can be difficult to model on a pseudo-orthogonal grid using conventional methods (e.g. White & Barton, 1999; Jackson et al., 2005). In contrast, it is simple to reproduce these geometries faithfully, even at the centimetre scale, using SBM in conjunction with the stratigraphic operators.

A model is produced through application of the operator Preserve Between (Figure 2.10). The uninterpreted field photo is shown in Figure 2.10A, followed by the interpretation of the top and base bounding surfaces of the cross-bed (Figure 2.10B). No operators are required to create the top and base surfaces because they do not intersect. The final model is shown in Figure 2.10C, after creation of internal surfaces, which represent the boundaries of sandstone laminae and mudstone drapes, through use of the operator PBW. The result is a series of discrete surfaces bounding areas of similar lithologic composition and grain size. Figure 2.10D shows detail of interpreted individual mudstone drapes, which are bounded above and below by closely spaced stratigraphic surfaces. Not all surfaces extend across the model, but all surfaces conform or truncate against other surfaces. The model was created using the following steps:

1. Create initial surfaces (Figure 2.10B):
    a. Create the bounding surfaces which extend across the model area

2. Using Preserve Between (Figure 2.10C):
    a. Define the top and base boundaries of a cross-bed set as the surfaces to Preserve Between
    b. Create surfaces that bound the individual sandstone laminae within the cross-bed set in any order.
3. Using Preserve Above or Preserve Below (Figure 2.10E)
    a. Create surfaces above or below individual sandstone laminae that represent mudstone drapes in any order.

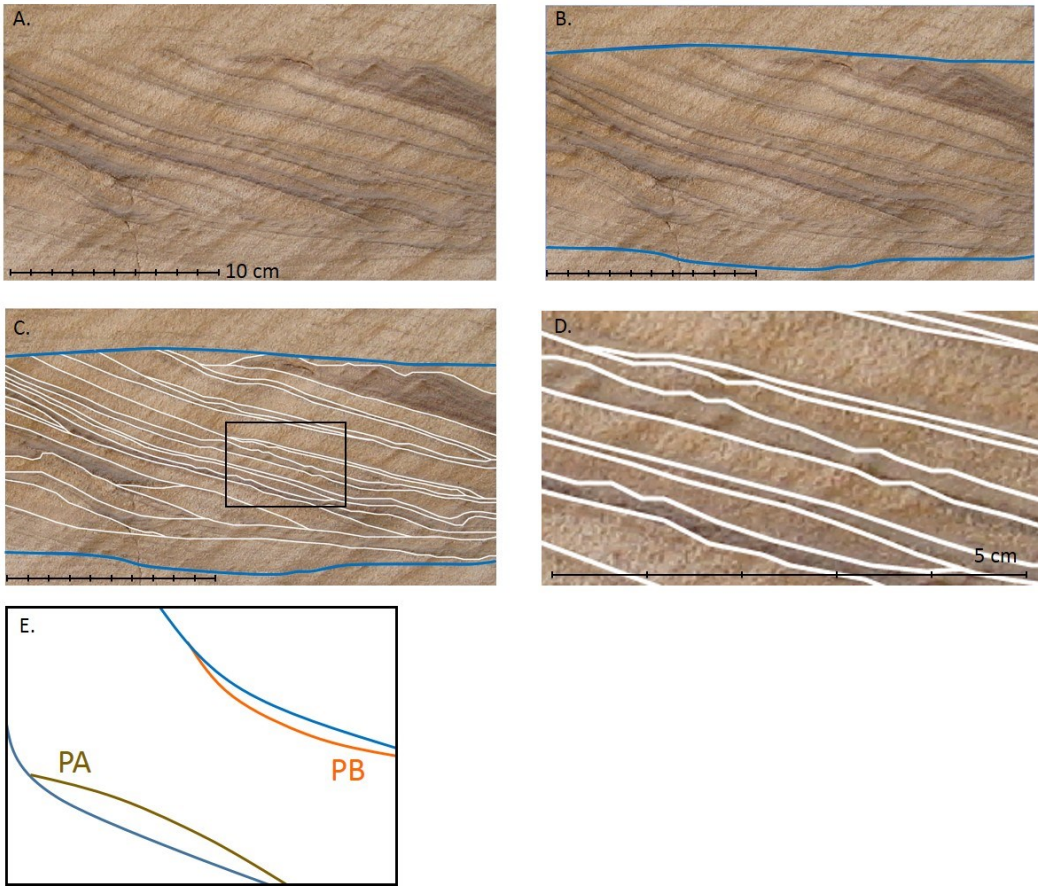

Figure 2.10. Illustration of handspecimen-scale model of heterolithic, cross-bedded sandstones, showing: (A) input outcrop data (after Legler et al., 2015; Massart et al., 2016a); (B) creation of top and base bounding surfaces (blue); (C) creation of internal surfaces with the operator Preserve Between and resultant completed surface-based model, (D) detail of surfaces that bound sandstone laminae and shale drapes along laminae (see inset box in D for location), and (E) a sketch showing how individual shale drapes can be created using the operator Preserve Above (brown) or Preserve Below (orange) in a model that includes existing surfaces (blue). Note that not all surfaces extend across the entire model, therefore some surfaces become coincident. The scale bar in A, B and C is 10 cm. The inset box D is approximately 5 cm across.

The modelled surfaces are not created in stratigraphic order. For ease of modelling, the top and base bounding surfaces of the cross-bed set are generated first, so that surfaces bounding sandstone laminae and mudstone drapes can be easily truncated against them using operator Preserve Between. Within these bounding surfaces, the order in which laminae- and drape-bounding surfaces are generated is flexible. The fundamental geological rules do not allow surfaces to terminate within a model domain (Figure 2.1B). Despite this requirement, it is possible to create a model that represents discontinuous mudstone drapes (e.g. along laminae toesets in the cross-bed set; Figure 2.10D) as watertight volumes bounded by surfaces that are coincident where the mudstone drapes are absent (rather than as surfaces with associated transmissibility modifiers; e.g. White & Barton, 1999). Surfaces can be added using the operators PA or PB until the model contains the required level of detail, for example adding additional mudstone drapes along sandstone laminae boundaries (Figure 2.10E). The benefit of the operators is that the interpretation of the number of mudstone drapes can be modified without the need to change pre-existing surfaces, as would be required if surfaces were added in stratigraphic order.

Small-scale stratigraphic architectures, such as those described above for heterolithic cross-bedded sandstones, are not modelled and used to simulate flow routinely during hydrocarbon reservoir characterization projects, where the focus of modelling effort tends to be at larger scales (although there are notable exceptions; e.g. Jackson et al., 2005; Ringrose et al., 2005, 2008; Massart et al., 2016b). Consequently, the effects of such architectures on hydrocarbon recovery are poorly constrained, despite their influence being widely recognized (e.g. Weber, 1986). One benefit of our approach is that it is independent of length scale and depositional process or geological interpretation; the same set of operators may be used to represent detailed stratigraphy across a wide range of scales.

2.9 Case Study 2B: Basin-scale model of carbonate platform depositional environment generated using seismic data

Here a model is presented based on a published seismic cross-section of carbonate platform deposits from the Late Miocene Central Luconia Province of the Sarawak Basin, offshore northwest Borneo (Kosa et al., 2015). These carbonate platform deposits are characterized by mounded geometries with thin, low-relief wedges, referred to locally as 'wings', that extend out from the main platform and are intercalated with adjacent siliciclastic deposits (Figure 2.11). The wings are thin (30-200 m) relative to the platforms (1-2 km) and can extend for up to 12 km laterally (Kosa et al., 2015). The resulting geometries are complex, due to the pronounced thickness differences between the platforms and associated wings, the low aspect ratio (thickness:width) of the wings, and the non-monotonic ("overhanging") nature of the boundary between carbonate platform-and-wing deposits and adjacent siliciclastic deposits. However, by using the stratigraphic operators presented in Sections 2.5 and 2.6, it is quick and easy to produce a model that accurately represents the geometric complexity of the strata.

A model is produced through application of the operators Preserve Between, Preserve Above and Remove Below Intersection (Figure 2.11). Three surfaces bounding the condensed sections, that form marker horizons across the entire basin, are modelled first (Figure 2.11B), then the simplified, near-vertical edges of the carbonate platform (Figure 2.11C), next the carbonate wings that extend from the platform (Figure 2.11D), and lastly the isolated carbonate buildups and surfaces in siliciclastic deposits adjacent to the carbonate platform (Figure 2.11E). The resulting model combines the platform and its lateral wings into a single contiguous volume of carbonate deposits, different from the geological interpretation of Kosa et al. (2015). It would be simple to add additional surfaces inside the carbonate platform, if required. The model was created using the following steps:

1. Create surfaces (Figure 2.11B):

    a. Create the top of the condensed section surfaces which extend across the model area

2. Using Preserve Between and Preserve Above (Figure 2.11C):
    a. Select the condensed section top surfaces to Preserve Between
    b. Create the simplified, near-vertical boundaries of the carbonate platform between the condensed section top surfaces
    c. Select the uppermost condensed section top surface to Preserve Above
    d. Create the mounded top of the carbonate platform
3. Using Remove Below Intersection (Figure 2.11D):
    a. Create the surfaces by sketching the surfaces as a single, non-monotonic surface bounding the carbonate wings along the simplified, near-vertical boundaries of the carbonate platform; the segments of the carbonate platform surface that lie below the newly generated carbonate wing boundaries are removed
4. No operator required (Figure 2.11E):
    a. Create the top surfaces that bound isolated carbonate buildups and bedding surfaces within siliciclastic deposits adjacent to the carbonate platform.

The final model contains surface-bounded volumes of carbonate platform-and-wing deposits. Such geometrically complex volumes are difficult to generate using SBM approaches that require surfaces to be constructed in stratigraphic order or using conventional modelling approaches based on pillar grids, which cannot accommodate non-monotonic surfaces (see Section 4.6.3 for further discussion of non-monotonic surfaces). An alternative method of model construction that does not require non-monotonic surfaces would be to create the top of the wing surface with the remove below operator, and the base of the wing surface with the remove above operator. However, it is simpler to use a single, non-monotonic surface.

Construction of a model that contains simply defined carbonate platform-and-wing volumes would allow efficient estimation of carbonate rock volumes and the hydrocarbon resources that they may host. The flexibility of the stratigraphic operators also ensures that the resulting model could be used as a basis for further investigation. For example, the effect of varying carbonate rock-property distributions at scales below seismic resolution could be investigated, by generating multiple scenarios for surface-defined stratigraphic architectures and facies distributions within the framework of traced seismic surfaces. For example, additional internal surfaces could be created within the carbonate platform, more wings could be created at the platform edges, or the lateral extent of the wings could be modified.

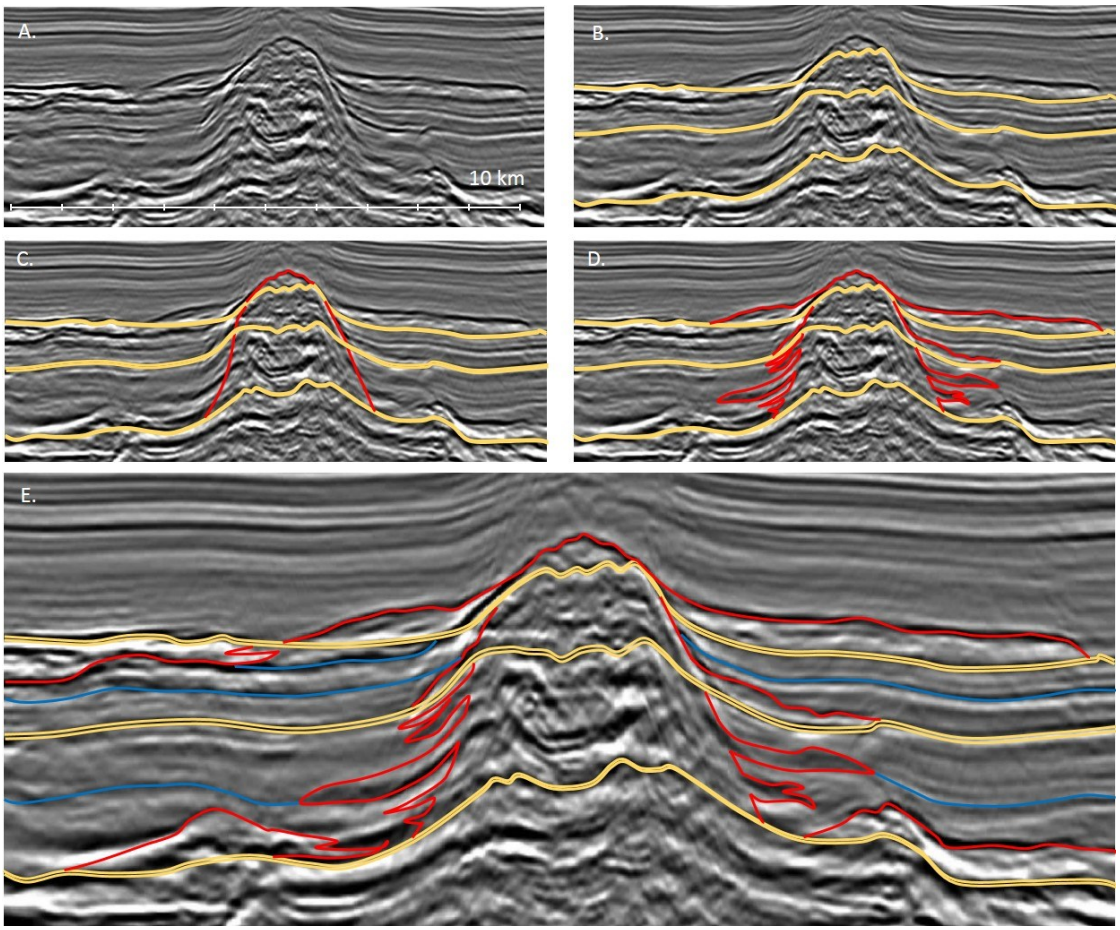

Figure 2.11. Illustration of basin-scale model of carbonate platform and lateral wings, showing (A) input seismic data (after Kosa et al., 2015); (B) generation of surfaces representing condensed sections (yellow); (C) generation of carbonate platform edges and mounded top using operators Preserve Between and Preserve Above (red); (D) addition of wings to edges of carbonate platform with operator Remove Below Intersection; and (E) completed surface-based model including isolated carbonate buildups (red) and surfaces in siliciclastic deposits (blue) adjacent to the main carbonate platform and its wings. The scale across the seismic image is approximately 10 km, shown in A.

2.10 Case Study 2C: Reservoir-scale model of deep-marine depositional environment generated using conceptual block diagram

Although models are often constructed from outcrop and subsurface data, as in the previous two examples, it is also useful to create models from conceptual block diagrams, for prototyping purposes, for example. This is simple to achieve with a SBM approach that uses surface operators.

The conceptual block model presented here (Figure 2.12) is adapted from an idealised cross-section of shallow seismic data, constrained by wells (after Posamentier & Kolla, 2003). The original data are from deep-water basin floor fan deposits of the Makassar Strait, Indonesia and include condensed-section deposits, mass-transport deposits, levee deposits, channel-fill deposits and lobe (frontal-splay) deposits (Posamentier & Walker, 2006). The spatial organisation of these depositional elements corresponds to a widely applied sequence stratigraphic model of a basin-floor fan deposited during a fall and subsequent lowstand of relative sea-level (Mutti, 1985; Posamentier & Vail, 1988; Posamentier & Walker, 2006). A lower mass-transport deposit is overlain by a series of lobe deposits. These are eroded and overlain by a channel-levee complex, which in turn is eroded by an upper mass-transport deposit that is draped by condensed-section deposits. To demonstrate application of the stratigraphic operators in three dimensions, the original idealised cross-section has been extended to create a block diagram.

Figure 2.12 shows two different model-construction pathways for two perpendicular cross-sections of the block diagram. The operators are applied in the order outlined below. After insertion of each surface the operators ensure that the resulting SBM is valid. Construction of the model is described below from stratigraphic base to top (Figure 2.12A-E, K), however it can be created in any order.

1. No operator required (Figure 2.12A-B):
    a. Create the basal surface of the lower mass-transport deposit
    b. Create the basal surface of the lowest lobe deposit
    c. Create the top surfaces of each of the overlying lobe deposits

2. Using Remove Above (Figure 2.12C):
    a. Create the basal surface of the channel-fill deposits; any intersected lobe-deposit surfaces are removed above the channel-fill basal surface
3. Using Preserve Between (Figure 2.12D):
    a. Select the channel-fill basal surface and lobe deposit top as the surfaces to Preserve Between
    b. Create the basal surface of the upper mass-transport deposit
4. Create surfaces (Figure 2.12E):
    a. Create the top surface of the channel-fill deposit
    b. Create the top surface of the condensed-section deposit
5. Using Preserve Between (Figure 2.12K):
    a. Define the upper mass-transport deposit basal surface, channel-fill deposit basal surface, and the lobe deposit top surface as the surfaces to Preserve Between
    b. Create levee deposit surfaces.

Construction of the same model using surfaces that are not created in stratigraphic order is now described below (Figure 2.12F-K).

1. No operator required (Figure 2.12A, F):
    a. Create the basal surface of lower mass-transport deposit
    b. Create the levee surfaces
2. Using Remove Above (Figure 2.12G-H):
    a. Create the basal surface of the upper mass-transport deposit; any intersecting levee surfaces are removed above the mass-transport deposit basal surface
    b. Create the top surface of the condensed-section deposits; any intersected mass-transport-deposit and levee-deposit surfaces are removed above the condensed-section top surface

3. Using Remove Above Intersection (Figure 2.12I):
    a. Create the channel-fill basal surface; any intersected mass-transport-deposit and levee-deposit surfaces are removed above the channel-fill basal surface
4. Using Preserve Below and Remove Below Intersection (Figure 2.12J-K):
    a. Define the channel-fill basal surface as the surface to Preserve Below, and in combination with Remove Below Intersection, create lobe-deposit surfaces and the top surface of lower mass-transport deposit. Any intersected levee deposits are removed below lobe-deposit surfaces. Operators are used concurrently in this step, which is allowed in our framework.

Application of the operators differs in the two model-construction pathways described above, but they result in the same model (Figure 2.12). This example demonstrates that the operators are compatible with three-dimensional modelling, with the use of conceptual information, and that surfaces can be added in any order with operators used flexibly to create a valid geological model.

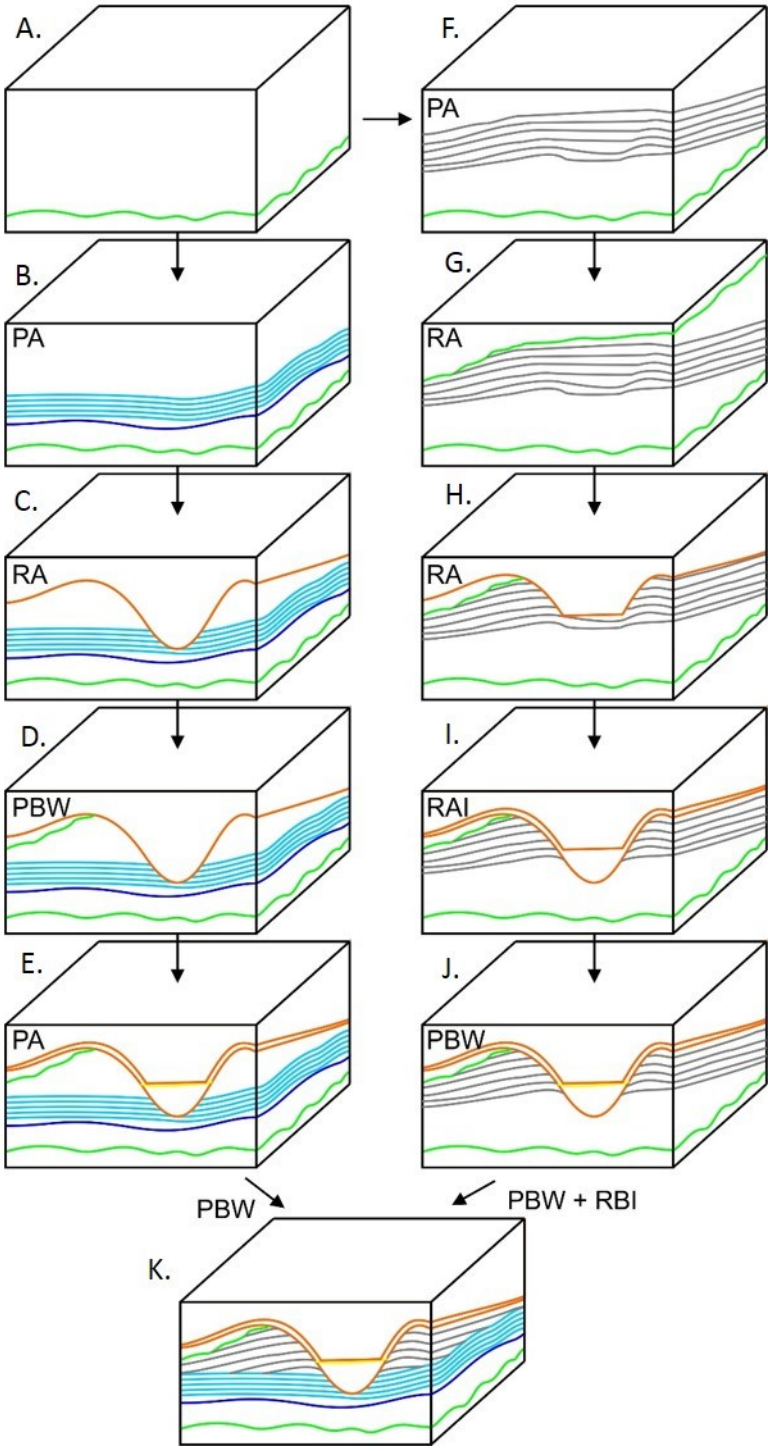

Figure 2.12. Illustration of reservoir-scale model of deepwater basin-floor fan deposits, showing a completed surface-based conceptual model (K) based on a conceptual deepwater depositional cross-section (after Posamentier & Kolla, 2003; Posamentier & Walker, 2006). The model generation pathway illustrated on the left is constructed predominantly from stratigraphic base to top. (A) First the lower mass-transport-deposit base is created (green surface); (B) next the mass-transport-deposit top surface (purple) and lobe-deposit surfaces (blue) are generated; (C) application of the Remove Above operator allows creation of the channel-base surface (orange) and removes the intersected lobe-deposit surfaces; (D) the basal surface of an upper mass-transport deposit (green) is generated below the channel-base surface; (E) the channel-fill top surface (yellow) and condensed-

section top surface (red) are generated above the channel-base surface; (K) lastly, internal levee surfaces are generated between the channel base, upper mass-transport-deposit base, and lobe deposit top surface, resulting in a complete conceptual surface-based model. The model generation pathway illustrated on the right is constructed predominantly from stratigraphic top to base. First (F) the levee surfaces are created by Preserving Above the lower mass-transport-deposit base; (G) next the basal surface of the upper mass-transport deposit is created with Remove Above; (H) next the condensed-section top surface is created with operator Remove Above; (I) then the channel base is created using operator Remove Above Intersection; (J) next the channel-fill top surface is created by using the operator Preserve Between; (K) lastly the lobe-deposit surfaces and top surface of the lower mass-transport deposit are created with the combined operators Preserve Below and Remove Below Intersection; any intersected levee deposits are removed below the lobe deposits. The two distinct modelling pathways result in the same geological model, demonstrating the flexibility of the operators.

2.11 Discussion

The operators presented here for SBM of stratigraphic surfaces are simple and flexible. Regardless of the method used to create surfaces, the operators apply, at any length scale, to any depositional environment, and to any data type. The three examples outlined above (Figures 2.10, 2.11, 2.12) demonstrate that the stratigraphic operators can be used to honour fundamental, widely used stratigraphic and sedimentological concepts such as the law of superposition, Walther's Law, sequence stratigraphy, and facies models. The weakness of our approach is that the surfaces do not directly integrate information about depositional processes during definition of rock property distributions (cf. "stratigraphic rule-based models" *sensu* Pyrcz et al., 2015). If needed, the stratigraphic organization of the surfaces thus needs to be derived separately. The strength of our approach lies in flexibility and practicality; surfaces can be generated in any sequence, and the operators can be applied in any order.

Returning to the three SBM examples given in the introduction (Section 1.2, this thesis), which were generated on a case-by-case basis, the method for generating these models using the operators is described. Unlike previous SBM approaches, the operators do not require that surfaces be generated in stratigraphic order or according to hierarchical spatial organisation.

1. Pyrcz et al. (2005) modelled lobe-bounding surfaces in stratigraphic order, from oldest to youngest. This model could be constructed using the operator Preserve Above, with each newly added surface becoming the surface to which the PA operator is applied.
2. The hierarchical modelling approach of Sech et al. (2009) captures facies boundaries between clinoform surfaces, which are in turn bounded by transgressive surfaces. The resulting model thus uses a three-level hierarchy of stratigraphic surfaces. Using the operators, clinoform surfaces could be Preserved Between the upper and lower transgressive surfaces, or Removed Above Intersection with the upper transgressive surface if they conform to the lower transgressive surface. Facies boundaries are Preserved Between each pair of clinoform surfaces.
3. Massart et al. (2016a, 2016b) modelled the boundaries of sandstone laminae and mudstone drapes within a cross-bed set using a mixture of stratigraphic and hierarchical ordering of stratigraphic surfaces. In this case, laminae boundaries could be Preserved Between the top and base surfaces of the cross-bed set. The boundaries of mudstone drapes along the foreset-to-toeset regions of the sandstone laminae could be Preserved Above or Preserved Below the laminae boundaries.

The benefit of our work is that it formalizes the operators in a way that easily allows for their implementation across a range of modelling methods. Additionally, our approach greatly increases modelling flexibility, because it allows rapid modification of existing models as new data are added or new geological concepts are explored without modifying the stratigraphic hierarchy or depositional order that is already in place.

Current implementations of our operators include a sketch-based interfaces and modelling (SBIM) method (Jackson et al., 2015a) and as metadata for a parametric (NURBS) surface-based method (Jacquemyn et al, 2019). Jackson et al. (2015a) present a modelling method where surfaces are sketched directly by a user (adapted for the Rapid Reservoir Modelling program presented in

Chapter 3). The operators presented here allow these sketches to be geologically possible, while allowing the user flexibility in the order in which the components of the model are drawn. Models that represent multiple geological scenarios can be generated easily and quickly to test, for example, which aspects of the stratigraphic architecture are significant in controlling hydrocarbon drainage efficiency by adding or removing surfaces without the need to construct new models from the start. Jacquemyn et al. (2019) use the operators as information contained within metadata for models built from NURBS surfaces across different levels of a stratigraphic hierarchy. The operators in the metadata allow surfaces to be combined automatically in a geologically possible way.

SBM is geologically intuitive, because surfaces are used to conceptualise and communicate geology in fundamental tools such as maps, cross-sections and block diagrams. This aspect of SBM is augmented by our stratigraphic operators, which provide a flexible framework for any future SBM method. In addition to existing applications in the exploitation of hydrocarbon, mineral and groundwater resources, such as cutting cycle times and improving the accuracy of resource estimation, there are clear but unrealised applications of SBM in education, for example in developing students' skills in visualising and testing geological interpretations.

2.12 Conclusions

This chapter has presented a set of seven universal operators that define the interactions between new and existing stratigraphic surfaces within a surface-based framework for constructing geological models. The operators are simple and flexible, because they can be applied in any order, are scale-independent, and are not specific to any sedimentological process or depositional environment. The stratigraphic operators are each summarized below:

- Preserve Above (PA) defines a target surface that a newly created surface(s) is generated above;

- Preserve Below (PB) defines a target surface that a newly created surface(s) is generated below;
- Preserve Between (PBW) defines two or more surfaces that describe a target volume within which a newly created surface(s) is generated;
- Remove Above (RA) creates a new surface(s), above which all existing surfaces and all sections of intersected surfaces are removed;
- Remove Above Intersection (RAI) creates a new surface(s), above which all sections of intersected surfaces are removed (and above which all existing, non-intersected surfaces are preserved);
- Remove Below (RB) creates a new surface(s), below which all existing surfaces and all sections of intersected surfaces are removed;
- Remove Below Intersection (RBI) creates a new surface(s), below which all sections of intersected surfaces are removed (and below which all existing, non-intersected surfaces are preserved);

The operators can be used in various combinations to generate surface-defined architectures that mimic fundamental, widely used stratigraphic and sedimentological concepts. The operators can be applied to any input data type, including outcrop, seismic and conceptual data, and they can be applied to any surface-based modelling method, including those based on sketches and algorithms. The application of a flexible and generic operator set for stratigraphic surfaces within a surface-based modelling context is geologically intuitive for the user, because the components and processes of model construction are similar to those used to conceptualise and communicate geology in maps, cross-sections and block diagrams. In Chapter 3, the stratigraphic operators will be demonstrated in 3D using the sketch-based modelling program Rapid Reservoir Modelling.

3 Application of operators to 3D Sketch-based Interface and Modelling through use of Rapid Reservoir Modelling

3.1 Summary

Sketch-based interface and modelling (SBIM) can be used to create 3D computational geological models rapidly and intuitively. SBIM uses surfaces sketched in a computational environment to represent all geological heterogeneity of interest. SBIM can complement existing geological modelling workflows by allowing rapid prototyping of geological concepts. In order to create geological models using SBIM, rules are required to govern how sketched surfaces interact such that resulting models are geologically sound. A comprehensive set of explicit and universal rules to govern the interaction of stratigraphic surfaces for SBIM has now been formalized, as presented in Chapter 2.

In this chapter, the seven operators that define how stratigraphic surfaces interact for SBIM such that universal geological rules are obeyed are demonstrated in 3D using the research prototype software Rapid Reservoir Modelling (RRM). Three case studies are presented using examples of siliciclastic and carbonate strata from different depositional environments, at length scales from meters to kilometres, and using seismic, outcrop, and well log data to constrain and guide the sketches. The case studies also demonstrate three different techniques for moving from 2D sketch to 3D model. These applications demonstrate the flexibility and broad applicability of the operators for SBIM for stratigraphy.

3.2 Introduction

In Chapter 2, the stratigraphic operators were introduced and demonstrated on hand-sketched models. In this Chapter, three case studies are presented to test the functionality of the operators within the sketch-based reservoir modelling software Rapid Reservoir Modelling (RRM), to demonstrate functionality of the operators in 3D and to show the broad applicability and flexibility

of our approach. The first example demonstrates a 3D model of deepwater deposits from the Rakhine Basin, offshore Myanmar (Xu et al., 2016). Each 3D surface in the model is created by interpolating between multiple 2D sketches made on parallel, vertical cross-sections. Each 2D sketch is guided by a corresponding cross-section through a 3D seismic dataset imaging the deposits of interest. The second example shows a 3D conceptual model of lacustrine carbonate microbialite bioherms and grainstones based on outcrop observations (Bohacs et al., 2013). Some 3D surfaces in this model are created by interpolation between sketches made on 2D vertical cross-sections; others are created by sketching 2D contours in plan-view. The final example shows multiple 3D models created from a suite of interpreted and simplified borehole logs through a meandering fluvial deposit (Colombera et al., 2018). These three examples demonstrate that the operators can be used at any scale, in any depositional environment and with a range of input data types.

3.3 Stratigraphic Operators for SBIM

In Chapter 2, the operators for SBM of stratigraphy were presented and defined (Sections 2.5 and 2.6, this thesis; Figures 3.1 and 3.2). The stratigraphic operators are summarized again below:

- Preserve Above (PA) defines a target surface that a newly created surface(s) is generated above;
- Preserve Below (PB) defines a target surface that a newly created surface(s) is generated below;
- Preserve Between (PBW) defines two or more surfaces that describe a target volume within which a newly created surface(s) is generated;
- Remove Above (RA) creates a new surface(s), above which all existing surfaces and all sections of intersected surfaces are removed;

- Remove Above Intersection (RAI) creates a new surface(s), above which all sections of intersected surfaces are removed (and above which all existing, non-intersected surfaces are preserved);

- Remove Below (RB) creates a new surface(s), below which all existing surfaces and all sections of intersected surfaces are removed;

- Remove Below Intersection (RBI) creates a new surface(s), below which all sections of intersected surfaces are removed (and below which all existing, non-intersected surfaces are preserved);

These seven stratigraphic operators are implemented in RRM. In the RRM SBIM approach, the selected operator is applied immediately after each surface has been sketched and before the next surface is added. Application of the operators to a given surface as it is created is an important aspect of the SBIM workflow, as it allows surfaces to be sketched without having interpreted, *a-priori,* the stratigraphic order or hierarchy. A video of the operators being used to create a variety of geometric stratal configurations using the RRM research software is provided in the supplemental material (Appendix 1; Supplemental Material, Video 1).

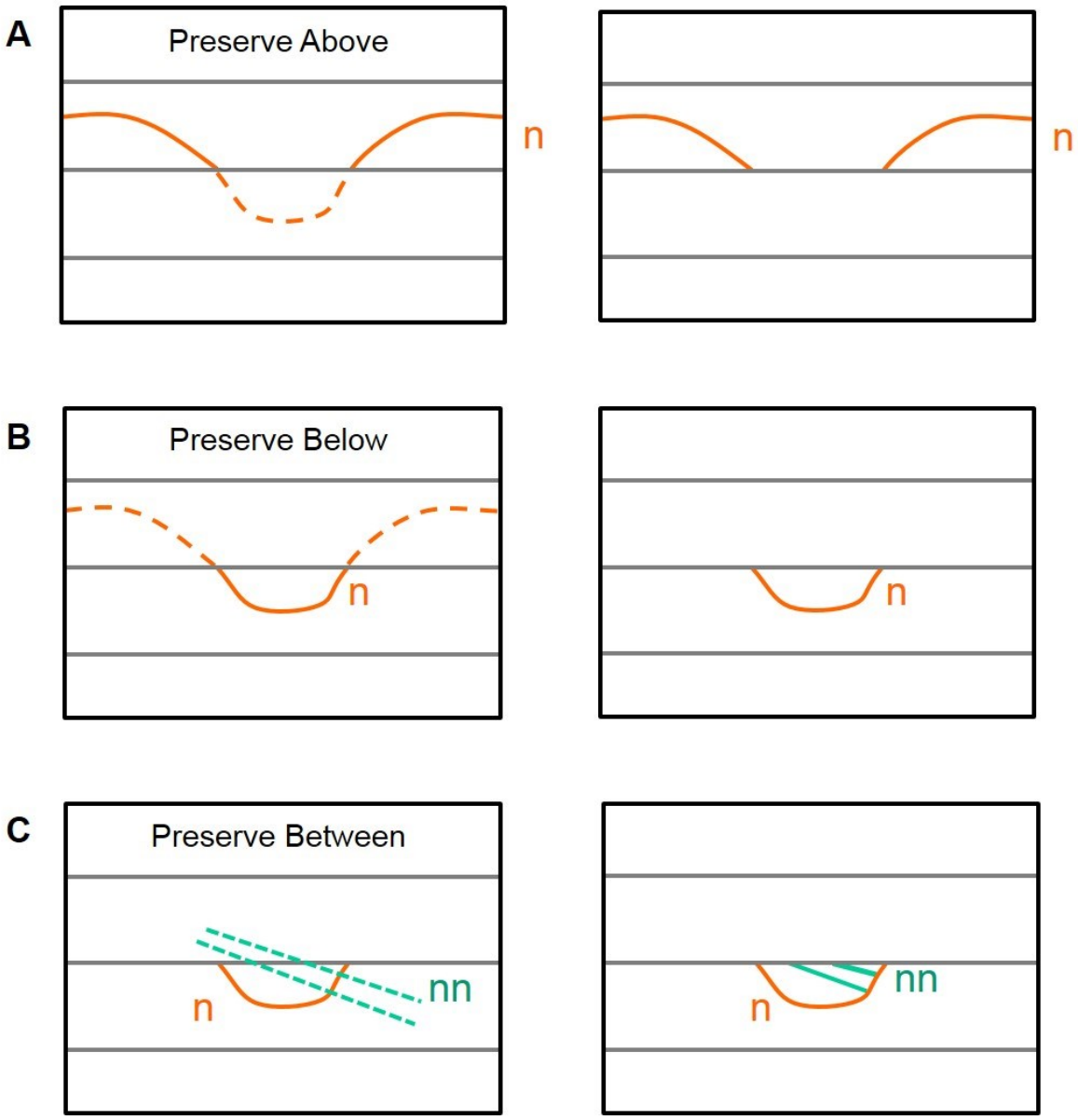

Figure 3.1. These figures illustrate operators applied to a new surface *n* when it intersects the existing central surface. A shows the result of application of the Preserve Above (PA) operator, where only parts of new surface *n* that lie above the central surface are preserved. B shows the result of application of the Preserve Below (PB) operator, where only parts of new surface *n* that lie below the central surface are preserved. C shows the result of application of the Preserve Between (PBW) operator, where only parts of new surfaces *nn* that lie between the central surface and the channel form *n* are preserved. In C, the central surface and the channel form *n* are selected as the surfaces to Preserve Between (PBW); only the parts of new surfaces *nn* that are between the selected surfaces are preserved.

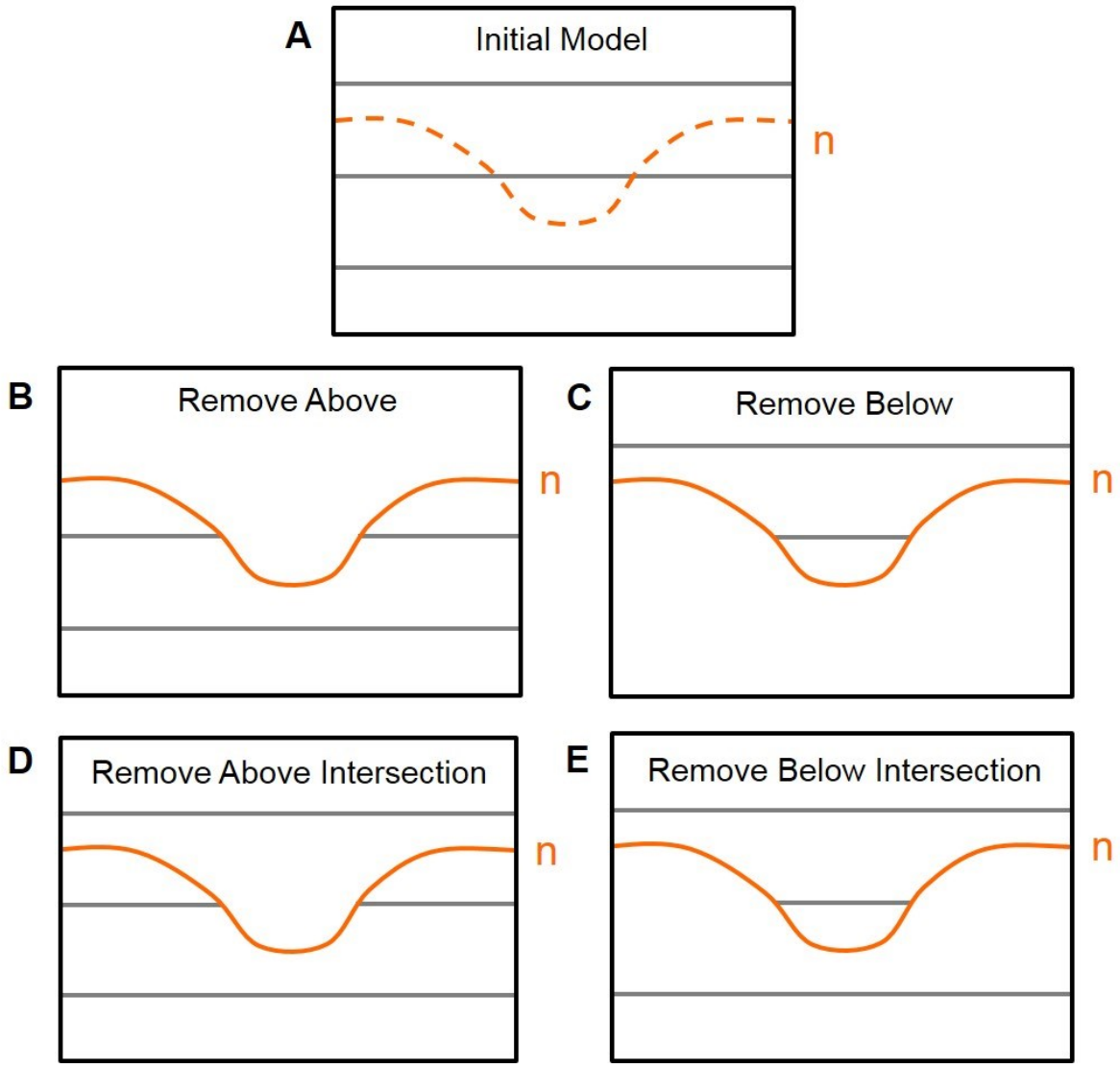

Figure 3.2. These figures illustrate operators applied to surfaces in an existing model (A) when a new surface *n* is inserted (dashed orange line). B shows the result of application of the Remove Above (RA) operator, where all surfaces that lie above *n* are removed. C shows the result of application of the Remove Below (RB) operator, where all surfaces that lie below *n* are removed. D shows the result of application of the Remove Above Intersection (RAI) operator, where only surfaces that are both above and intersected by *n* are removed. E shows the result of application of the Remove Below Intersection (RBI) operator, where only surfaces that are both below and intersected by *n* are removed.

3.4 Creating 3D models from 2D sketches

The sketching operators presented above have been defined here in a 2D sketching plane but are applied to 3D surfaces after these surfaces have been created from a 2D sketch. Three different approaches have been implemented to create 3D surfaces from 2D sketches in RRM. In all cases, the

chosen stratigraphic operator is applied in 3D to each surface after it is created, rather than to the 2D sketches.

1. Sketch the projection of the surface on multiple vertical 2D cross-sections and interpolate between the sketches. This approach is demonstrated in Case Study 3A (Section 3.5) and is suitable for sketching stratigraphic features that have poorly defined geometry between the cross-sections.
2. Sketch depth contours in plan-view. This approach is demonstrated in Case Study 3B (Section 3.6). The surface can be sketched on multiple horizontal 2D planes and then interpolated between them, thereby creating a three dimensional surface.
3. Sketch the projection of the surface onto a vertical 2D section, and then sketch a trajectory in map-view. The cross-section is extruded along the trajectory to create a 3D surface (see Jacquemyn et al., 2019). This approach is demonstrated in Case Study 3C (Section 3.7). The trajectory can be re-used to create multiple surfaces; for example, to sketch a channel form and its internal channel-fill deposits. This approach is suitable for sketching stratigraphic features that have a well-defined geometry in cross-section.

Sections 3.5, 3.6 and 3.7 demonstrate application of the stratigraphic surface operators to three geological cases of different length scales and depositional environments, using different types of data to constrain and guide sketches, and different approaches to 3D surface construction. These three case studies are presented to illustrate the flexibility and effectiveness of the operators. The operators are demonstrated here in 3D using the SBIM prototype software Rapid Reservoir Modelling (RRM), developed jointly by the author and the RRM research team at Imperial College London, Heriot-Watt University and the University of Calgary (after Jackson et al., 2015a; Section 1.6, this thesis). Videos of each case study model being constructed in RRM are provided in Supplemental Material, Videos 2, 3, 4 and 5 (Appendix 1).

3.5 Case Study 3A: Seismic-scale prototype models of deepwater channel deposits using multiple parallel cross-sections

The following example is a model guided by data comprising parallel interpreted seismic cross-sections through deepwater deposits of the Rakhine Basin, offshore Myanmar (Xu et al., 2016). The Rakhine Basin deposits are Miocene to Pleistocene in age and include submarine canyons, confined slope channel complexes, aggradational channel-levee complexes, and frontal splays (Xu et al., 2016). The seismic lines used in this study are separated by 14-19 km and are interpreted to progress from a more proximal to a more distal location along the axes of confined slope channel complexes (Xu et al., 2016). The aim of SBIM here is to prototype a plausible 3D geometric model of confined slope channel complexes (*sensu* McHargue et al., 2011) from three 2D cross-sections (Figure 3.3A) following the interpretation of Xu et al. (2016). The complexes are strongly confined in the proximal cross-section, but show a greater degree of lateral offset in the distal cross-sections (Xu et al., 2016), which introduces uncertainty in the correlation of individual channel complexes between the cross-sections.

An initial prototype model was made based on the interpretation of Xu et al. (2016) which consists of four stacked channel complexes. The published seismic cross-sections are used as a base on which to build our prototype model. The operators allow us to work in any order, but here the interpretation moves from stratigraphic base (oldest) to top (youngest). The steps of the model construction are shown in Figure 3.3B-C and a video of the model construction process is provided in the supplemental material (Appendix 1; Supplemental Material, Video 2).

No operators are required to create the lowermost channel complex base surface, which extends across the model and does not interact with any existing surfaces. The surface is sketched on three parallel cross-sections and the software creates a surface by interpolating between each sketch, thereby creating a 3D model. The lowermost channel complex base surface is sketched on cross-section 1, representing a proximal location, and then sketch the surface again on cross-sections 2

and 3, which represent distal locations. The surfaces are correlated by the user, based on interpretation of each seismic cross-section. Correlation is non-unique and the user may consider building models for different correlations. The interpretation moves from proximal (cross-section 1), where there is more confidence, to distal (cross-section 3), where there is greater uncertainty in the interpretation (Figure 3.3B; Appendix 1; Supplemental Material, Video 2).

Once the lowermost channel complex base surface is in place, stratigraphically younger channel complex base surfaces are interpreted using the operator RAI. This operator prevents overlapping of surfaces by removing any segments of existing surfaces that lie above a new surface, in this example effectively simulating erosion. Again each surface is sketched on the three parallel cross-sections (Figure 3.3C; Appendix 1; Supplemental Material, Video 2). In cross-section 1, the second channel complex base surface is interpreted to occupy the existing lowermost channel complex base surface, indicating pronounced lateral confinement in proximal slope locations. In cross-sections 2 and 3, the second channel complex base surface is interpreted to be laterally offset from the lowermost channel complex base surface, indicating less lateral confinement in more distal locations on the slope. In a matter of minutes, a 3D prototype model of Xu et al.'s (2016) interpretation of the proximal to distal geometry of four channel complex base surfaces has been created from an interpreted correlation between the seismic cross-sections (Figure 3.4A). Using the same approach, multiple scenarios can be prototyped for how the channels are correlated from proximal to distal, with an alternative prototype model shown in Figure 3.4B. Interpolation of the channel complex base surfaces between sparse cross-sections results in low sinuosity plan-view geometries for the channel complexes (Figure 3.4), which is consistent with conceptual models and examples of such features (e.g. Mayall et al., 2006; McHargue et al., 2011).

The operators can be applied at multiple hierarchical levels; therefore, the same operators can be used to add stratigraphic detail to the internal architecture within individual channel complexes (Figure 3.5; Appendix 1; Supplemental Material, Video 3). The individual channel complex to be

interpreted are selected using the operator PBW to define the volume to sketch within. The RA operator is then used to sketch surfaces representing individual channel elements (*sensu* McHargue et al., 2011) within the channel complex (Figure 3.5A). Within the volume of the channel complex, the channel elements are interpreted to display a disorganised stacking pattern in which there is no systematic lateral or vertical arrangement of successive channel elements, as implied by the geological interpretations of Xu et al. (2016). Interpolation of the channel element bounding surfaces between sparse cross-sections results in low sinuosity plan-view geometries for the channel elements. Typically, such channel elements are more sinuous than those demonstrated (as before e.g. Mayall et al., 2006; McHargue et al., 2011), as also implied by seismic coherency and RMS amplitude maps of the stratigraphic interval of interest (Xu et al., 2016); sinuous channel elements are not included in the model shown here but could be incorporated by using sketched plan-view trajectories in combination with the seismic cross-sections (see Section 3.7, this thesis).

With the operator RB or RBI, a surface is also inserted representing the top of a slump or mass-transport element at the base of the channel complex, underlying the channel elements (Figure 3.5B; Supplemental Material, Video 3). Such slump or mass-transport elements are common features at the base of confined slope channel complexes, although they have variable lateral and along-axis continuity (e.g. Mayall et al., 2006).

With the method described here, combining SBIM and logical operators, it is quick and easy to prototype a range of interpretations by varying the correlation of the basal surfaces of channel complexes in between the different cross-sections (Figure 3.4), or to create multiple more detailed interpretations of the internal architecture of each channel complex (Figure 3.5; Appendix 1; Supplemental Material, Video 3). The user can quickly create a range of prototype models to test different proximal-to-distal correlation concepts. Additionally, the user can modify the prototype model out of stratigraphic order, for example to add internal details within channel complexes.

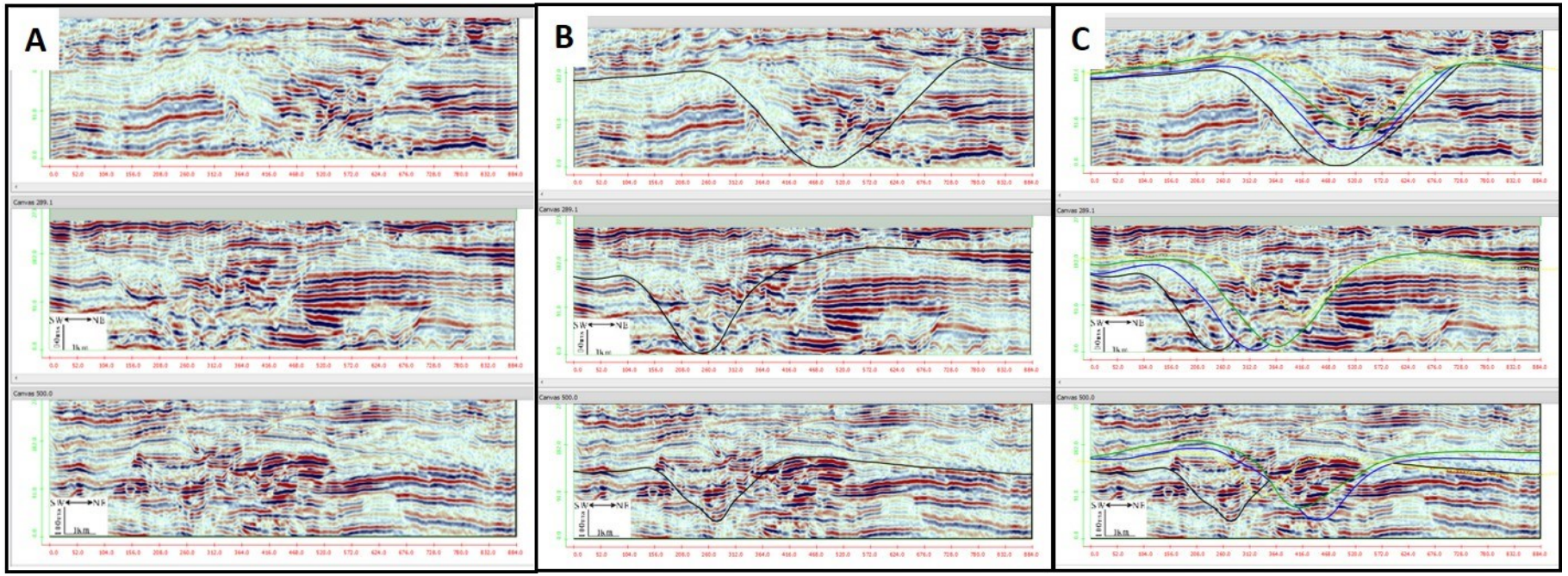

Figure 3.3. Illustration of steps for model construction from parallel seismic cross-sections of deepwater deposits from the Rakhine Basin, offshore Myanmar (Xu et al., 2016). The seismic cross-sections are loaded into the RRM software (A) based on their physical position from proximal (top) to distal (base). Each seismic cross-section has dimensions of ~400 m by 10 km, and seismic cross-section have 14-19 km spacing between them (Xu et al., 2016).X, y and z dimensions are not shown at the same scale, for visualisation purposes. Channel-complex base surfaces are interpreted and modified on each cross-section, sketching from base to top using the operator RAI. In B, the lowermost channel complex base surface is shown (black) in each cross-section. In C, three additional channel complex base surfaces are added. The resultant model is three-dimensional and honours the seismic cross-section data, and is shown in Figure 3.4A. A video of the prototyping is described in Appendix 1 and shown in Supplemental Material, Video 2.

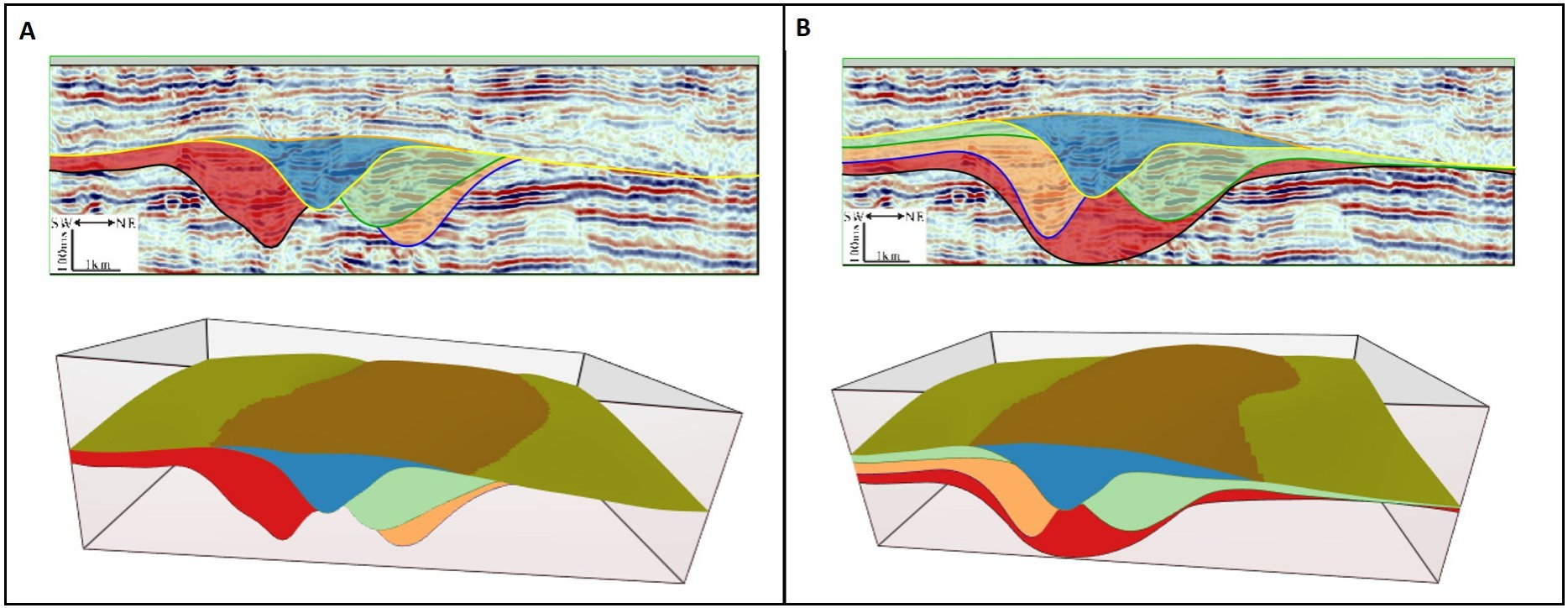

Figure 3.4. Illustration of prototype model construction from parallel seismic cross-sections of deepwater deposits from the Rakhine Basin, offshore Myanmar (Xu et al., 2016). In A, we show the result of the modelling process from Figure 3.3 using the distal seismic cross-section. This is the interpretation shown by Xu et al. (2016). In B, we show an alternative prototype model of the proximal to distal correlation of channel complex base surfaces. These alternative models were made in minutes and can be used to test different geological concepts and correlations.

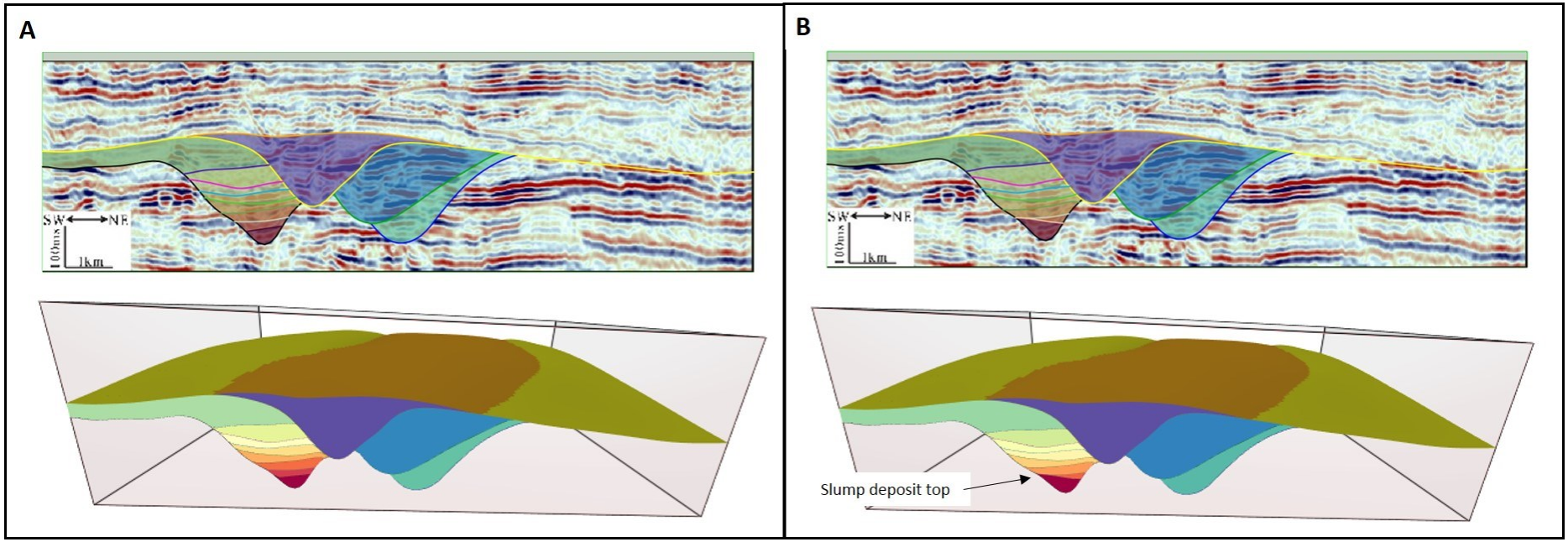

Figure 3.5. Illustration of updates to prototype model constructed from parallel seismic cross-sections of deepwater deposits from the Rakhine Basin, offshore Myanmar (Xu et al., 2016). The original model of Xu et al. (2016) is used as the initial model (Figure 3.4A). This model is then modified by adding additional architectural detail to the lowermost channel complex. Using the operator Preserve Between, we select the lowermost channel complex and add channel elements (A). Then, using the operator Remove Below, we add a slump deposit top at the base of the channel complex. The same technique could be applied to other channel complexes in the model, or to other prototypes of the correlation. A video of the prototyping is described in Appendix 1 and shown in Supplemental Material, Video 3.

3.6 Case Study 3B: Comparative outcrop-derived prototype models of lacustrine carbonates

In this example, two prototype models are created representing contrasting interpretations of lateral and vertical connectivity of a conceptual core section through lacustrine carbonates (after Bohacs et al., 2013). Bohacs et al. (2013) characterised the late Miocene Hot Spring Limestone at outcrop in Idaho, USA, where it comprises lacustrine carbonate strata that accumulated within the Lake Idaho depositional system. Thicknesses of microbialite and grainstone stratigraphic intervals in the Hot Spring Limestone are on the order of several meters, with the intervals extending on the order of tens to hundreds of meters laterally (Bohacs et al., 2013). The strata of the Hot Spring Limestone have been used as a depositional analogue for the data-poor Cretaceous pre-salt hydrocarbon reservoirs of the South Atlantic province (e.g. Moczydlower et al., 2012; Muniz and Bosence, 2015), to provide insights into controls on reservoir architecture and connectivity. Bohacs et al. (2013; their figure 19) contrast two potential interpretations 'A' and 'B' of a hypothetical core comprising alternating grainstone beds with microbialite bioherm deposits (Figure 3.6A). In Interpretation A, laterally continuous, sheet-like skeletal grainstone intervals alternate with laterally continuous, sheet-like intervals of microbialite bioherms, resulting in little to no vertical connectivity between grainstone strata. In Interpretation B, microbialite bioherm mounds and inter-mound grainstone are coeval, occur laterally in the same stratigraphic interval, and grainstone strata are thus connected vertically. The aim of SBIM here is to generate 3D prototype models that correspond to the two end-member Interpretations A and B for lacustrine microbialite and grainstone carbonates of Bohacs et al. (2013) by combining surfaces sketched on 2D vertical cross-sections (as in Section 3.5, this thesis) with surfaces sketched as depth contours in plan-view.

The prototype model of Interpretation A requires no operators. Interpretation A consists of surfaces that bound laterally continuous, sheet-like intervals, and therefore the prototype model can be made simply by extrapolating subparallel, non-intersecting surfaces sketched in any order on a 2D vertical cross-section (Figure 3.6B; Appendix 1; Supplemental Material, Video 4).

The prototype model of Interpretation B is made by sketching contours in plan-view to create the mounded surfaces that represent individual microbialite bioherms, confined within each stratigraphic interval by using the operator Preserve Between (Figure 3.6C; Appendix 1; Supplemental Material, Video 4). Starting with the surfaces sketched in Interpretation A, the region to sketch within (PBW) is selected; this region represents the stratigraphic interval within which a group of coeval microbialite bioherm mounds were developed. It is assumed that the bioherms are upwards-widening in cross-section (Figure 3.6) and approximately circular in plan-view (Bohacs et al., 2013). The lower plan-view (circular) geometry of the bioherm mound bases are sketched on a plan-view (horizontal) sketching plane positioned at the lower bound of the model volume (Figure 3.6C; Appendix 1; Supplemental Material, Video 4). The sketching plane is then moved to the upper boundary of the model volume and sketch the (larger, circular) plan-view geometry of the bioherm mound tops, using the (still visible) sketches of the mound bases as a guide (Figure 3.6C; Appendix 1; Supplemental Material, Video 4). The sketches on each plane (that essentially represent depth contours) are interpolated to generate upward-widening conical mounds of the form interpreted by Bohacs et al. (2013). This process is then repeated within a separate region to create a second stratigraphic level of coeval microbialite bioherm mounds and skeletal grainstones.

This example demonstrated how a pair of 3D prototype models representing different geological concepts can be created rapidly, including complex geometries. These prototype models serve as a starting point to investigate their implications for reservoir architecture and behaviour, for example by following the protocol for flow diagnostics outlined by Zhang et al. (2019). The model for Interpretation A would be straightforward to produce using conventional modelling techniques. In contrast, a model of Interpretation B, which includes mounded geometries with overhanging surfaces, would be possible to create stochastically with object-based modelling but would be difficult to create deterministically with standard modelling techniques. However, it is possible to quickly generate a deterministic model that contains mounded bioherm geometries using our technique of combining stratigraphic operators with sketched plan-view contours.

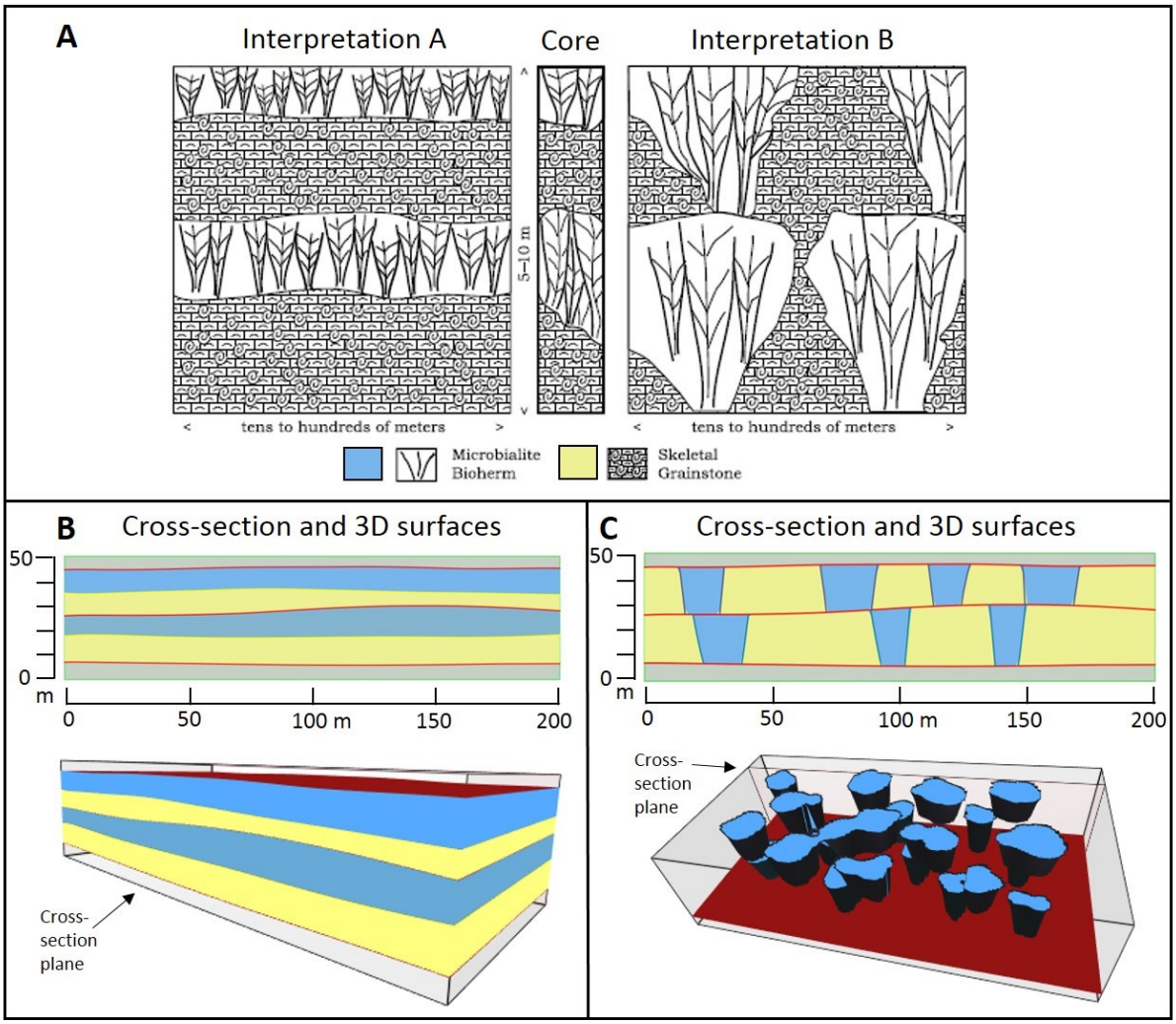

Figure 3.6. Illustration of models representing end-member Interpretations A and B for lacustrine microbialite and grainstone carbonates from Bohacs et al. (2013) (A). Interpretation A (left) comprises continuous interbedded microbialite bioherms and skeletal grainstones whereas Interpretation B (right) contains coeval mounded microbialite bioherms and skeletal grainstones. The model of interpretation A (B) shows the 3D model created from subhorizontal sketched surfaces. No operator or plan-view sketches are required to create this model because the surfaces do not intersect. The model of interpretation B (C) shows the 3D model created from the same base model as Figure B; the red top, base and central surfaces in both models are the same. To create interpretation B, the top and central surfaces were selected to Preserve Between (PBW). The sketching plane was then moved up and down vertically and circles were drawn in the plan-view to create the mounded geometries.

3.7 Case Study 3C: Comparative well-based prototype models of fluvial point-bar sandstones

In this example, two alternative prototype models of fluvial point-bar deposits are produced, based on a correlation panel of facies logs from wells, with the correlation style guided by a seismic time-slice map (Figure 3.7A-B). The data are taken from part of a fluvial reservoir composed mainly of

point-bar deposits in a single meander-belt sandbody (Colombera et al., 2018). Such sandstone reservoirs host significant resources (e.g. McMurray Formation, Athabasca heavy oil province), but their heterogeneity is difficult to characterise in subsurface data and to capture in reservoir models (e.g. Fustic et al., 2013; Martinius et al., 2017; Colombera et al., 2018). The seismic time-slice map (Figure 3.7A) shows a set of curved surfaces within the meander-belt sandbody, which correspond to successive positions of the point bar on the inner bend of the meander during its evolution. The wells each contain thin (<1 m) mudstone-prone intervals within the meander-belt sandbody (Figure 3.7B); outcrop analogue data indicate that such mudstone-prone intervals lie along point-bar accretion surfaces (e.g. Fustic et al., 2013; Martinius et al., 2017). However, the distribution and extent of mudstone-prone intervals between wells is uncertain, because they are poorly sampled by wells and are too thin to be directly imaged in seismic data. The aim of SBIM here is to generate two prototype models that correspond to end-member interpretations of mudstone-prone interval extent, by using surfaces sketched on a 2D vertical cross-section and extruded along a sketched plan-view trajectory. The first model tests an interpretation in which there is little or no sandstone connectivity between wells due to laterally extensive mudstone-prone intervals along point-bar accretion surfaces; the second model tests an interpretation in which there is a high degree of sandstone connectivity between wells due to mudstone-prone intervals of limited lateral extent.

To create a common stratigraphic framework for both models, the top and base surfaces of the meander belt that represents the reservoir interval are defined; no operators are required as the surfaces do not intersect. Both prototype models use the same top and base surfaces, and thus have the same volume. Next Preserve Between (PBW) is used in order to ensure that new surfaces are created only between the top and base reservoir surfaces. Point-bar accretion surfaces are sketched between the wells in the channel-belt reservoir volume. First, an accretion surface is sketched in cross-section, and then a plan-view trajectory for the surface is sketched to define its 3D geometry. The same trajectory is applied to each subsequently sketched accretion surface in this prototype, but one could choose to make each surface vary in 3D by sketching new plan-view trajectories. This

process is repeated until a set of point-bar deposits bounded by accretion surfaces have been defined. The result is the geometric framework for both models (Figure 3.7C; Appendix 1; Supplemental Material, Video 5).

Mudstone-prone intervals are then added to the point-bar deposits. A region is selected to Preserve Between (PBW), bounded by two point-bar accretion surfaces and the top and base reservoir surfaces, and then the top surface of the mudstone-prone interval is sketched. The top surface of the mudstone-prone interval is automatically trimmed where it intersects the region boundaries. The process is repeated across the model, again using plan-view trajectories to extrapolate the top surfaces of the mudstone-prone interval from cross-sections into three dimensions. The user controls the shape and extent of each mudstone-prone interval as it is sketched. The result in this case is a model with laterally continuous mudstone-prone intervals above each point-bar accretion surface (Figure 3.7D; Appendix 1; Supplemental Material, Video 5).

Returning to the geometric framework (Figure 3.7C), it is used to construct a second model in which mudstone-prone intervals cover only the upper 25-30% of the point-bar accretion surfaces (Figure 3.7E; Appendix 1; Supplemental Material, Video 5). It is simple and quick to do this with the RRM approach: the previous process is repeated, but the extent of the top surfaces of the mudstone-prone intervals is changed.

In a matter of minutes, models of two end-member scenarios for the lateral extent of mudstone-prone intervals in point-bar deposits in a meander-belt sandbody have been created. Many other models could be produced quickly with this approach. For example, the cross-sectional geometries of point-bar accretion surfaces could be changed, their plan-view trajectories modified, or the distribution and extent of mudstone-prone intervals changed. As noted above for the other example applications, the resulting suite of models could be used as a starting point to investigate the impact of these heterogeneities on reservoir behaviour (e.g. via application of flow diagnostics; Zhang et al., 2019).

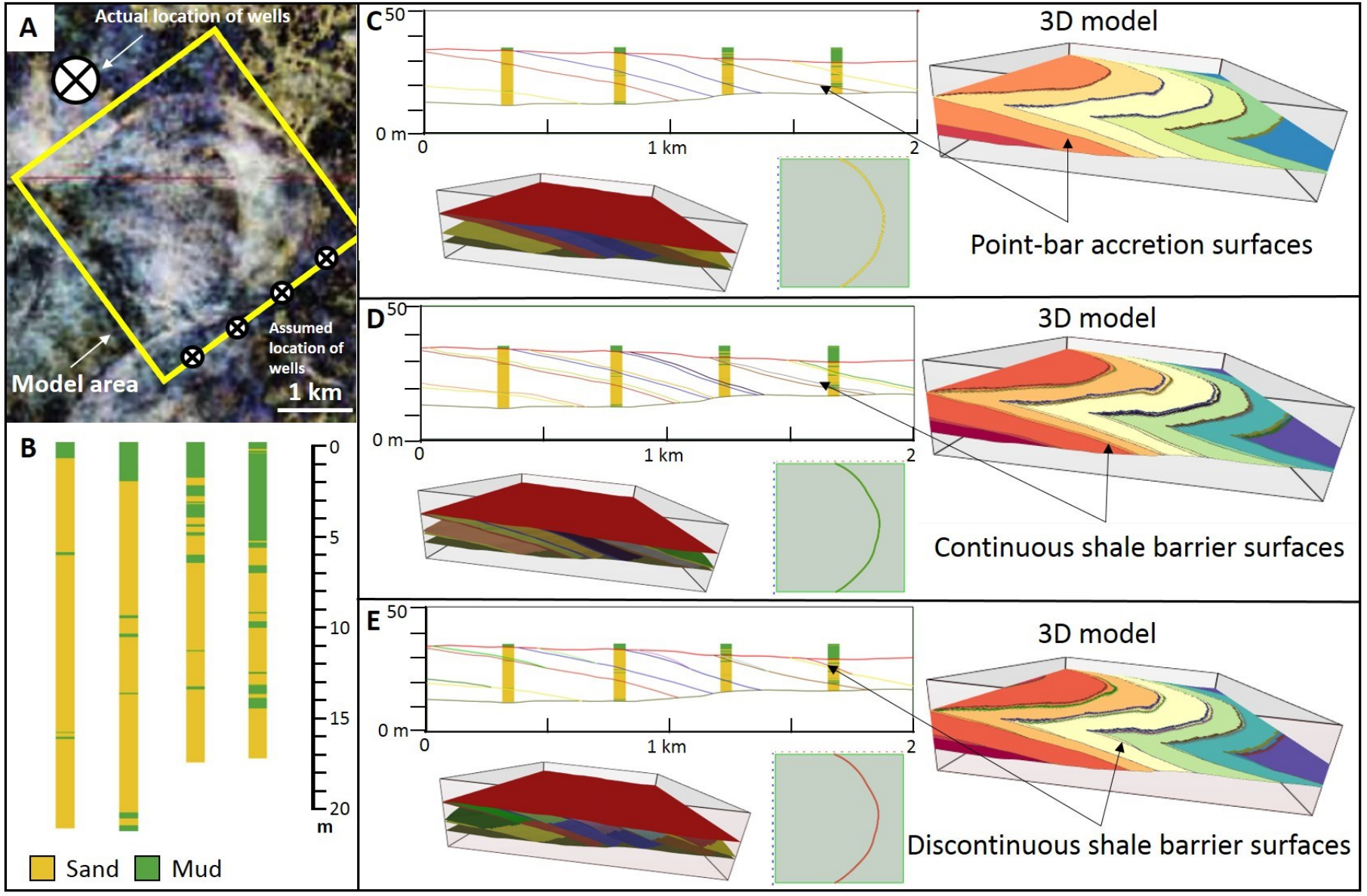
A
Actual location of wells
Assumed location of wells
Model area
1 km
B
0
5
10
15
20
m
Sand
Mud
C
50
0 m
0
1 km
2
3D model
Point-bar accretion surfaces
D
50
0 m
0
1 km
2
3D model
Continuous shale barrier surfaces
E
50
0 m
0
1 km
2
3D model
Discontinuous shale barrier surfaces

1

Figure 3.7. Illustration of models representing point-bar deposits in a meandering fluvial environment. The models are constructed over a correlation panel of facies logs (B) with sand-rich (yellow) and mud-rich (green) intervals with plan-view geometry based on a seismic time-slice map (A) (Colombera et al., 2018). The reported location of the wells from the paper is shown by the large white X on the seismic time-slice map (A); assumed locations of the wells are shown by the small white Xs along the bottom edge of the model area (A; yellow box). The correlations are based on a simple interpretation of correlated mud-rich intervals across the point-bars with assumed well separation of 500 m; the actual well separation and location data are not presented in the paper thus these assumptions were required. The models have dimensions of 2 km x 2 km x 50 m, and are shown at x10 vertical exaggeration. On the left of panels C-E, the correlation panel and sketched surfaces are shown above a 3D model of the surfaces and a plan-view map of the trajectory applied to surfaces. On the right of panels C-E, a 3D volume model is shown with colours representing relative stratigraphic depth. The geometric template used for both models (C) is constructed by defining the top and base of the meander belt. We select the area between the top and base reservoir with Preserve Between and sketch point bar accretion surfaces, applying a trajectory to each surface in plan-view to define the 3D geometry of the surfaces; this is the base geometric framework model. The trajectory and scale of point-bars is based on the seismic time-slice (A). The prototype model in D contains continuous shale barrier surfaces; these are constructed by sketching surfaces above the existing point-bar accretion surfaces using PBW. The prototype model in E contains discontinuous shale barrier surfaces; these are constructed by choosing to PBW individual point-bar accretion surfaces and sketching surfaces that intersect the lower point-bar accretion surfaces. The new surfaces are automatically trimmed to create a watertight volume between the discontinuous shale barrier surfaces and underlying point-bar accretion surfaces.

3.8 Discussion

SBIM provides a method for rapid prototyping of geological concepts. However, a “well defined set of sketching metaphors” (Lidal et al., 2013) is required to make geological SBIM possible. In this chapter, operators for SBIM of stratigraphic surfaces that are simple and flexible were demonstrated in 3D using RRM. The operators apply at any length scale, to any depositional environment, and to any data type. The three examples outlined above (Case Studies 3A, 3B, 3C; Figures 3.3, 3.4, 3.5, 3.6, 3.7; Appendix 1; Supplemental Material, Videos 2, 3, 4, and 5) demonstrate that the stratigraphic operators can be used to honour fundamental, widely used stratigraphic and sedimentological concepts such as the law of superposition, Walther’s Law, sequence stratigraphy, and facies models. The strength of our approach lies in flexibility and practicality; surfaces can be sketched in any order to reflect different interpretations, or interpretations that evolve during sketching. Additionally, in this chapter the 3D functionality of the operators was demonstrated. Multiple methods of moving from 2D sketch to 3D model add flexibility to the way models can be constructed. The benefit of our

work is that it formalises the operators in a way that easily allows for their implementation in any sketch-based modelling method. Our approach further provides modelling flexibility, because it allows rapid modification of existing models as new data are added or new geological concepts are explored without modifying the stratigraphic hierarchy or depositional order that is already in place (e.g. Figures 3.5, 3.6C, 3.7D-E; Appendix 1; Supplemental Material, Videos 3, 4, 5). In Chapters 4 and 5, similar operators that apply to structural and diagenetic surfaces will be presented.

As demonstrated above, the operators function at all scales and at multiple levels of hierarchy. However, that does not mean that RRM should be used to create a large model that covers multiple scales. To investigate multiple scales within a reservoir, it would be best to use RRM to create models of Representative Elementary Volumes (REV, e.g. Nordahl & Ringrose, 2008). One could quickly sketch REV at multiple levels within a hierarchy, simulating each level for representative flow properties, and then using those values as the model is progressively upscaled. Attempting to capture all reservoir heterogeneity in a single model across multiple scales would become very computationally intensive and would undermine the rapidity with which RRM can be used. So although it would technically be possible to create large, multiscale models with RRM, it would not be the most effective use of the software.

It is important to note that there remains room for improvement in the 3D functionality of the RRM prototype. The use of simple extrusion, though useful, is not ultimately satisfactory as a method for creating 3D surfaces. Extrusion is effectively a 2.5D process, where a surface is copied along a trajectory perpendicular to the model boundaries. A result of this is that meandering rivers cannot be properly rendered with this technique (Figure 3.7). The meander bends are cut off and the channel appears to have been shifted linearly; this is inaccurate. In order to solve this problem, a new method is under development to all 3D extrusion following a trajectory. The new extrusion method creates a vector field along which a surface is created; this allows the surface to rotate in

space as defined by the vector field. With this method, it will be possible to accurately capture the meandering of a river through the use of a cross-section and vector-field extrusion.

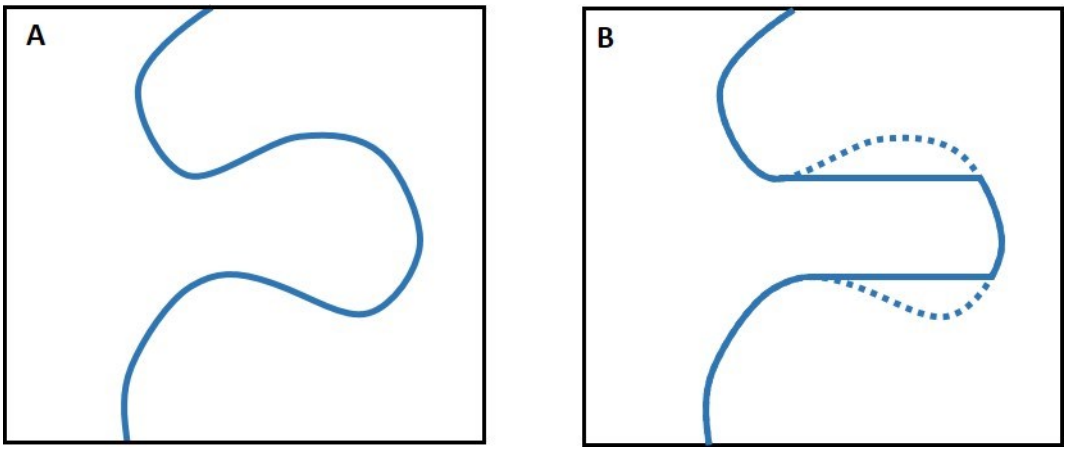

Figure 3.8. Schematic figure showing a pair of plan-view river trajectories as originally sketched (A) and as rendered in RRM (B). A) shows a series of meander bends sketched in a trajectory window of RRM. B) shows how that meander would be rendered in RRM using extrusion (solid line), where the surface is extruded parallel to the model boundaries rather than rotating along the trajectory. The original meander form that is removed using extrusion is shown with the dashed line. This results in an erroneous shape for the river trajectory. An improved version of extrusion using a vector field to rotate surfaces along a trajectory, thus eliminating this problem, is currently under development.

Although in this chapter the operators are presented in the context of an SBIM implementation, the operators have the potential to be applied to other SBM methods. Wherever surfaces intersect, regardless of the method of surface creation, their intersection must be defined so that overlapping volumes are not created (White and Barton, 1999). To ensure non-overlapping volumes, model construction can follow purely stratigraphic ordering of surfaces, from oldest to youngest (e.g. Pyrcz et al., 2005), purely hierarchical ordering of surfaces, from large scale to small scale (e.g. Sech et al., 2009), or a combination of stratigraphic and hierarchical ordering (e.g. Massart et al., 2016a). It is possible to apply the operators demonstrated in this chapter to previous SBM approaches, as shown in Section 2.11.

Jacquemyn et al. (2019) used the operators as information contained within metadata for surface-based models built from parametric (non-uniform rational B-splines (NURBS)) surfaces across different levels of a stratigraphic hierarchy. The metadata describe how one or more operators are

used to define surface interactions, such that the resulting model creates watertight, non-overlapping volumes. The benefit of this approach is that many models can be created both stochastically and automatically, provided that each surface has its metadata defined prior to model creation. In contrast, in the SBIM approach described here, each surface is sketched, but there are no specific constraints on the surface itself a priori (e.g. hierarchical level, interpreted stratigraphic surface type). Each surface interacts with existing surfaces in the way that is defined by the selected operator and the geometry of the model; this requires that operators are applied as each new surface is sketched. The result is that our approach allows the user to construct a model "on the fly," without a model definition prior to sketching. This approach allows flexibility in the way models are created, as well as allowing flexibility in the type of models that can be created. Additionally, existing models can be readily updated.

Our approach, combining operators with SBIM implementation, is not designed to replace existing reservoir modelling software packages. Instead, our modelling approach allows rapid prototyping of a range of model concepts in order to select those that are useful for further investigation. For example, our method could be used where there are limited seismic data and a range of models are desired, or when working in the field creating a model based on outcrop observations. In both cases, the benefit of our approach is being able to work intuitively as one would when creating a paper sketch or conceptual block diagram, with the result of that sketch being a 3D model that could be used to make volumetric calculations or as a basis to analyse flow (e.g. Zhang et al., 2019). SBIM is geologically intuitive, because sketched surfaces are used to conceptualize and communicate geology in fundamental tools such as maps, cross-sections and block diagrams. This aspect of SBIM is augmented by our stratigraphic operators, which provide a flexible framework for any future SBIM method. In addition to applications in the exploitation of hydrocarbon, mineral and groundwater resources, such as cutting cycle times and improving the accuracy of resource estimation, there are clear applications of SBIM in education; for example, in developing students' skills in visualizing and testing geological interpretations in the classroom and field.

3.9 Conclusions

The stratigraphic operators presented in Chapter 2 have been implemented in 3D in the sketch-based modelling program Rapid Reservoir Modelling (RRM). The three case studies presented here demonstrate the applicability of the stratigraphic operators to three different geological settings (deepwater slope systems, lacustrine carbonates and fluvial point-bar deposits) with three different data types (seismic, outcrop and wells) and with three different methods for creating three-dimensionality (multiple cross-sections, plan-view contours and applied trajectories).

Case Study 3A demonstrated that multiple 3D models of deepwater slope system deposits can be quickly and easily produced using RRM by varying the correlation of basal surfaces. Deepwater slope system 3D models were created using the stratigraphic operators applied to surfaces across multiple parallel cross-sections. These models show that additional detail (e.g. interpretation of internal channel architecture) can be added to a model once it is constructed and that geologically sound models can be created when sketching surfaces out of stratigraphic order.

Case Study 3B demonstrated how a pair of 3D prototype models representing different geological concepts can be created rapidly, including complex geometries. One prototype model includes mounded geometries with overhanging surfaces; this model would be difficult and time-consuming to create with standard modelling techniques. However, these 3D mounded bioherm geometries were created rapidly in RRM using the technique of combining stratigraphic operators with sketched plan-view contours.

In Case Study 3C, models of two end-member scenarios were created to model the lateral extent of mudstone-prone intervals in point-bar deposits in a meander-belt sandbody. The prototype models were based on vertical well data and a seismically derived map, and 3D geometries and were created by combining sketched cross-sections with plan-view surface trajectories. The prototype

models were produced in minutes; other models could also be produced quickly with this approach. For example, the cross-sectional geometries of point-bar accretion surfaces, their plan-view trajectories, or the distribution and extent of mudstone-prone intervals could all be modified.

All case study prototype models serve as a starting point to investigate their implications for reservoir architecture and behaviour. The power of the stratigraphic operators implemented in RRM is the speed and simplicity with which the models were created and modified. Various prototype models of an area of interest can be made quickly, and the influence of the model variations can be tested. In Chapter 4, the applicability of the stratigraphic operators will be tested for structural modelling.

4 Logical Operators for Sketch-based Interfaces and Modelling of Structure in Rapid Reservoir Modelling

4.1 Summary

Structural geological surfaces are an integral part of reservoir modelling. The previous case studies presented in this thesis have been applied to stratigraphic settings without structural complications. In this chapter, the stratigraphic operators are employed in RRM to create structural models. Test cases are a conjugate fault model and a physical model of a salt-influenced passive margin. Gaps in the capability to leverage the stratigraphic operators for all 'sketch-what-you-see' structural models are identified, and future updates to RRM are recommended.

4.2 Introduction and Previous Research

Rapid Reservoir Modelling (RRM) is a sketch-based geological modelling program developed to create 'sketch-what-you-see' geological models. RRM aims to represent the final product of geological processes, rather than to model the processes themselves. For example, the stratigraphic operators presented in Chapters 3 and 4 are based on the logic required to sketch what you see; they are not designed to create forward stratigraphic models. In the same way, the goal for structural modelling in RRM is not to perform structural restorations or forward models of deformation processes, but to be able to quickly and easily sketch a 3D structural geological interpretation at a fixed point in time. Just as with the stratigraphic operators, RRM can be used to create multiple interpretations rapidly, allowing investigation of a range of structural scenarios interpreted from ambiguous data (as in the scenario-based approach of Bentley and Smith, 2008).

3D structural geological computer modelling is a topic that has been under investigation for over thirty years (e.g. Gjøystdal et al., 1985; Fagin, 1991; Hamilton & Jones, 1992; Mallet, 1992; Turner, 1992; Houlding, 1994; de Kemp & Sprague, 2003; Groshong, 2006; Matthäi et al, 2007; Caumon et al., 2009). Specific software packages have been designed to enable geologists to create structural

models (e.g. GoCAD, Move). In conventional reservoir modelling workflows, the structural framework of a reservoir is commonly constructed prior to representing stratigraphy (e.g. Bryant & Flint, 1993). Typically this structural framework consists of stratigraphic surfaces of the top and base reservoir, and major faults that offset these two surfaces. Top-reservoir and base-reservoir surfaces and major fault surfaces are typically derived from seismic mapping. Thus, the typical first step of a conventional reservoir model can be considered to be constructed by a form of surface-based modelling (e.g. Denver & Phillips, 1990; Hamilton & Jones, 1992), albeit one in which surface geometry may be inaccurately represented on a pillar grid of a certain resolution. Smaller-scale structures, such as fracture networks, are typically not represented explicitly in conventional reservoir modelling workflows.

Caumon et al. (2009) set out guidelines for 3D surface-based model construction with a focus on structural modelling. They define logical rules for building structural models, with a goal of representing faults and horizons interpreted from sparse subsurface data (Caumon et al., 2009). Although these rules are compatible with sketch-based modelling (Caumon et al., 2009), they are not explicitly designed for this approach.

A recent review of structural modelling by Wellman and Caumon (2018) provides a full presentation and discussion of modern structural modelling techniques, including the use of parametric surfaces (e.g. De Kemp, 1999), triangulated surfaces (e.g. Caumon et al., 2009), or volumetric approaches (e.g. Frank et al., 2007; Calgano et al., 2008; Hjelle & Petersen, 2011; Souche et al., 2013). Much modern structural modelling aims to probabilistically create a range of scenarios which can then be used to propagate uncertainties throughout the modelling process (Wellman & Caumon, 2018). Geological volumes and surfaces are commonly created in these techniques by the use of an algorithm and/or probabilistic method. In introducing a special issue of Mathematical Geosciences focused on 3D structural modelling, Caumon and Collon-Drouaillet (2014) state that “3D modelling still raises suspicion from some geologists who remain sceptical about mathematics and numerical

computations and instead prefer sound conceptual thinking and well-accepted methodologies implemented with paper and pencil." Naturally there are opportunities for both; what we aim to do with RRM is to provide an outlet for that inherent desire of geologists to sketch the geology they envision, as a prototype for or complement to algorithm-based methods that are predominantly used in reservoir modelling.

The RRM approach differs from the conventional structural modelling approach in three specific ways. Firstly, we aim to follow a scenario-based *deterministic* approach to model a range of different scenarios (after Bentley & Smith, 2008). Secondly, we aim to create these deterministic models rapidly through the tool of *sketching*. Thirdly, we aim to allow *flexibility* in the way a model is constructed by avoiding restrictive workflows in which structure and stratigraphy are modelled consecutively. In the previous chapters, the effectiveness of using RRM to create sketched surface-based models of stratigraphy has been demonstrated in detail. In this Chapter, I will first present the ways in which the stratigraphic operators, as currently implemented in RRM, can be leveraged to create structural models in the conventional-modelling-workflow order of faults first and stratigraphy second (Section 4.3). I will then describe how the addition of a new rule and operator, and additional modifications to the way RRM operates would allow the user to work with increased flexibility, for example interpreting first stratigraphy and then faults. With these updates, the structural model no longer has to be interpreted before the stratigraphic model – both the structure and stratigraphy can be interpreted concurrently. These updates to RRM will provide the increased functionality required to make RRM more robust for thorough 'sketch-what-you-see' structural modelling (Section 4.6).

4.3 Operators for Interactions of Structural Surfaces Using Existing Stratigraphic Operators

The operators created for sketch-based modelling of stratigraphic surfaces, implemented in RRM, can be successfully leveraged to create a variety of structural models. However, not all structural

models can be created with the stratigraphic operators. In this section, I will: (1) present the fundamental geological rule framework for structural surfaces in contrast to stratigraphic surfaces, (2) present the stratigraphic operators, (3) discuss their implementation and limitations, and (4) present two case studies in which the stratigraphic operators have been used to create 3D structural models in RRM.

4.3.1 Stratigraphic Operators: Uses and Limitations

Seven stratigraphic operators have been created to allow logical interaction of stratigraphic surfaces for sketch-based modelling (Sections 2.5 and 2.6, this thesis):

1. Preserve Above (PA) defines a target surface that a newly sketched surface(s) is generated above;
2. Preserve Below (PB) defines a target surface that a newly sketched surface(s) is generated below;
3. Preserve Between (PBW) defines two or more surfaces that describe a target volume within which a newly sketched surface(s) is generated;
4. Remove Above (RA) is used to sketch a new surface(s), above which all existing surfaces and all sections of intersected surfaces are removed;
5. Remove Above Intersection (RAI) is used to sketch a new surface(s), above which all sections of intersected surfaces are removed (and above which all existing, non-intersected surfaces are preserved);
6. Remove Below (RB) is used to sketch a new surface(s), below which all existing surfaces and all sections of intersected surfaces are removed;
7. Remove Below Intersection (RBI) is used to sketch a new surface(s), below which all sections of intersected surfaces are removed (and below which all existing, non-intersected surfaces are preserved).

These stratigraphic operators were not originally designed to model structural surfaces, however, in many instances they can be leveraged to create accurate structural models. There are a variety of structural surfaces in geology including folded strata, faults, fault zones and joints. The logic used for stratigraphic surfaces applies directly to folded stratigraphic surfaces. Any folded strata can be created with the operators defined for stratigraphy, however the implementation of the stratigraphic operators in RRM requires that surfaces be monotonic. Therefore, recumbent folds and other folds with overturned strata, though logically possible with the operators, cannot currently be sketched in RRM (Figure 4.1). Any folded surfaces that are monotonic can be created with the existing stratigraphic operators (Figure 4.1).

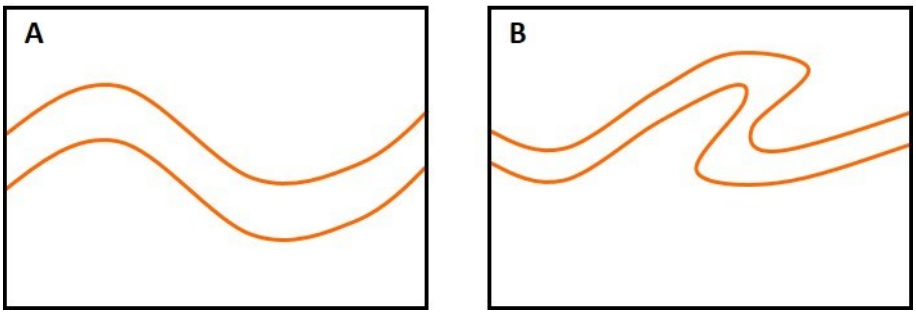

Figure 4.1. Sketch showing a pair of gently folded stratigraphic surfaces, which are monotonic (A) and a pair of recumbently folded stratigraphic surfaces, which are non-monotonic where overturned (B). Both sketches could be modelled in RRM given the logic of the operators, however, only A can be created in practice as non-monotonic surfaces are not allowed in the current software prototype.

The stratigraphic operators can be applied to fault or joint surfaces that are through-going across the model or terminate at existing surfaces (e.g. another fault surface) (Figures 4.2A and 4.2B). The stratigraphic operators cannot be applied to structural surfaces that terminate within a stratigraphic volume (e.g. where fault throw decreases to zero) (Figure 4.2C). Stratigraphic surfaces are forbidden from terminating within the model and thus, fault terminations cannot be accommodated with the stratigraphic operators.

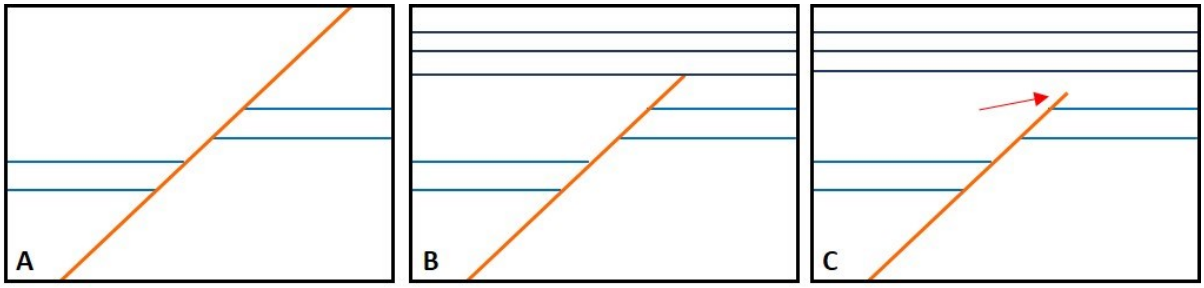

Figure 4.2. Sketch showing a pair of gently folded stratigraphic surfaces, which are monotonic (A) and a pair of recumbently folded stratigraphic surfaces, which are non-monotonic where overturned (B). Both sketches could be modelled in RRM given the logic of the operators, however, only A can be created in practice as non-monotonic surfaces are not allowed in the current software prototype.

The stratigraphic operators were designed to allow surfaces to be sketched in any order: they do not need to be constructed in stratigraphic or hierarchical order. Thus a model does not need to be interpreted prior to construction and the model can be created 'on the fly'. However, this is not true when the stratigraphic operators are applied to fault or fracture surfaces. The location of the fault or fracture surfaces will impact the order in which surfaces must be sketched using the stratigraphic operators (Figure 4.3). In Figure 4.3, the examples provided in Figure 4.2A and 4.2B are broken down into the steps required for construction using the stratigraphic operators. Flexibility remains in the way that surfaces are added by using different approaches to the order of surface addition during model construction, however there is a limit to the possibilities. For example, to create model 4.2A of a simple through-going reverse fault, there are three different paths that could lead to the resulting model (Figure 4.3A, Table 4.1). To create model 4.2B of a normal fault eroded by overlying strata, four different paths could be chosen (Figure 4.3B, Table 4.2). Therefore, some flexibility exists when applying the stratigraphic operators to these structural surfaces, but the sketching order needs to be considered at the outset of modelling when including fault and fracture surfaces.

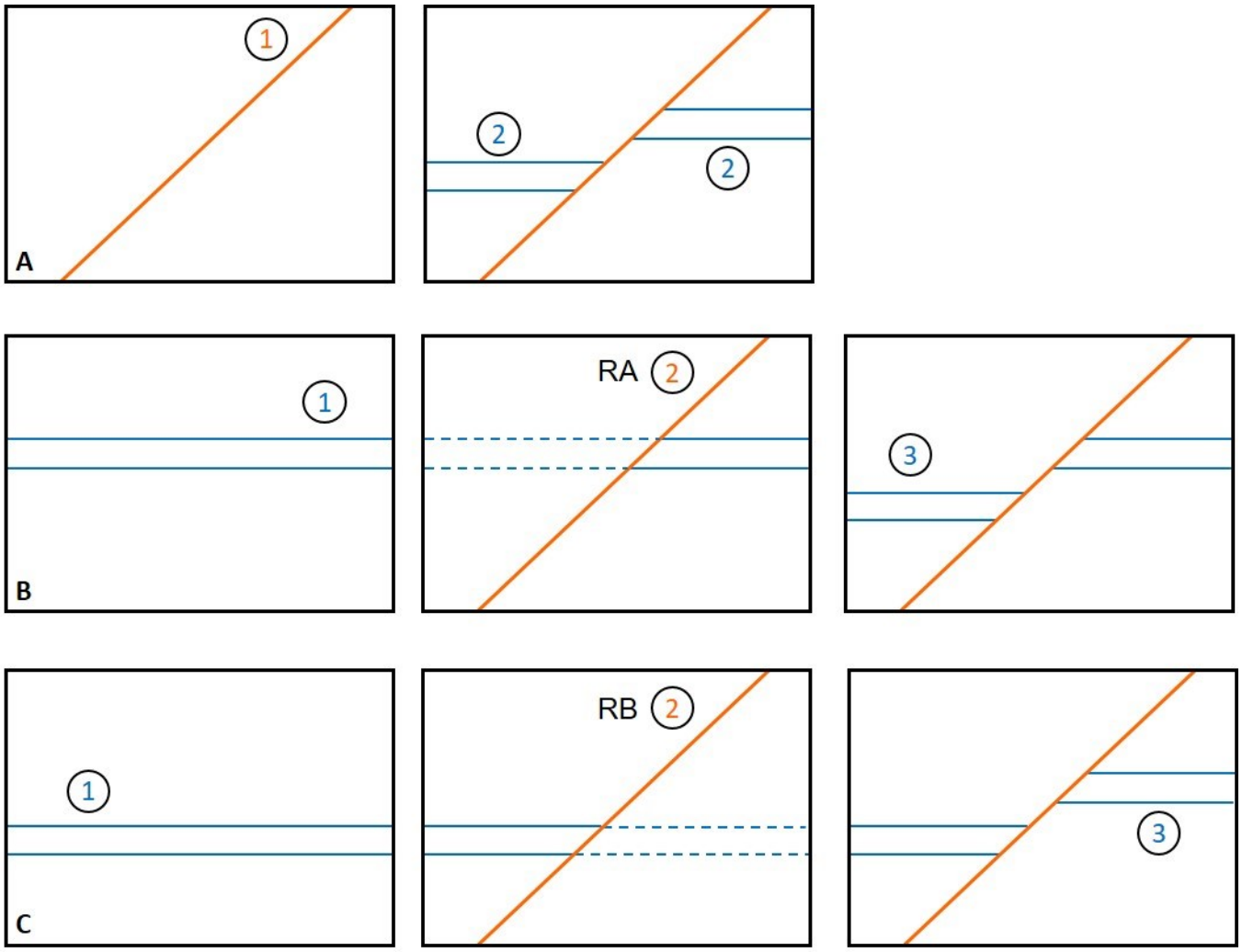

Figure 4.3. These figures demonstrate the different ways that models in Figure 4.2A (4.3A-C, above, Table 4.1) and Figure 4.2B (4.3D-G, below, Table 4.2) can be made using the stratigraphic operators in RRM. Details of each model creation pathway are shown in the tables following the figures.

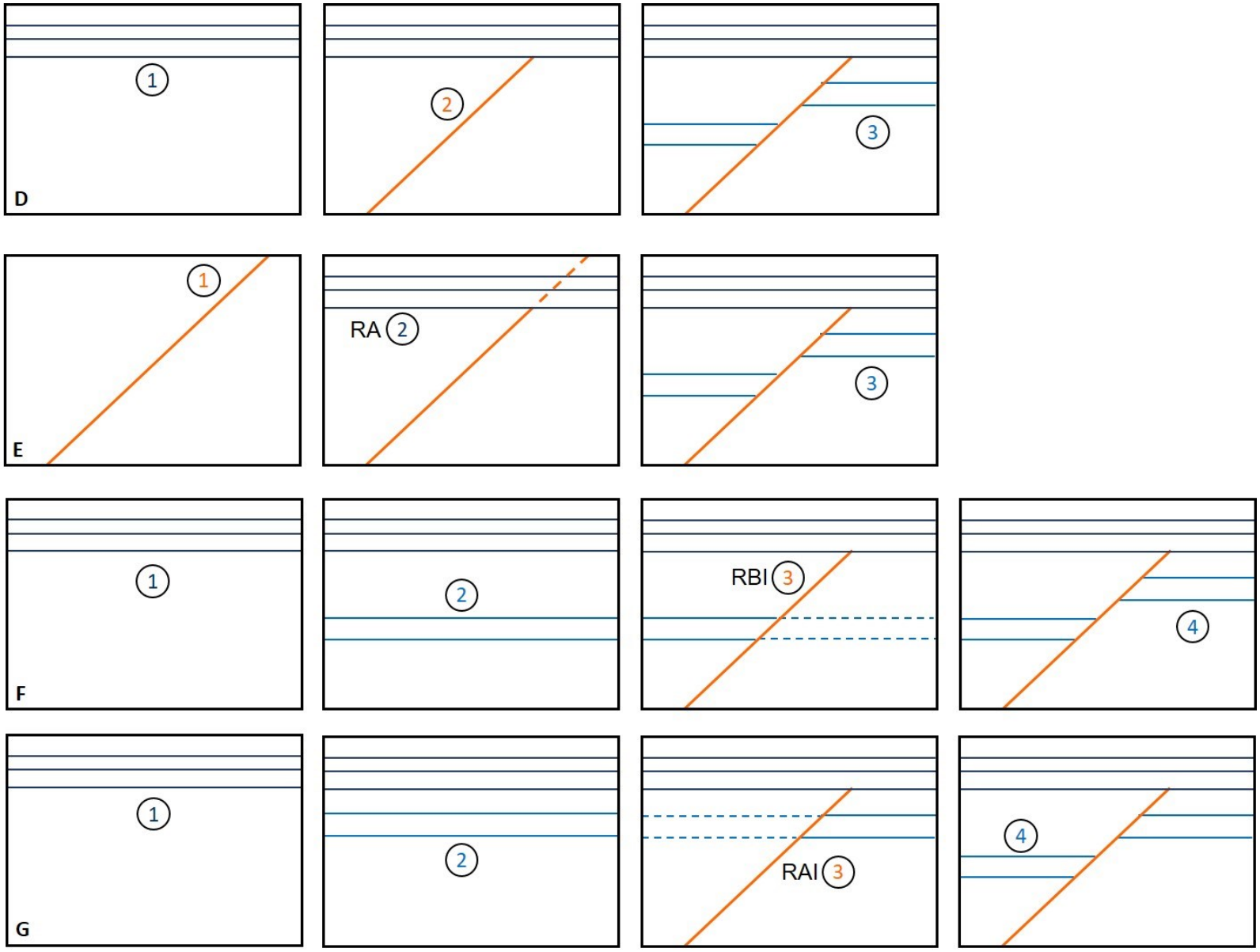
D
1
2
3
E
1
RA 2
3
F
1
2
RBI 3
4
G
1
2
RAI 3
4

	Figure 3A	Figure 3B	Figure 3C
1.	Sketch fault surface	Sketch upper stratigraphic surfaces	Sketch lower stratigraphic surfaces
2.	In any order, sketch stratigraphic surfaces terminating against the fault surface	Select Remove Above (RA), sketch fault surface	Select Remove Below (RB), sketch fault surface
3.		Sketch lower stratigraphic surfaces terminating against the fault surface	Sketch upper stratigraphic surfaces terminating against the fault surface

Table 4.1. Three different paths to create model in Figure 4.2A.

	Figure 3D	Figure 3E	Figure 3F	Figure 3G
1.	Sketch top set of stratigraphic surfaces	Sketch fault surface	Sketch top set of stratigraphic surfaces	Sketch top set of stratigraphic surfaces
2.	Sketch fault surface	Select Remove Above (RA), sketch lowermost of top set of stratigraphic surface then additional top-set stratigraphic surfaces	Sketch lower set of faulted stratigraphic surfaces	Sketch upper set of faulted stratigraphic surfaces
3.	In any order, sketch faulted set of stratigraphic surfaces	In any order, sketch faulted set of stratigraphic surfaces	Select Remove Below Intersection (RBI), sketch upper set of faulted stratigraphic surfaces	Select Remove Above Intersection (RAI), sketch lower set of faulted stratigraphic surfaces

Table 4.2. Four different paths to create model in Figure 4.2B.

Despite the caveats of considering sketching order and not allowing faults to tip out within a volume, many structural models can be made with the stratigraphic operators. The following sections demonstrate this by showing construction of 3D structural models for two examples, the first based on a conceptual NURBS-based conjugate fault model and the second based on an experimental model of a salt-influenced passive margin. Three dimensionality is achieved through the use of plan-view trajectories and multiple cross-sections (e.g. Sections 3.5 and 3.7, this thesis).

4.4 Case Study 4A: Conjugate Fault Model

The following example model is guided by a surface-based model of a simple conjugate fault system (Jacquemyn et al., 2016, 2019). The surface-based model was created to test the NURBS (non-uniform rational basis spline) modelling method designed by Jacquemyn (see Jacquemyn et al., 2016, 2019) and the IC-FERST flow simulation software developed by the Novel Reservoir Modelling and Simulation group at Imperial College London (e.g. Jackson et al., 2015b; Salinas et al., 2017; Salinas et al., 2018). The model is designed with two flat-lying, alternating stratigraphic units that are then cut by a conjugate fault set, with faults oriented at 60 degrees to each other in strike view, with opposing dip polarity, and dipping at 60 degrees (C. Jacquemyn, pers. comm.) (Figure 4.4). Conjugate faults of this geometry are a common occurrence in extensional settings (e.g. Price & Cosgrove, 1990) and are thus a good test case for the stratigraphic operators as applied to structural surfaces. Additionally, this type of model can be difficult to create and simulate using conventional reservoir modelling packages such as Petrel, particularly when surface geometries are constrained by an underlying grid (e.g. Jackson et al., 2015a; Jacquemyn et al., 2019).

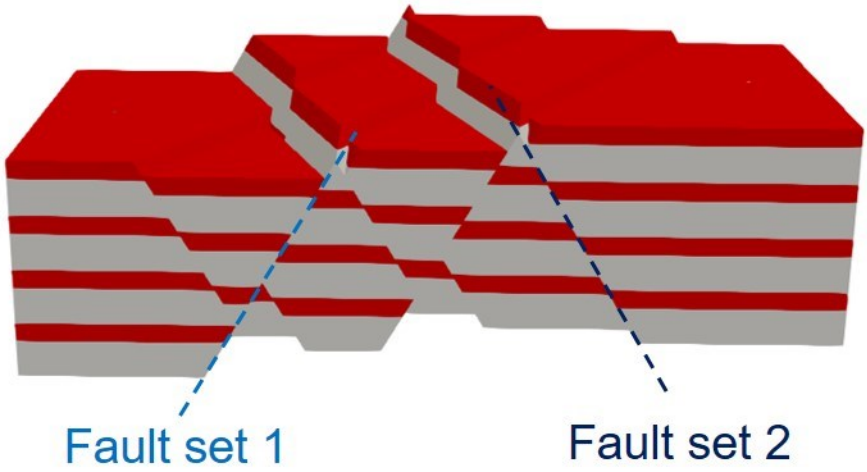

Figure 4.4. 3D model of a conjugate fault set with offset strata. The model was created by C. Jacquemyn using the IC-SERF software program and is reproduced here with permission. A fault belonging to fault set 1 is shown dipping to the left (light blue), a fault belonging to fault set 2 is shown dipping to the right (dark blue), and strata (grey and orange) are horizontal. This model forms the basis for the example case shown in Figure 4.5 and 4.6. The model has no implied scale.

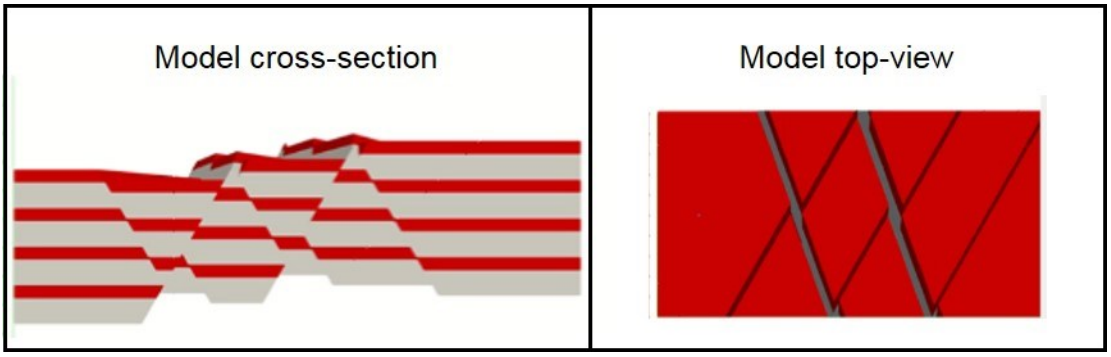

Figure 4.5. This figure shows the cross-section (left) and top-view (right) of the Jacquemyn model (Figure 4.4) that was used in RRM. These images were used to guide sketching of the model shown in Figure 4.6.

The original model was created by an algorithm and assembled from input data (Jacquemyn et al., 2016). To recreate the model by sketching in RRM using the stratigraphic operators, a single cross-section of the original model is used, combined with the original model top-view showing fault-strike orientations (Figure 4.5). As stated previously, the order of surface sketching is an important consideration when using the stratigraphic operators to create faults. This example is sketched on the cross-section view working backwards through time, beginning with the most recent set of

faults, then the earlier faults and lastly the offset stratigraphy. As a result, the most recent through-going faults (set 1) are sketched first so that other surfaces can terminate against them. After surfaces have been sketched in cross-section, the trajectory is sketched in plan-view. It is then applied to the surface and the surface adopts this orientation. This technique is used to orient the faults to match the original model (see also Section 3.7, this thesis).

To create the model, no operators are required to sketch the two youngest fault surfaces, set 1. The first fault of set 1 is sketched in cross-section and the trajectory of the fault is traced in plan-view and applied to the fault surface (Figure 4.6A; Appendix 1; Supplemental Material, Video 6A). The second fault of set 1 is then sketched; the previous trajectory is re-used so that the second fault has an identical orientation to the first fault. Fault set 1 surfaces will now be used to truncate set 2 fault surfaces. The sketching order of the two set 1 faults is interchangeable because they are parallel to each other and do not terminate against existing stratigraphy.

The operator PBW is used to create the conjugate fault set, set 2. Again, the order in which these five set 2 fault surfaces are sketched is interchangeable, but they must be sketched after the set 1 faults and before the stratigraphy. A region of the model is selected to constrain the extent of the fault surface (PBW), the fault surface is sketched, then the set 2 trajectory is traced in plan-view and applied to the fault surface (Figure 4.6B; Appendix 1; Supplemental Material, Video 6B). The conjugate fault is then created only within the selected fault block. This process is then repeated for the remaining four fault surfaces in set 2.

Again the operator PBW is used to sketch the stratigraphic surfaces. The stratigraphic surfaces are parallel and are sketched independently within each fault block; as such, the order of the stratigraphic-surface sketching is interchangeable within each fault block. The operator PBW is used to select an individual fault block, then each stratigraphic surface is sketched (Figure 4.6C; Appendix 1; Supplemental Material, Video 6C). No trajectory is applied because the stratigraphic surfaces are flat-lying. Once all strata within a fault block are sketched, another region is selected to PBW and the

next set of stratigraphic surfaces are sketched. This process is repeated for all eight fault blocks. In principle, it is possible to sketch the stratigraphy in any order within the constituent fault blocks of the model. However, in practice it most efficient to sketch the stratigraphy within each fault block, hence this was the sketching order employed here. The resultant model faithfully recreates the original model of Jacquemyn (Figure 4.6D; Appendix 1; Supplemental Material, Video 6D).

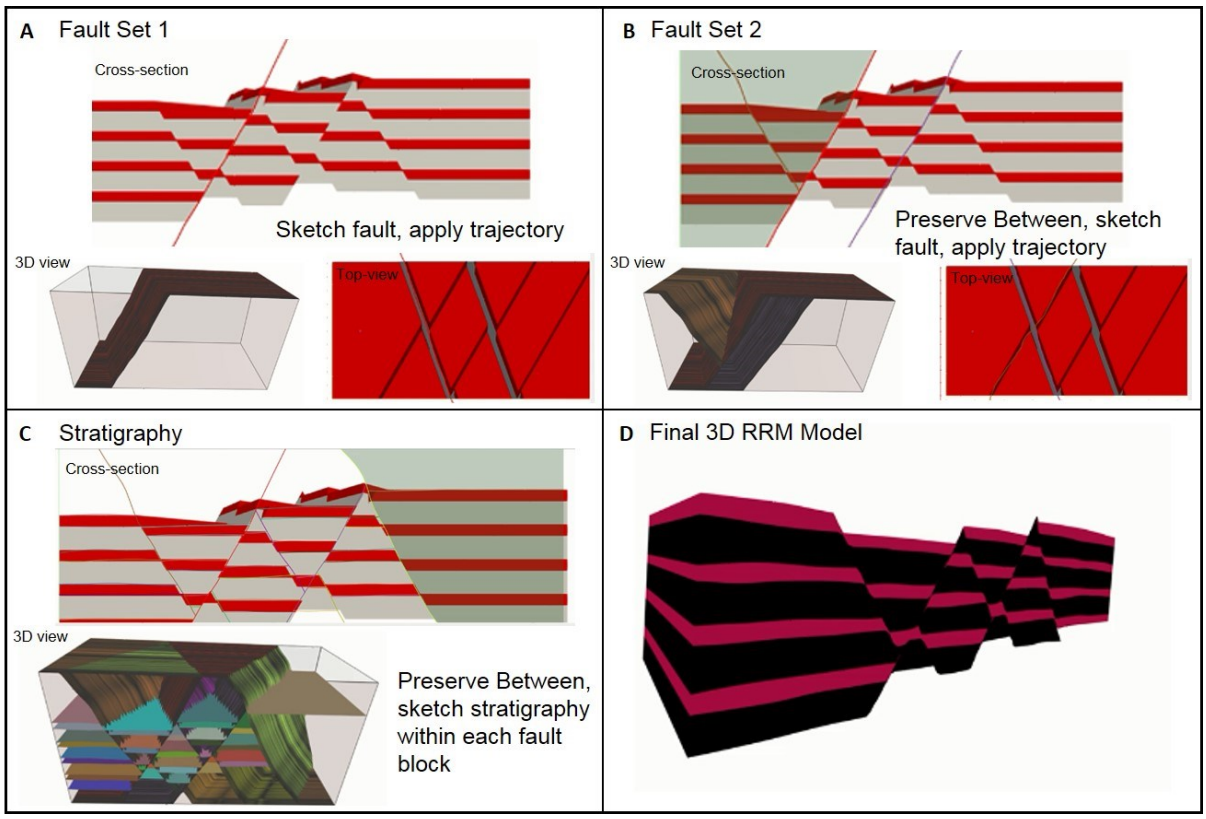

Figure 4.6. Four sequential steps used to sketch the conjugate fault model (cf. Figure 4.4) in RRM. (A) Creation of fault set 1 (two faults) with the cross-section sketching window (top), the 3D view (bottom left) and top-view (bottom right). The faults in set 1 are sketched in cross-section, then their trajectory is sketched in top-view, and finally the surface is constructed and shown in the 3D view. (B) Creation of the conjugate fault set 2 (five faults). First the existing fault block that contains each fault in set 2 is selected using Preserve Between (green shaded region in cross-section). Then the faults in set 2 are sketched in their respective region of the cross-section with the trajectory sketched in the top-view. Finally, the surface is constructed and shown in the 3D view. (C) Creation of stratigraphic surfaces. Once the faults have been created, each fault block can be selected as the region to Preserve Between. The stratigraphic surfaces are then sketched within each fault block. In Figure 4.6C, fault blocks on the left already contain stratigraphic surfaces, as seen in the 3D view (bottom). The furthest right fault block is selected (green shaded region in cross-section) and stratigraphic surfaces are sketched. (D) Final model created in RRM; a 3D conjugate fault model was constructed using only the stratigraphic operators by considering the sketching order carefully before modelling. A video of the prototyping is described in Appendix 1 and shown in Supplemental Material, Video 6.

This conjugate fault model example has demonstrated how the stratigraphic operators can be applied to structural surfaces. This required that the sketching order be constrained; future structural operators could be created to allow more flexibility in the sketching of faults (see Section 4.6, this thesis). In order to improve the usability of RRM for structural purposes, it may be useful to have 1) the ability to input a map orientation (e.g. 060), 2) a linear guide to create straight lines, 3) the ability to select top and base points and extrapolate a surface between them and 4) the inclusion of template surfaces. Inputting a map orientation could be preferable to sketching the trajectory on the plan-view window if a model was created from detailed field measurements (e.g. Amorim et al., 2014). It is still useful to be able to sketch the plan-view trajectory directly, for example in a scenario where a fault trace bends over the modelling area. For occasions when a flat surface is appropriate, it may be useful to have a linear guide to create straight lines when sketching. An alternative, but similar, approach to a linear guide would be the ability to sketch the location of the top and base of a surface and interpolate linearly between points. Template surfaces could be useful in the conjugate fault model, for example. The user may want to copy and paste a particular fault geometry; creating a reusable template surface could increase the efficiency of sketching. The various sketching tools listed above would increase user-controlled flexibility in sketching models.

Another limitation of the current RRM software is that surfaces are required to extend to the model boundaries. Therefore, there are volumes above and below the modelled strata that exist within the model volume, but are not desired for the final model. They are visible in Figure 4.6B and 4.6C as green shaded areas above and below the model.

There is no inherent relationship between stratigraphic surfaces across the different fault blocks. Each stratigraphic surface segment is treated as unique by the RRM software, rather than as part of a single unit that was truncated by faults. This feature can be useful in models for which there is little information and the user would like to retain flexibility in the way stratigraphic correlations are made across faults. Conversely, this feature can be frustrating if the user knows the stratigraphic

correlations across faults with a high degree of confidence. It is important to allow ambiguity in RRM so that the user is free to interpret their own across-fault stratigraphic correlations, rather than having them determined automatically by the software. Once the surfaces are sketched in RRM, it is possible to group the regions into domains. In this example, the individual stratigraphic units would be grouped into one of two domains to match the original model of alternating stratigraphic units (grey and orange in Figure 4.5). In the future, it would be beneficial to be able to tag segments of the same stratigraphic surface to interrogate offsets across faults, as discussed further in Section 4.6.8.

4.5 Case Study 4B: Salt-influenced Passive Margin Analogue Model

The second example model is constructed using three parallel cross-sections taken from a physical (i.e. sandbox) model at one point in time during a deformation experiment. The experiment was undertaken by S. Evans of the Basins Research Group at Imperial College London, and the cross-section images are used with permission. The physical model shows the basal relief and internal deformation of a salt layer, and the experiment was designed to test how sediments stack and faults propagate during translation across ramps of variable dip on a salt-influenced passive margin (S. Evans, pers. comm.). The experiment was designed with three ramps dipping at 9^{o} at the margin, 4^{o} on the slope-basin transition, and 0^{o} along the basin floor (S. Evans, pers. comm.). The sediment stack is made up of one prekinematic sand layer, a silicon layer thinning updip and syn-kinematic sediments that fill topography during the experiment (S. Evans, pers. comm.). Figure 4.7 shows cross-sections through the physical model.

The three-dimensionality of the model in RRM is created by using three parallel cross-sections (Figure 4.7) loaded into RRM in their relative position (see also Section 3.5, this thesis). Individual fault surfaces are then traced across the three different cross-sections, thereby creating a 3D model of the data. As has been mentioned previously, the order of surface construction must be determined prior to modelling in order to use the existing stratigraphic operators to create structural surfaces.

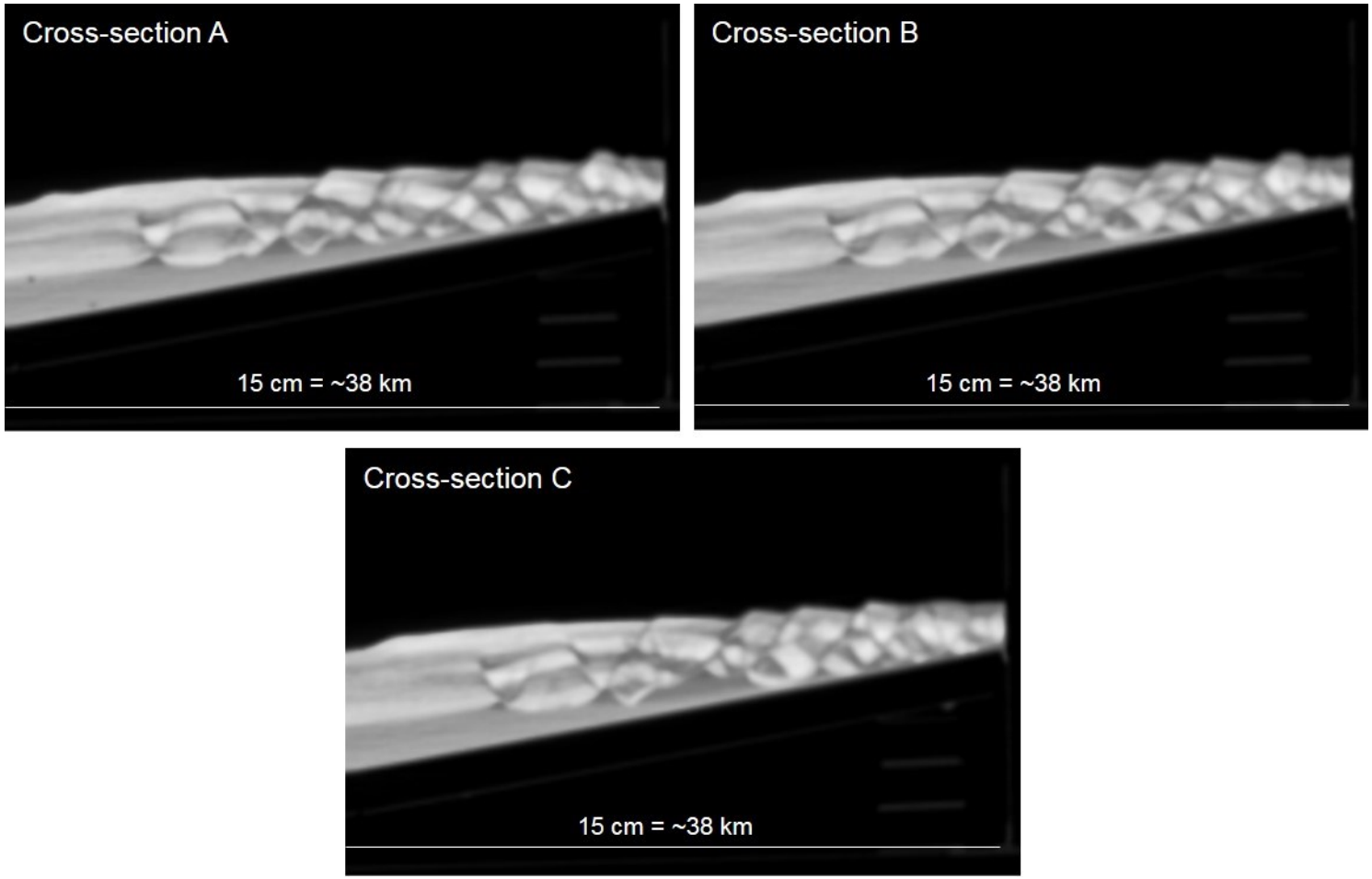

Figure 4.7. Three cross-section slices from a physical model (Evans, pers. comm.) to create a 3D structural model in RRM (Figure 4.8). The cross-sections are approximately 15cm long in real space, equivalent to approximately 38 km at the scale of analogous passive margins. The slices are spaced approximately 20 mm apart (equivalent to ~5 km). This part of the physical model is dipping basinward (left) at ~9°; a full view of the analogue-model cross-section that contains cross-section A can be seen in Figure 4.9. The cross-sections were shortened horizontally for sketching purposes.

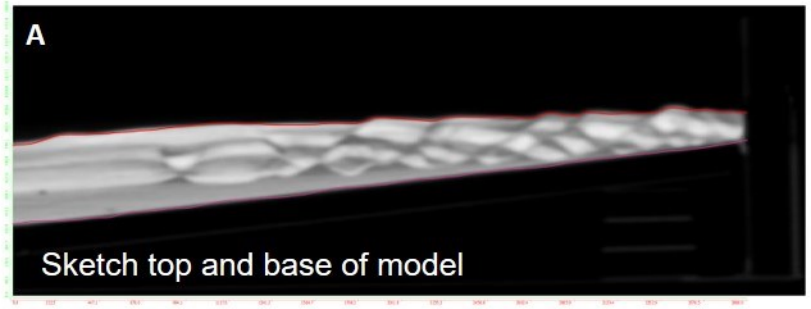
A
Sketch top and base of model

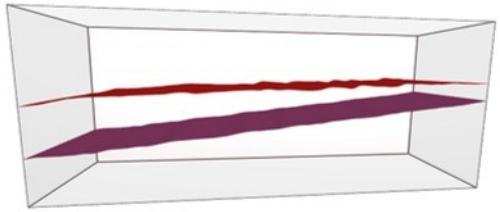

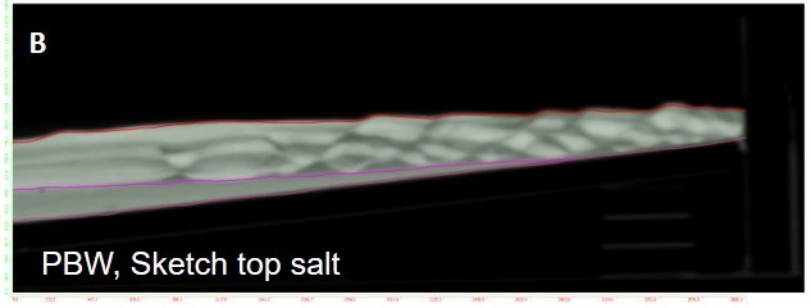
B
PBW, Sketch top salt

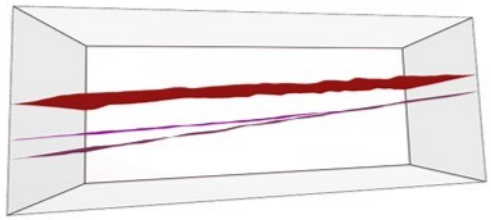

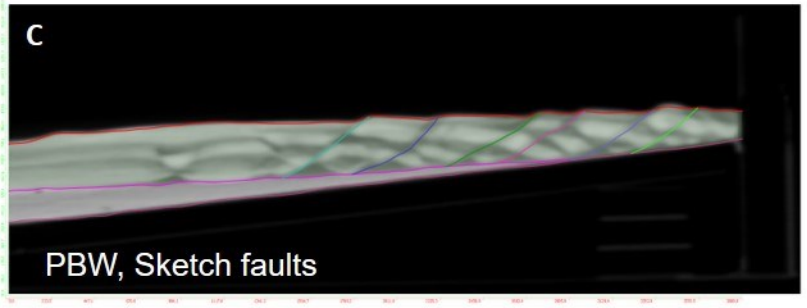
C
PBW, Sketch faults

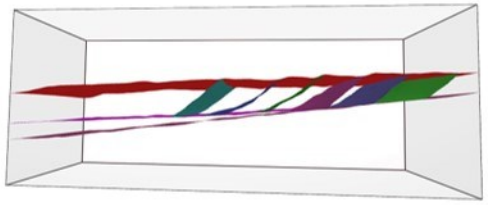

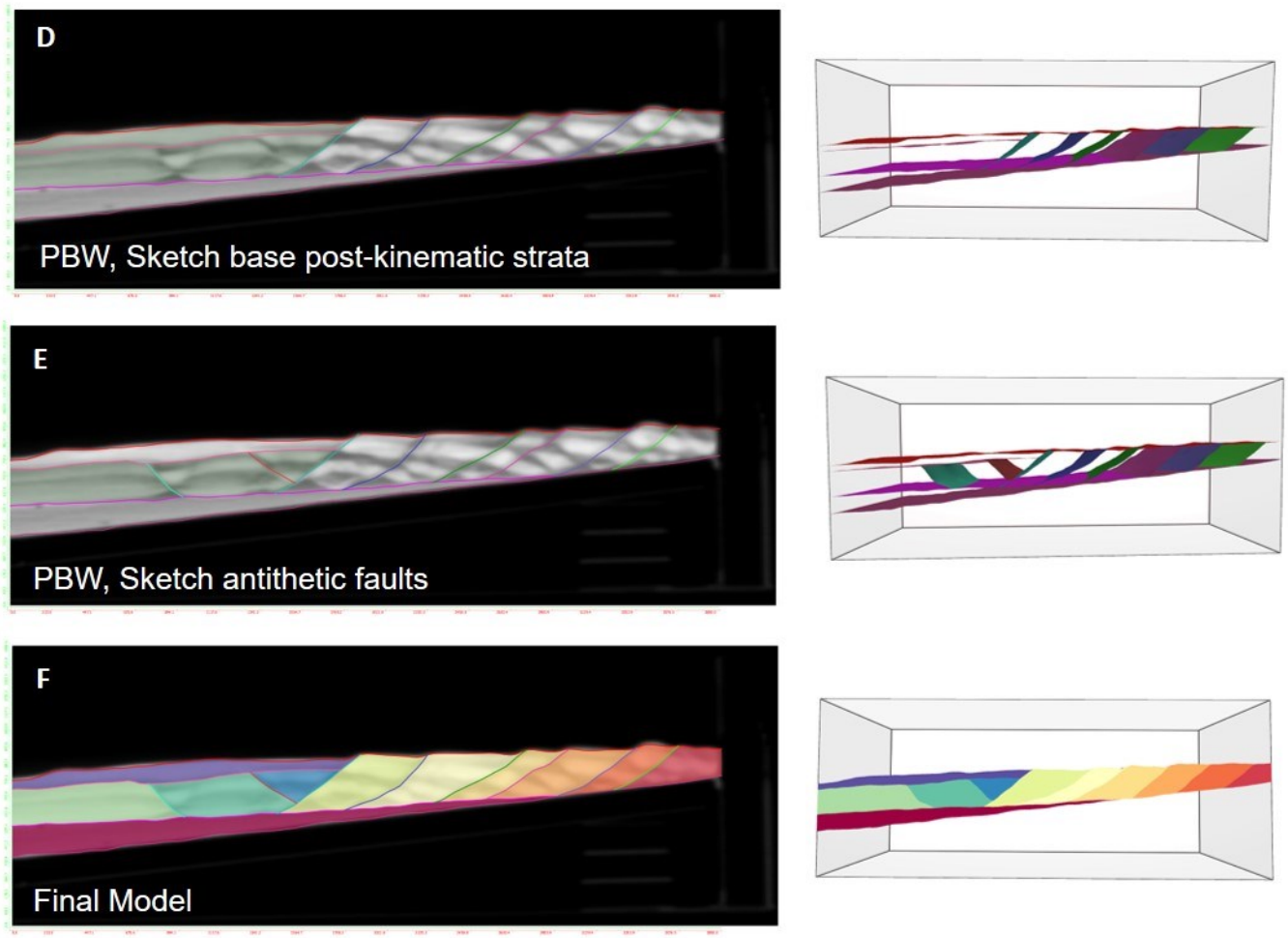

Figure 4.8. Six sequential steps used to sketch the analogue model (cf. Figure 4.7) in RRM. Images on the left show cross-section A (Figure 4.7) with strata and faults interpreted in RRM. Images on the right show the 3D volume created at each step in RRM. (A) The base and top of the model are sketched as stratigraphic surfaces. These surfaces will be used as boundaries for later sketching. (B) Creation of the top-salt surface; the base and top of the model are selected to Preserve Between (PBW, green shaded region). The top-salt surface is then sketched. (C) Six basin-dipping, synthetic faults are sketched in the

volume bounded by the three existing stratigraphic surfaces (green shaded region), which is selected using PBW. (D) The most basinward synthetic fault (dark green), the top-salt surface and the top-model surface are selected to PBW. The base surface of post-kinematic strata is then sketched. (E) Two antithetic faults are sketched in the volume bounded by fault 1, the top-salt surface, and the base surface of post-kinematic strata (green shaded region), which is selected using PBW. (F) Final model created in RRM. A video of the prototyping is described in Appendix 1 and shown in Supplemental Material, Video 7.

Figure 4.9. Complete cross-section through the analogue model (Evans, pers. comm.). The model is 39 cm in length in real space which corresponds to an analogous passive margin approximately 100 km long. The blue box highlights the basinal toe of the ramp, where salt has formed non-monotonic fold structures, which cannot be recreated in the current version of the RRM software prototype. The red box highlights possible antithetic faults (orange dashed lines) in the up-dip section. These faults are difficult to discern at the resolution of the data, and also are difficult to correlate between cross-sections (cf. Figure 4.7). Therefore they were not included in the RRM model

To create the model, no operators are required to sketch the base of the salt ramp and the top of the model, both of which are sketched as stratigraphic surfaces (Figure 4.8A). Next, the base of the salt ramp is selected to Preserve Above (PA) and the top of the model is selected to Preserve Below (PB). The top-salt surface is then sketched, also as a stratigraphic surface (Figure 4.8B; Appendix 1; Supplemental Material, Video 7). The area within these three surfaces is then selected as the area to Preserve Between (PBW). All basin-dipping, synthetic fault surfaces can now be sketched and they may be sketched in any order relative to each other. This model is sketched from left to right (Figure 4.8C; Appendix 1; Supplemental Material, Video 7). Each fault is traced on all three cross-sections before the surface is committed to (i.e. finalised in) the RRM model. Then, the next fault is traced, and so on. Six basin-dipping, synthetic faults in total are interpreted in this model (Figure 4.8C; Appendix 1; Supplemental Material, Video 7).

Antithetic faults are found in a basinward position, dipping towards the ramp. To add these to the model, a stratigraphic surface is sketched to mark the base of the post-kinematic strata above the antithetic faults using the operator PBW applied to the region defined by the top-salt, top-model, and most basinward fault (termed 'fault 1') surfaces (Figure 4.8D; Appendix 1; Supplemental Material, Video 7). The operator PBW is then used to select the region bounded by the top salt, fault 1 and the base post-kinematic strata. The two antithetic faults are now sketched (Figure 4.8E; Appendix 1; Supplemental Material, Video 7); the order in which the two faults are sketched is interchangeable. The resulting RRM model (Figure 4.8F) is a faithful 3D interpretation of the structure in Evans' physical model.

RRM can be a powerful way to add value to existing models and data. In this example, a physical model of salt-influenced deformation and sedimentation can be sketched, creating a 3D reservoir model. This RRM model was created in minutes and has the potential to be used to study how fluids move through the different units and interact with faulted strata. The work of Evans and colleagues is aimed at understanding how salt structures evolve in 4D with potential application to

understanding basin development in areas like offshore Angola and Lebanon (S. Evans, pers. comm.). The benefit of creating RRM models of the physical models is clear: the experimental data can be leveraged to investigate how the resultant geometries affect the flow of fluids within the basins.

As with the example shown in Section 4.4, it was necessary to determine the order of surfaces to be sketched prior to modelling. Structural surfaces must terminate at existing surfaces in this example, and therefore the bounding stratigraphic surfaces are sketched first. Despite the need for some surfaces to be created in a specific order, flexibility remains within the details. For example, the basin-dipping, synthetic faults could be added in any order relative to each other. In fact, one fault could be added, then stratigraphy, then another fault that removes that stratigraphy. But in this example, a more straightforward and efficient order was chosen (sketching from left to right) rather than attempting to show each permutation of surface sketching order that could be used (e.g. Figure 4.3).

Another limitation with the model shown here is that the toe of the salt ramp, located in a basinal position, was not included in the sketched RRM model. The salt folds at the toe of the ramp, and the folded base-salt surface is non-monotonic (Figure 4.9) and therefore cannot be sketched in the current RRM software prototype. As a result of this limitation, the physical model cross-sections were cropped to remove the toe of the salt ramp from the RRM model volume.

It appears in some of the cross-sections that there may be small antithetic faults in the upper left of the model (Figure 4.9). These were difficult to discern at the resolution of the physical model cross-sections, and are difficult to trace between cross-sections. Therefore, they were not included in the RRM model. However, if these small faults were deemed to be important, then the user could develop an interpretation(s) of their correlation between the cross-sections. Once the RRM software has the additional functionality of allowing faults to terminate within the model volume (see Section 4.6.2), features such as these small antithetic faults could be added simply and efficiently.

Structural surfaces must terminate against an existing surface or model when using the stratigraphic operators. However, there are places where faults should terminate within the volume of the RRM model shown in Figure 4.8. It was chosen not to represent these faults in the RRM model.

When interpreting data of low resolution, it can be difficult to decide the relative timing of different faults, although this information is needed to determine the sketching order when creating a model using stratigraphic operators. Because the relative timing of faults can be ambiguous, it would be preferable to be able to sketch multiple faults into the model at the same time. However, RRM was designed to create geologically realistic 3D models of a static volume and to do so, operators must be applied to each surface as it is sketched. Therefore, it is not possible to sketch multiple faults at once, so the interpreter is required to make a judgement of fault timing when creating the model. The flexibility of RRM, however, allows the interpreter to make an alternative model quickly if multiple structural interpretations are considered to be equally valid.

Although limitations exist when leveraging the stratigraphic operators for structural purposes, this example again demonstrates that it is possible to create a model in the current RRM software prototype with faults and stratigraphy if the sketching is done thoughtfully. Three dimensionality is achieved through using multiple cross-sections, which allows flexibility in the way surfaces are sketched and with the types of data that can be used. Sketching the model can be carried out quickly, in hours, even taking into account the need to consider the sketching order.

4.6 New operators and operations required to fully implement structure in RRM

The two example cases presented in Section 4.4 and 4.5 demonstrate that it is possible to create structural models using the stratigraphic operators, and that the stratigraphic operators are not sufficient for all structural modelling. Therefore, new structural operators and functionality are required in RRM to create ‘sketch-what-you-see’ models. In the following section, the fundamental geological rule framework required for structural surfaces is presented (Section 4.6.1). Next, the

ways that these geological rules are accounted for and what modifications can be made to the existing stratigraphic operators so that 'sketch-what-you-see' 3D structural modelling is possible in RRM is presented. These include the ability to sketch faults that terminate within a domain (4.6.2), to create non-monotonic surfaces (4.6.3), to insert faults and modify stratigraphy (4.6.4), to sketch directly on a fault plane (4.6.6), to interrogate structural information (4.6.7) and to manage the information contained within the models as they are sketched (4.6.8).

4.6.1 Geological rule framework for SBM of structure

To create operators that define the interactions of stratigraphic surfaces for SBIM, the following fundamental geological rules were set out (Section 2.4, this thesis) (e.g. White and Barton, 1999; Jackson et al., 2005; Caumon et al., 2009):

1. Surfaces cannot cross.
2. Surfaces cannot end within a domain.
3. Surfaces can either terminate against (truncate or conform) or remove (erode), existing surfaces.

These rules form the basis for the stratigraphic operators described in Section 4.3. However, they are not sufficient to capture all of the requirements of structural surfaces. The fundamental geological rules required for structural fault surfaces differ in that (e.g. White & Barton, 1999; Jackson et al., 2005; Caumon et al. 2004, 2009):

1. Surfaces can end within a domain.

Caumon et al. (2004) state that a result of the free border rule is that only fault surfaces may have logical borders not connected to other surfaces. Thus it is a requirement that structural fault surfaces can end within a domain, but only where their displacement is zero (Caumon et al., 2009) (e.g. Figure 4.2C). The result is that structural surfaces may not, by definition, create a closed, watertight volume such as those bounded by stratigraphic surfaces. However, the combined regions

surrounding a fault tip will create a watertight volume around the termination, as discussed in more detail in Section 4.6.2.

The focus for the work presented here is on fold and fault surfaces, thus joint systems and diagenesis associated with structural surfaces will not be specifically addressed here (see Section 5.2, this thesis). It is noted that structural surfaces and structurally modified stratigraphic surfaces, such as those present in folded strata, can be non-monotonic. Such non-monotonic surfaces must be allowed in the RRM software prototype if the full geological range of folds are to be sketched in 3D, as discussed in more detail in Section 4.6.3.

4.6.2 Surfaces that terminate within the model volume

The stratigraphic operators were designed to create discrete volumes, bounded by surfaces, to enable rock properties to be assigned to regions of common geological properties (e.g. Jackson et al., 2015a). As a result, it is a requirement that stratigraphic surfaces must terminate along model boundaries or against existing surfaces. This requirement cannot exist for fault surfaces where fault displacement is zero. Thus, faults must be allowed to terminate within an existing volume. If a 3D stratigraphic surface has been offset by a fault, there would be a tear in the stratigraphic surface where the fault it is present. This geometrical configuration is shown in Figure 4.10, which compiles images created by RRM collaborator J.D. Machado Silva in demonstration software, and are used with permission. Therefore, structural fault surfaces in future RRM software will need to be allowed to terminate within the model volume, and are not required to bound closed volumes.

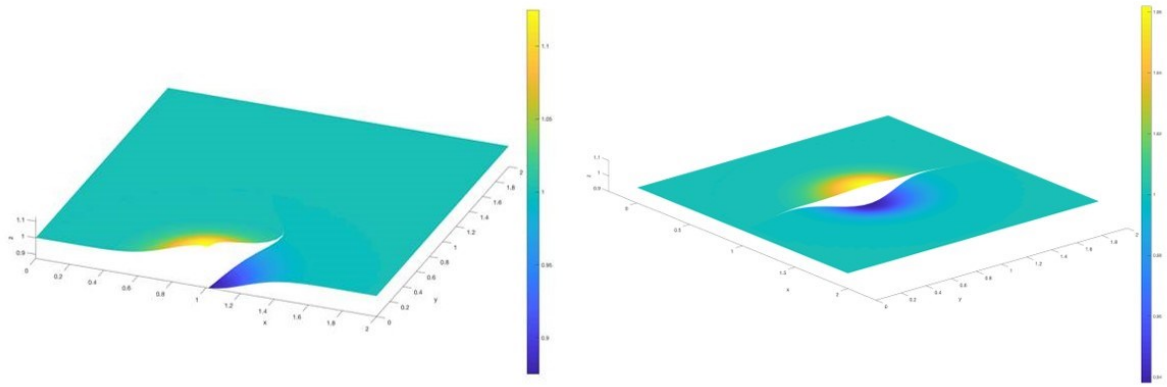

Figure 4.10. Representations of faults that offset a stratigraphic surface and terminate within the model volume (Machado Silva pers. comm.). The upper image shows a fault that partly extends beyond the model volume (i.e. the model volume contains one fault tip), and the lower image shows a fault that terminates within the model volume (i.e. the model volume contains one fault tip). The models have no implied scale, and colour shows the arbitrary depth of the offset stratigraphic surface relative to horizontal.

One way for faults to terminate within a model domain, but still fit the stratigraphic surface requirement of forming closed volumes, would be to have faults represented as volumes (i.e. fault zones). For example, a fault surface could be sketched and then automatically duplicated, with a small volume added between the two surfaces except at the fault tips where the surfaces would terminate against each other (Figure 4.11). This solution would be computationally expensive because each fault zone would likely contain many small elements for volume discretisation when it is gridded. However, there is no logical reason to preclude this option. Sketching faults as a zone also provides a mechanism for assigning flow properties directly to the fault itself, for example to model fault gouge. Representing faults as volumes would remove any need to assign transmissibility barriers to fault surfaces.

A method for using the stratigraphic operators to allow a fault termination in an existing stratigraphic volume is to include a ‘dummy’ stratigraphic surface against which the fault terminates (Figure 4.12). The volumes on either side of the ‘dummy’ surface would be assigned the same properties, and so would effectively belong to the same region. The addition of ‘dummy’ surfaces would add computational expense, particularly in gridding RRM models. Additionally, the ‘dummy’

surface would appear as an anomalous surface in the hierarchically or chronostratigraphically ordered list of surfaces generated for a model. Therefore, this solution is not satisfactory in the long-term, but is a viable option in the short-term.

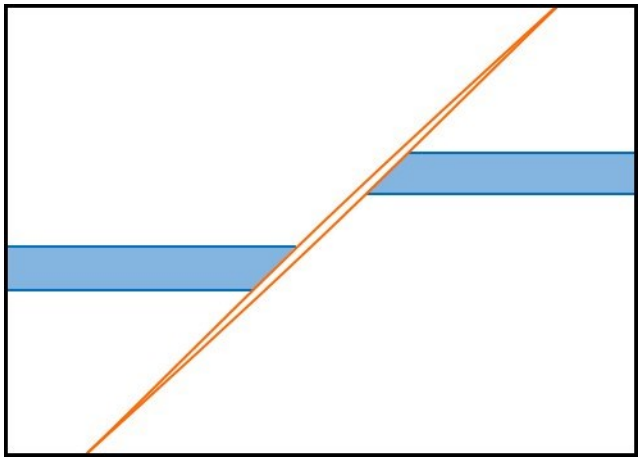

Figure 4.11. Fault represented by a pair of surfaces (orange) separated by a small volume. Rock properties could be assigned directly to the volume representing the fault volume, rather than assigning a transmissibility barrier to a fault surface, for example.

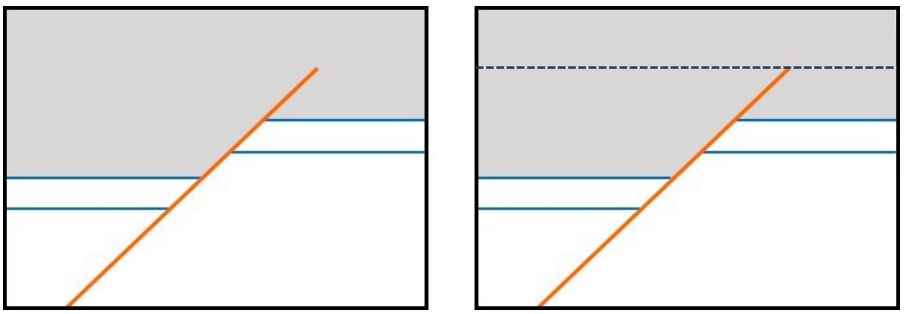

Figure 4.12. This figure shows a model that includes a fault that tips out within a region (left), which is not allowed by the stratigraphic operators in RRM. A potential solution using the stratigraphic operators would be to create a 'dummy' stratigraphic surface (dashed line in image on right). The dummy stratigraphic surface would be sketched first, allowing the fault to terminate against it. The three grey regions created by the addition of the dummy surface would be selected and grouped together in RRM, so that they are assigned the same properties.

4.6.3 Allow sketching of non-monotonic surfaces

A clear limitation of the current RRM software prototype is the inability to sketch non-monotonic surfaces. This inability is a result of the way in which the operators are implemented in the software, rather than a limitation of the logic of the operators. Provided that surfaces do not intersect, there is

no logical reason that surfaces cannot be multivalued in the z-direction (e.g. Case Study 2B), so recumbent folds or overhanging diapirs could be sketched (Figure 4.13A-B).

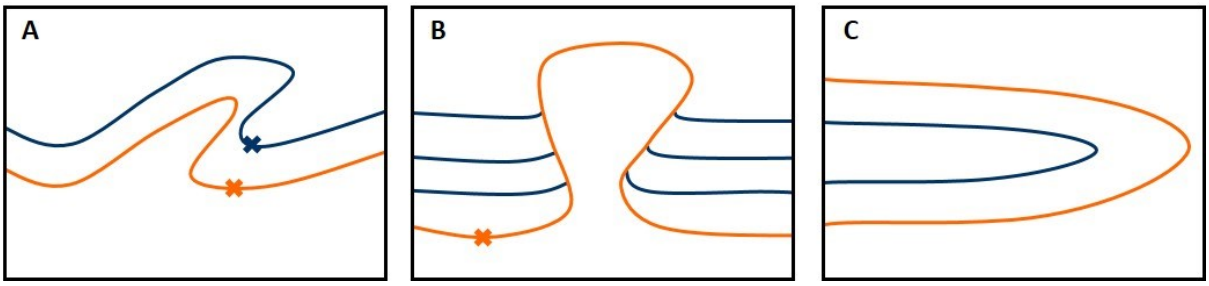

Figure 4.13. Definition of 'above' and 'below' for implementing stratigraphic operators in structurally modified settings. (A) Fold with overturned limb, in which parts of the orange surface are located 'above' parts of the blue surface in the z direction. However, by taking the lowermost point in z of each surface (orange and blue crosses), an appropriate relative position can be determined (blue above orange). (B) Diapir and flanking strata, which the diapir crest is located above the flanking strata. However, the lowermost point in z on the top-diapir surface (orange cross) is located 'below' the lowermost point in z of the flanking strata (blue cross). Thus, the diapir is determined to be below the strata. (C) Part of a recumbent fold is contained in the model volume, but additional contextual information is lacking. Consequently, the orange surface is located above and below the blue surface on different limbs of the fold. Therefore, the assignment of 'above' and 'below' to the two surfaces is ambiguous.

Where newly sketched surfaces intersect existing non-monotonic surfaces, then the software must be able to determine whether the multivalued surface(s) is above or below the new surface. A possible way for RRM to do this would be to define the lowermost point in z of each surfaces, and to use that point as a reference for comparison with other surfaces (Figure 4.13A-B). In the example cases shown in Figure 4.13A-B, the Remove Above, Remove Below, Preserve Above and Preserve Below operators could be unambiguously applied, because the lowermost point in z of newly sketched surfaces (blue) is higher than the lowermost point in z of the existing, non-monotonic surface (red). However, complications arise in the use of Remove Above, Remove Below, Preserve Above and Preserve Below operators where termination relationships are absent or recumbent-fold geometries cannot be related to pre-kinematic stratigraphic relationships. For example, Figure 4.13C shows a set of recumbently folded surfaces, some of which are entirely contained within other surfaces such that the former are simultaneously above and below the latter. In these specific

scenarios, it would be appropriate for RRM to return an error to the user stating either that they are not allowed to use the Remove Above, Remove Below, Preserve Above and Preserve Below operators for this surface, or that the user needs to provide additional (interpretative) information to remove ambiguity in the application of these operators. RRM is also able to determine relative stratigraphic age based on the ordering of surfaces, and this information can be contained in or assigned to surface metadata (see Section 4.6.8). Relative stratigraphic age is not currently utilized with the operators, but if known, it could be used rather than relative position in z. Testing of future RRM software prototypes will be key to determine how problematic these considerations are in the long term.

4.6.4 Modify stratigraphy in an existing model with insertion of a fault plane

In order to realise the full functionality of structure within the RRM software, it must be possible to deform previously interpreted strata by inserting a fault or fold. For example, a geologist interpreting seismic data might trace a package of strata that appear to be monoclinally folded (Figure 4.14A). Upon reflection, the geologist interprets that the strata are folded, but have instead been offset across a normal fault. It would be desirable for the geologist to insert a sketched fault surface, rather than having to re-sketch the stratigraphic and structural surfaces. In order to achieve this goal, fault surfaces would need to be allowed to cut stratigraphy. There would then be options for how to update the faulted strata. The strata could be:

(1) cut by the newly sketched fault surface, but retain the geometry of the initial interpretation (Figure 4.14B),

(2) cut by the newly sketched fault surface, and then re-sketched or over-sketched where offset by the fault, or

(3) cut by the newly sketched fault surface, and then extrapolated linearly (or with a defined bend) to the fault surface where offset (Figure 4.14C-D).

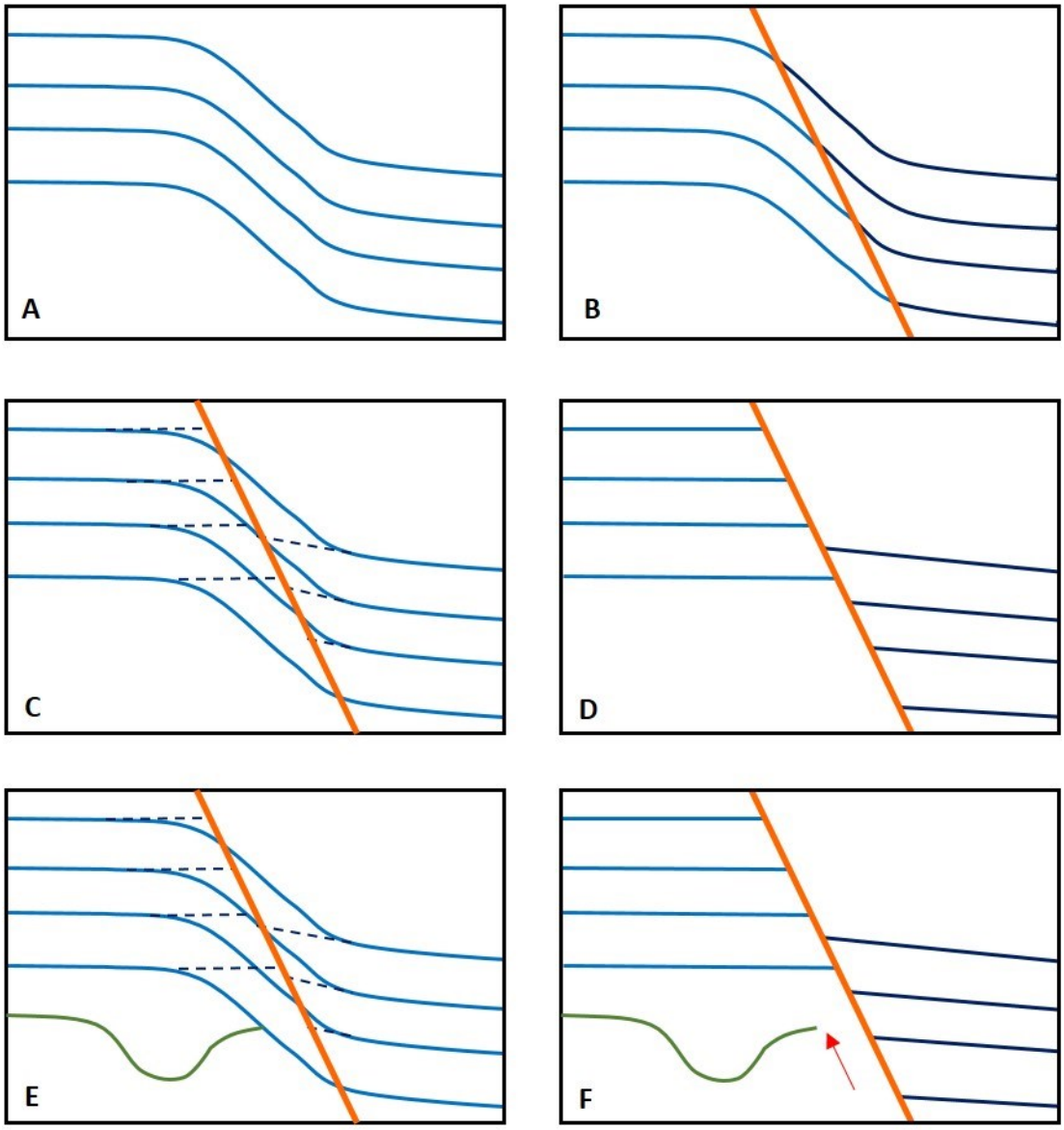

Figure 4.14. Potential options to accommodate insertion of a newly sketched fault into previously sketched strata. (A) A series of monoclinally folded strata have been interpreted. (B) The fault surface (orange) cuts the strata, but the original folded geometry of the stratigraphic surfaces is retained. (C) The original folded strata (solid blue lines) are cut by the fault surface (orange), and then extrapolated linearly to the fault surface (dashed black lines) from the region of undeformed strata, to give a resulting model (D). (E) existing stratigraphic surfaces (e.g. solid green line) that terminate against stratigraphic surfaces (blue lines) may be left with hanging ends due to modification of the latter after insertion of a fault (orange line), to give a resulting model (F).

Options (1) and (3) could both be automatic options in RRM (potentially within a defined distance from the fault surface for option 3), with option (2) allowing more user flexibility. It is important to note that stratigraphic operators would not be applied to the updated strata in option (2); operators

are applied as a surface is initially sketched, and therefore cannot modify surfaces that have been committed (i.e. finalised). This is a requirement of the 'sketch-what-you-see' modelling approach of RRM.

An additional consideration relates to the geometry of surfaces that lie close to, but do not intersect, the inserted fault. Figures 4.14E-F illustrates one such scenario, in which a channel form was sketched adjacent to strata that have been modified by linear extrapolation (option 3) to a newly inserted fault surface. In this scenario, one default option would be to remove any strata that have "hanging ends" after modification of stratigraphic surfaces that intersect the newly inserted fault surface. This option may have unintended consequences, so should be used cautiously. Alternatively, future prototypes of the RRM software could highlight areas of disrupted geometry to the user, so that they can modify strata as they see fit.

All sketched surfaces in RRM models have the potential to contain information including their location, type (e.g. structural or stratigraphic) and the location of intersection nodes as metadata (Section 4.6.8). Where faults are inserted into pre-existing stratigraphy, such metadata will retain the information that the surface was once continuous, and will thus be able to relate segments of a previously continuous surface. This information will be useful for more detailed analysis of structural modifications of a model (see Section 4.6.8).

4.6.5 New operator required: Remove Between – RBW

In addition to changing the fundamental rules in RRM which allow the location, geometry and continuity of structural surfaces, an additional operator is required to assign rock properties to fault zones: Remove Between. The Remove Between operator would be used to remove parts of existing surfaces that lie in between them two or more newly sketched surfaces (Figure 4.15). In this way a fault zone represented by a pair of newly sketched surfaces (e.g. Figure 4.11) could be assigned

properties, for example to account for gouge or cataclasite within the fault zone. This operator could also be used to model diagenesis (see Chapter 5, this thesis).

The implementation of RBW will require a modification to the way in which the operators are currently implemented: two surfaces will need to be inserted prior to the application of an operator, rather than after each surface.

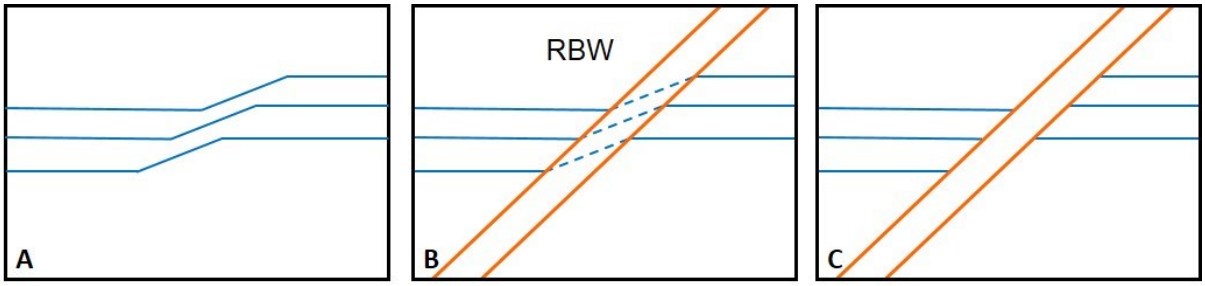

Figure 4.15. Sketch showing the proposed new operator Remove Between (RBW). (A) A series of kink-folded strata (blue) have been interpreted. (B) A pair of surfaces defining a fault zone (orange) have been inserted with the operator RBW. (C) The previously sketched strata between the two surfaces bounding the fault zone are removed, and the fault zone is assigned its own specific properties.

4.6.6 Sketch stratigraphy onto fault surface

The ability to select an arbitrary plane on which to sketch surfaces is planned for future RRM software prototypes, and will enable the user to select an existing fault plane on which to sketch stratigraphic surfaces. Allan diagrams (Allan, 1989) or fault juxtaposition diagrams (e.g. Knipe, 1997) could then be created by sketching the hanging wall and footwall strata directly onto the fault plane (Figure 4.16). This would allow the modeller to assess the validity of the model by examining displacement patterns along the length of the fault (e.g. Caumon et al., 2009), and to investigate the potential sealing effects of stratigraphic juxtaposition across the fault (after e.g. Allan, 1989; Knipe, 1997). Where the existing stratigraphic surfaces have been modified by a newly sketched fault surface or zone, then future RRM software prototypes will be able to produce Allan and fault juxtaposition diagrams automatically, by calculating the intersections of the stratigraphic surfaces with the fault surface. Lateral variations in fault displacement and layer thickness across the fault could be checked for their compatibility with interpreted fault kinematics (Walsh et al., 2003).

Once strata can be sketched directly onto a fault plane, it will be possible to sketch a tip line loop on the footwall, hanging wall or both (Figure 4.16B). This envelope could then be used to constrain how strata bend along the fault plane. It would also be beneficial to be able to sketch cross-sections showing the offset and thickness of strata across the fault at a particular location, with strata then extrapolated along the fault plane following a particular template. For example, normal faults are commonly assumed to have a characteristic fault-displacement profile along their strike (e.g. Price & Cosgrove, 1990), and various conceptual models of fault displacement-length relationships could be incorporated into RRM modelling. A library of template fault displacement-length models could potentially be used to guide 3D extrapolation of stratigraphic surfaces in RRM models.

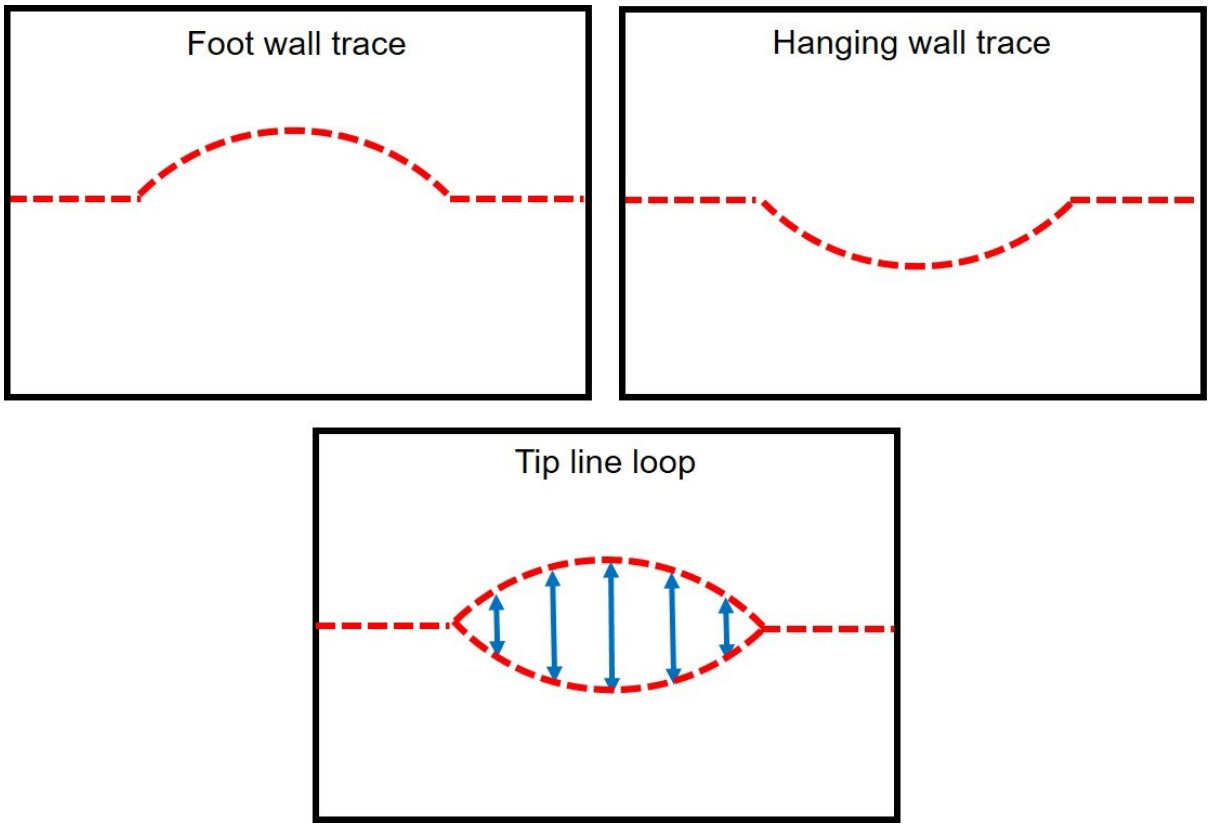

Figure 4.16. Sketch showing the potential uses of sketching directly onto a fault plane. In the top two images, the foot wall trace and hanging wall trace of a stratigraphic surface have been sketched directly onto the fault plane, or extrapolated on to the fault plane from previously sketched stratigraphic surfaces. The lower image shows the creation of a tip line loop created by combining the hanging wall and foot wall traces of the stratigraphic surface. The sense and magnitude of displacement of stratigraphic surfaces can be calculated along the fault (blue arrows), as a way to validate the stratigraphic and structural relationships that have been sketched in the model.

4.6.7 Checking fault throw, sense and type with visual inspection

RRM allows the validity of structural models to be assessed visually once they have been sketched. For example, a user could sketch faults and strata in multiple cross-sections. The user would then be able to inspect stratal offsets across the faults in order to check whether they make geological sense.

Improving the visualisation functionality of the current RRM software prototype would enhance the user's ability to perform geological "sense checks" on their sketched models. For example, the introduction of a cutting tool would allow the user to cut a model along arbitrary cross-sections. The ability to pull apart stratal layers to view their 3D geometry would also be a useful visualisation tool (e.g. Amorim et al., 2014).

4.6.8 Metadata for structural surfaces

Metadata associated with structural surfaces can be leveraged to interrogate or define aspects of sketched models (e.g. Melnikova et al, 2016; Jacquemyn et al., 2016, 2019). For example, all intersection points of interacting surfaces are calculated as the model is constructed. If a marker stratigraphic surface has been identified, then RRM can potentially calculate how the stratigraphic surface changes across a fault in 3D, for example to determine the fault sense, throw or type. This information can be used as a "sense check" of a sketched model and the interpretations that underpin it. RRM could also use that same methodology to tag faults as normal, strike-slip or reverse based on analysis of the metadata. This information could be included in the fault surface information, along with its name (e.g. fault 1) and relative position within the model. If the interpretation is ambiguous, RRM could leave the fault unassigned.

The user would also have the option to tag a fault directly in the metadata, for example as a normal fault. RRM would then be able to check that throw across the fault was consistent with a normal fault interpretation, and flag to the user any instances of incongruence. For example, the fault could be flagged by RRM if the throw changes sense (from positive to negative on the same side) or if the throw sense does not match the metadata tag.

An additional use for the intersection point calculations would be to interpret impossible geometries across a fault. For example, a tip line loop could be constructed based on the occurrence of a marker bed. This envelope could then be inspected to ensure that the hanging wall and footwall traces do not overlap, which would indicate an error in modelling (e.g. another fault is missing from the model) (Figure 4.16, Section 4.6.7, this thesis). A tip line loop could also be used to quantify offset across and along a fault.

If a fault is inserted into existing stratigraphy (Section 4.6.4, this thesis), then the metadata associated with each stratigraphic surface cut by the fault would include the information required to correlate each surface across the fault. In this way, RRM would by default maintain a set of marker beds following insertion of newly sketched faults. Where interpretation is ambiguous, stratigraphic surfaces in different fault blocks could be tagged by the user to denote across-fault correlation. At least one marker bed must be defined if automatic checking of fault throw, sense and type are desired. Another use for the fault-surface metadata would be to assign properties, such as transmissibility modifiers, to fault surfaces.

Another way that metadata could be used in RRM is to check the consistency of stratigraphic relationships which are affected by faulting. If faults have offset an existing set of stratigraphic surfaces, then these stratigraphic surfaces will have the same ordering relative to each other. If they are tagged as the same across faults, or if they are offset by insertion of a fault after sketching, RRM would have the necessary geometrical information in the metadata to check that the stratigraphic surfaces have a consistent ordering across fault blocks. Similarly, the user could interpret sets of strata as pre-, syn-, or post-kinematic, adding those labels to metadata. RRM could use the metadata associated with these stratigraphic packages to check that their geometry matched the kinematic interpretation, thus providing another way to quality check the validity of the interpretation.

4.7 Discussion

The sketch-based approach used in RRM generates one or more deterministic structural models that each illustrate a different geological concept, in contrast to conventional modelling approaches that tend to generate probabilistic models based on a single geological concept. Additionally, conventional modelling workflows create the structural template first, followed by stratigraphy (e.g. Bryant & Flint, 1993) whereas our approach aims to allow surfaces to be created in any order. The current RRM prototype, containing only stratigraphic operators, is suitable for the conventional workflow of modelling structure followed by stratigraphy, provided that faults are continuous and through-going in the model volume. The additional operator and functionality proposed in this chapter would allow more flexibility in the sketching order and continuity of structural surfaces.

The ability to assess uncertainty associated with models is a significant area of current research into structural modelling (e.g. Wellman & Caumon, 2018). How geologically valid are the models, how can that validity be assessed, and how can the integrity of geologically valid models be propagated through the course of their use? For example, surface curvature analysis has been used to assess the validity of structural models (Samson & Mallet, 1997; Mallet, 2002; Pollard & Fletcher, 2005; Groshong, 2006), as has restoration of structural models to their depositional state (Rouby et al., 2000; Maerten & Maerten, 2006; Moretti, 2008). The sketch-based design of RRM aims to allow the user to investigate uncertainty by prototyping a range of deterministic interpretations or focussing updates of the model directly on areas of uncertainty. Thus RRM is not suitable for probabilistic characterisation of model uncertainty. However, the ease of use and flexibility of RRM provide a unique tool that allows initial assessment of uncertainty, as a basis for further, more detailed analysis.

Another advantage of the sketch-based modelling approach in RRM over conventional modelling workflows is the flexibility to update models that have been previously created. The conventional modelling workflows is to create a base-case model that honours a single geological concept (e.g.

structural framework) and then to vary stochastically input parameters used for subsequent model construction (e.g. for history matching), rather than to construct alternative base-case models, even as new data that potentially conflict with the base-case model are acquired (e.g. Bentley & Smith, 2008). The sketch-based approach that is being developed via RRM provides flexibility by specifically addressing how new surfaces interact with existing surfaces; in the case of structure, fault surfaces could be inserted into a model that has already been constructed. This type of surface interaction allows the user to update readily an existing model. Thus models can be made and updated in a straightforward and quick manner.

The current RRM software prototype can be leveraged to create a variety of structural models, despite it being designed for sketching stratigraphic surfaces. In this chapter, the ability of the current RRM software prototype to construct sketch-based structural models of conjugate fault sets and salt-detached listric faults has been presented. Models of different structural configuration could be constructed, provided that faults are through-going or terminate at 'dummy' surfaces, and the order in which surfaces are sketched has been considered carefully at the outset. Further 3D functionality exists in the current RRM software prototype, such that sequential structural contours could be sketched in the map-view plane to construct a model of a monotonically folded and/or faulted stratigraphic surface.

Once the proposed structural functionality has been added to future RRM software prototype, then it must be tested. I propose the following three test cases as a starting point. (1) Constructing a sketch-based model of a flower structure would allow the sensitivity with which 3D fault curvature and convergence (splaying) of high-angle faults can be represented to be assessed. It would also be an ideal test case for modelling complex structure using a combination of cross-section sketches and sketched plan-view trajectories: can one sketch a cross-section through the centre of a flower structure and a map-view of anastomosing faults to create a 3D model that makes geological sense? (2) Constructing a sketch-based model of a metamorphic core complex or duplex would allow testing

of how vertically stacked faults and related folds, which potentially define non-monotonic structural and stratigraphic surfaces, merge onto a master detachment surface at depth. Additionally, the sketching of a metamorphic core complex would allow testing of how the RRM prototype handles both brittle and ductile structural deformation in the same model. (3) Constructing a sketch-based model of an incipient rift zone would allow sketching of faults that terminate within the model volume to be tested. The test cases proposed above would enable further development of RRM software, and would likely be useful for identifying unforeseen modifications required to fully enable 'sketch-what-you-see' structural modelling.

A final testing area for RRM is quality checking of models. Several methods for leveraging the metadata inherent in RRM are presented above (Section 4.6.8) and these should be tested once additional structural operators have been incorporated into RRM. Visual inspection is already employed and additional functionality could be incorporated into RRM to improve visual inspection, for example, the ability to cut arbitrary cross-sections and separate volumes (Section 5.2, this thesis). When models are sketched, it is possible to have volume balance problems across fault blocks. This could be indicated by RRM with a flag if fault blocks do not balance. However, detailed quality checking measures, for example back-stripping of models or structural balancing, are beyond the scope of the RRM program. RRM is not designed to be able to do everything that existing software packages can, it should be used in conjunction with them. RRM provides a tool to rapidly prototype a range of models. If the modelling in RRM reaches a level of complexity where additional validity checking is needed, the surfaces can be exported to a program that is designed for this purpose (e.g. 3D Move or TrapTester for structural models). Once quality checking has been completed, modelling could be continued within RRM if desired. Section 5.3 presents a further discussion of where the RRM program fits within the larger reservoir modelling community.

4.8 Conclusions

After demonstrating the broad applicability of the operators to create stratigraphic models, it was demonstrated in Chapter 4 that the existing stratigraphic operators in RRM can be used to create a variety of structural models, provided that the sketching order of surfaces is determined prior to sketching. Case Study 4A demonstrated that a model of conjugate normal fault sets could be created in RRM by sketching faults oriented in 3D with plan-view trajectories. Case Study 4B demonstrated that output from a physical model could be sketched in RRM using multiple cross-sections to create 3D geometries of listric extensional faults along a salt detachment. However, the current RRM software prototype lacks the functionality to create all 'sketch-what-you-see' structural models.

To enable full representation of 'sketch-what-you-see' structural models in RRM, fault surfaces must be allowed to terminate within the model volume. The new operator Remove Between (RBW) would allow the insertion of a pair of surfaces to create a fault zone, to which specific rock properties could be assigned. Additional updates to future RRM software prototypes that would improve functionality for sketching structural surfaces include: (1) to implement sketching of non-monotonic surfaces; (2) to update existing stratigraphic surfaces within a model by inserting fault surfaces (when RBW is not employed to sketch fault zones); (3) to sketch stratigraphic surfaces onto fault planes; (4) to use the intersections of stratigraphic surfaces and fault surfaces to analyse fault displacement profiles and stratigraphic juxtaposition relationships; and (5) to leverage the metadata associated with structural surfaces to check and assign fault throw, sense and type.

Through the application of a small number of stratigraphic rules and operators, RRM can be used to create a wide variety of sketched stratigraphic and structural surface-based models. With the additional structural functionality outlined above, RRM will be able to capture even more structural complexity.

5 Discussion

5.1 Potential for Broad Use of Stratigraphic and Structural Operators

The stratigraphic operators presented in this thesis are implemented in RRM, however they can be applied in any SBIM or SBM software. Any modelling software that requires surfaces to interact in a geologically valid way can be guided by the operators when defining surface interactions. For example, the concepts of the operators are being utilised by Jacquemyn et al. (2019) as part of surface metadata to define how surfaces terminate and truncate in 3D. In their method, the surfaces are created with an algorithm rather than being sketched, but the logic of the operators remains valid irrespective of how the surfaces are constructed.

Sketch-based modelling and prototyping are underused in current reservoir modelling workflows, largely because the community lacks an appropriate tool for doing so. An appropriate sketch-based modelling tool not only must enable sketching, but it must enable models to be constructed such that results are geologically valid in 3D. Preferably, the tool would also be intuitive and easy to use without lengthy training. RRM provides this tool; it has a simple interface and small number of operators, allowing anyone with geological experience to create a model. The stratigraphic operators combined with multiple methods of 3D construction provide the geological underpinning of the sketching software. The software has been designed and tested with the end-user in mind, aiming to be easy to use and easy to understand.

The ability to create models quickly means that prototyping can be used to its fullest extent, since a range of models can be constructed to investigate the specific problem of interest. In an area of sparse data, multiple large-scale models could be produced to test a range of conceptual interpretations. In an area of abundant data, a detailed base model could be modified with prototype models of small-scale features that lie below data resolution. Model outputs can be used in various ways. For example, they may be visually inspected to evaluate the implications of a particular geological interpretation, they may provide quantitative data to assess static reservoir

parameters (e.g. facies proportions, facies-body connectivity), or they may be used to evaluate flow diagnostics (e.g. Zhang et al., 2019) or as input for flow simulation. The geological community has identified the value in our approach, as evidenced by the most common question after this work is presented: “When is it being commercialised?”

In the future, RRM 3D sketching will be fully integrated with flow diagnostics. This integration will allow the modeller to consider fluid movements as the model is being constructed, rather than once the model has been finalised. However, sketched RRM surfaces can already be exported to other software packages (e.g. IRAP-RMS, Petrel) in which flow simulation can be carried out. Prototype models can be made quickly in RRM, then surfaces imported to the program of choice to complete additional studies. This flexibility makes RRM a useful tool when only specific software programs are approved for use, for example to quantify and audit resource volumes. Thus the models that have been presented in this thesis and that result from RRM modelling are more than pretty pictures in a software prototype, they are full 3D models that can be interrogated in a meaningful way for resource estimation or reservoir characterization.

RRM can also be used as a tool to add value to existing work and as a compliment to geological teaching. Researchers and students often produce geological models, whether they are outcrop-based, conceptual block diagrams or physical models such as Case Study 4B, for example. The simplicity of RRM means that it can be used by the broader community to add value quickly and easily to work that has already been carried out. A researcher could create 3D computational geological models from their physical experimental studies, thus enabling additional research avenues to be explored (e.g. fluid movement for various time-steps of the physical experiment). 3D conceptual models of widely visited field localities could be constructed to add value to field teaching. Conventional reservoir modelling workflows are too time-consuming and require specialist training, which provides a high entry barrier for non-specialists to follow their curiosity.

Three-dimensional thinking can be a tricky concept for students to grasp. The ability to sketch an interactive block diagram would be very beneficial in developing students' ability to understand how geological surfaces interact in 3D. Additionally, the portability of RRM enables it to be used on a tablet in the field. For example, RRM could be used by an undergraduate in situ to construct a 3D model of their mapping area. This model could be compared to students' maps and cross-sections. Students would have the opportunity to think about 3D architectures when they are in the field making observations; this could precipitate new ideas or could encourage additional data collection. In higher level courses, students could create 3D reservoir models in the field based on outcrop observations. These models could then be used to look at subsurface flow or architectures. Geology is an inherently creative discipline and the opportunity to create meaningful models from drawings can be leveraged widely for teaching.

The operators were created to be logical rather than to be process-based (i.e. mimicking one or more geological processes). Therefore, the models that can be made with RRM are not limited to a particular stratigraphic or structural setting. There is potential to create a range of models with the existing prototype and further flexibility for model construction once proposed updates are made for structural modelling. For example, volcaniclastic-flow deposits can have similar geometries to conventional turbidite deposits, and thus RRM could be suitable for modelling a volcaniclastic terrain. Salt tectonics create varied structural and stratigraphic geometries, but if surfaces could be sketched such that they were monotonic, perhaps by combining multiple surfaces or using 'dummy' surfaces, it could be possible to model an area with salt tectonic influence. The key point is that because models are constructed by sketching and without underlying reference to processes (which may not be known or understood), any model with geometrical relationships that are geologically valid could be constructed in RRM.

5.2 Future Work

To further this research, first the prototype changes proposed in section 4.5 of this thesis to allow full 'sketch-what-you-see' structural modelling in RRM should be implemented. Once the changes have been made, the proposed test cases (metamorphic core complex or duplex, flower structure, incipient rift zone) should be modelled to determine if additional operators or functionality adaptations are required to create such models in RRM. The testing phase of the research will be a key step in achieving structural modelling capability in RRM; the logic of the proposed updates appears sound but implementation of that logic can be challenging or reveal unintended logical consequences (e.g. Figures 4.13 and 4.14).

There are clear development directions to advance the functionality of RRM beyond 'sketch-what-you-see' models of stratigraphy and structure, in particular for diagenesis. There are two rules and two operators needed to allow diagenesis to be represented in RRM models. The two new rules for diagenesis are: (1) surfaces must be allowed to cross and (2) surfaces must be allowed to self-intersect. If these two rules are enabled, further operators for diagenesis can be created. The two new operators needed to update a model with diagenetic overprinting are Modify Within (MW) and Remove Within (RW) (Figure 5.1). The operator RBW can also be used to represent diagenesis.

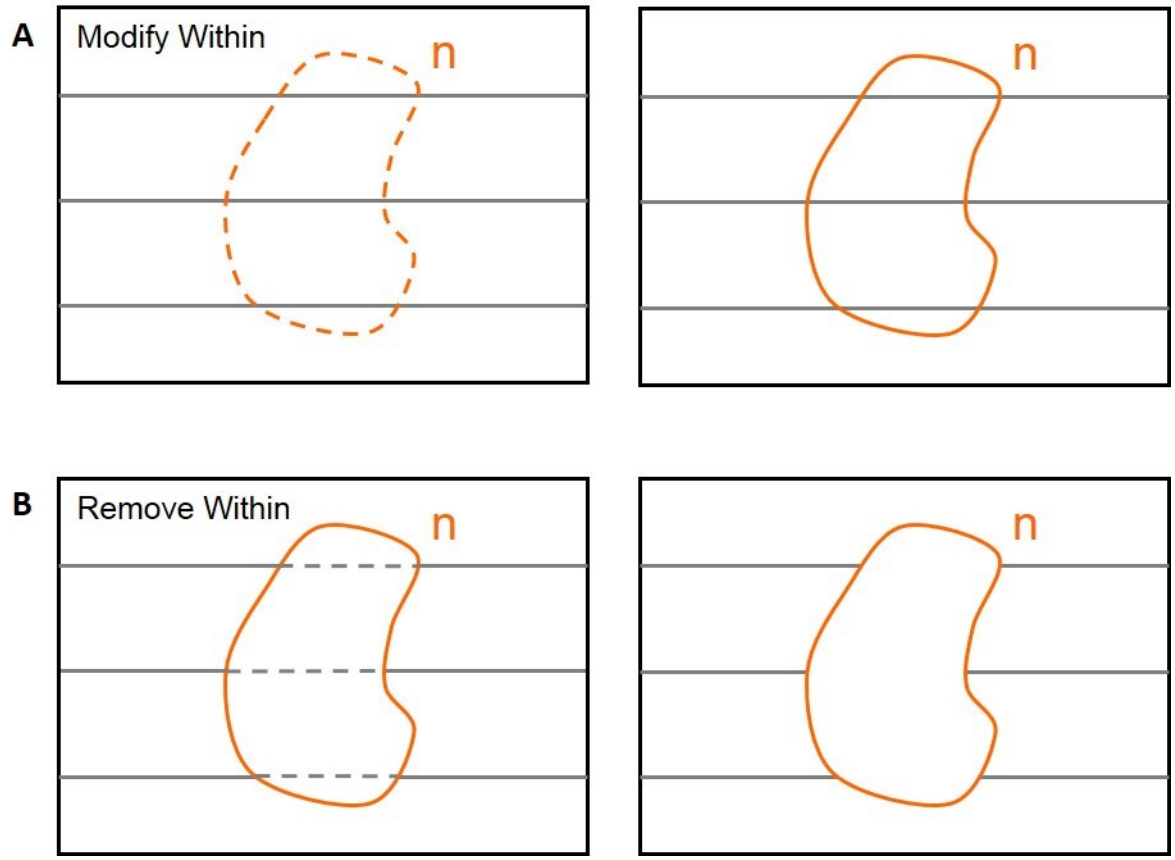

Figure 5.1. Illustration of proposed new operators applied to existing surfaces when new self-intersecting surface *n* intersects existing grey surfaces. A shows the result of application of the Modify Within (MW) operator, where all existing surfaces and *n* remain in the model; the four regions within *n* are now separated from six regions outside new surface *n*. B shows the result of application of the Remove Within (RW) operator, where surfaces that are intersected by and within *n* are removed; the entire region defined by RW forms one region.

The operator Modify Within (MW) creates a new, self-intersecting surface that preserves all existing surfaces and sections of intersected surfaces within it (Figure 5.1A). This operator could be used to define a volume within which the physical properties of the rocks have been modified by diagenesis, but not their geometry (i.e. structure or stratigraphy). Existing stratigraphic and structural surfaces remain and are divided into distinct domains on either side of the newly sketched surface. For example, the operator MW can be used to define the edge of a cemented zone.

The Remove Within (RW) operator creates a new, self-intersecting surface within which all existing surfaces and all sections of intersected surfaces are removed (Figure 5.1B). This operator differs

from RBW in that a single, self-intersecting surface is created by the operator RW. The operator RBW allows two separate surfaces to be inserted, with the strata between these new surfaces removed. The two RBW surfaces do not necessarily intersect. The RW operator could be used to define a diagenetic region(s) that cuts across previously formed structural and stratigraphic surfaces and within which rock properties are uniform. For example, the operator RW can be used to create zones of dissolution due to karstification.

The PW and RW operators can be applied to other geological settings as well. The operators MW and RW could be used to insert a new region of any geometrical form into an existing model. For example, the operator RW could be used to sketch a self-intersecting surface representing a cut-off salt diapir. The diapir form could be sketched in cross-section with plan-view contours being used to define the 3D geometry of the diapir. The operator RW could also be used to create injected sand bodies within an existing model. Both the diapiric and injected features described above would be very difficult to represent in conventional reservoir modelling workflows and tools.

The inclusion of template surfaces and a template surface library is a further development to RRM that would improve usability. Template surfaces would provide the modeller with the ability to use pre-defined surfaces of recurring geometry (e.g. clinoforms, channel bases and tops) and reuse ("copy and paste") their own sketched surfaces which would be useful. For example, a gently sloping template surface could be used to represent a series of point-bar accretion surfaces (e.g. Case Study 3C) or to represent sub-parallel faults (e.g. Case Study 4B). Pre-defined template surfaces could be provided in a template library within RRM, where the user could adapt their geometry to fit their model, for example changing the aspect ratio of a channel form or the dip of a gently curved surface. Additionally, RRM could have a 'template surface creation' tool that allows the user to sketch a template form that they can then re-use. This would be akin to the 're-use trajectory' tool that RRM already employs in the plan-view sketching window, but would be available in the cross-section sketching window.

Lastly, there are many additional improvements that can be made to the current RRM software prototype to improve 3D modelling and usability. These improvements include the following features:

- Ability to sketch on arbitrary cross-sections
- Ability to sketch the same surface on perpendicular and arbitrary cross-sections
- Ability to combine plan-view trajectories with sketching on multiple cross-sections
- Ability to control the way a surface is extrapolated away from or in between cross-sections, e.g. linearly for a channel form
- Ability to cut cross-sections arbitrarily through the model for visual inspection of the model interior
- Ability to pull apart regions of the model for visual inspection
- Ability to import surfaces from other modelling software packages
- Ability to geo-reference models
- Full integration of meshing and flow diagnostics within RRM

RRM has been shown to be an effective tool for prototyping 3D reservoir models. The breadth of models that can be produced will only be expanded with the improvements outlined above. The integration of meshing and flow diagnostics within RRM would allow the flexibility of sketching to be combined with quantitative measurements to truly produce a rapid analysis of the impact of sketched heterogeneities on fluid flow within prototyped models.

5.3 RRM in practice

RRM was never designed or intended to be a replacement to existing software packages. The RRM approach is fundamentally different; deterministic sketching of surfaces using simple operators as a means to quickly prototype reservoir models. This is where the value of RRM lies. It can be used to

create a range of base models, to update existing models or to create deterministic REV for model upscaling. It is not a replacement for Petrel or other existing software packages that are designed (or attempt) to do everything. Existing commercial software packages are often large, cumbersome, and extensive in their modelling capabilities. One can think of them like a reservoir modelling barge: solid, known, dependable on a straight course but ill-suited to changes in course. In contrast, RRM is like a reservoir modelling yacht: small, speedy, not suitable for all tasks but highly manoeuvrable. The best use of RRM is as a complement to existing workflows.

This research has not taken place in a vacuum. In fact, through all stages of prototype development, sponsor companies have used RRM to add value to their daily activities. The most common way that it has been used is to quickly create surfaces through sketching. These surfaces are then imported into another software package like Petrel or IRAP-RMS, where tasks such as flow simulation can be done. In cases of joint-ventures, often a specific software tool is legally required for reporting metrics like reservoir volumes. The ability of RRM to produce exportable surfaces allows it to be used in conjunction with these approved software tools. RRM has also been used to create models of exploration areas where there are large uncertainties in of the subsurface volumes and complicated geometrical relationships. The flexible sketching within RRM allows these complicated geometries to be captured, and the ease of sketching allows a range of models to be made.

The addition of structural operators into RRM will further allow the integration of prototypes with existing modelling packages. For example, to carry out detailed volumetric balancing across fault blocks, a model sketched in RRM could be imported to 3D Move. To check a sketched RRM model for hydrocarbon traps, it could be imported to TrapTester. What RRM allows is the ability to quickly create a variety of deterministic models in a geologically intuitive way. It is best used in tandem with existing software packages. The ability to sketch stratigraphy in a deterministic way is what separates RRM from existing software packages.

6 Synopsis and Conclusions

6.1 Synopsis

This thesis has defined seven universal operators for the creation of surface-based stratigraphic operators and has demonstrated their broad applicability with three case studies of drafted models. The stratigraphic operators are then tested through implementation in the Rapid Reservoir Modelling (RRM) software prototype. The results show three case studies of full 3D geological models and two case studies of full 3D structurally modified geological models. Additional rules, operators and functionality needed to for full 'sketch-what-you-see' structural modelling have been described in detail, and future RRM development has been outlined.

In Chapter 2 the set of seven universal operators were presented that define the interactions between new and existing stratigraphic surfaces within a surface-based framework for constructing geological models. The stratigraphic operators are simple and flexible, because they can be applied in any order, are scale-independent, and are not specific to any sedimentological process or depositional environment. The stratigraphic operators are each summarized below:

- Preserve Above (PA) defines a target surface that a newly created surface(s) is generated above;
- Preserve Below (PB) defines a target surface that a newly created surface(s) is generated below;
- Preserve Between (PBW) defines two or more surfaces that describe a target volume within which a newly created surface(s) is generated;
- Remove Above (RA) creates a new surface(s), above which all existing surfaces and all sections of intersected surfaces are removed;

- Remove Above Intersection (RAI) creates a new surface(s), above which all sections of intersected surfaces are removed (and above which all existing, non-intersected surfaces are preserved);
- Remove Below (RB) creates a new surface(s), below which all existing surfaces and all sections of intersected surfaces are removed;
- Remove Below Intersection (RBI) creates a new surface(s), below which all sections of intersected surfaces are removed (and below which all existing, non-intersected surfaces are preserved);

The operators can be used in various combinations to generate surface-defined architectures that mimic fundamental, widely used stratigraphic and sedimentological concepts. The operators can be applied to any input data type, including outcrop, seismic and conceptual data, and they can be applied to any surface-based modelling method, including those based on sketches and algorithms. The application of a flexible and generic operator set for stratigraphic surfaces within a surface-based modelling context is geologically intuitive for the user, because the components and processes of model construction are similar to those used to conceptualise and communicate geology in maps, cross-sections and block diagrams.

These surface-based operators have been implemented in a sketch-based modelling software prototype, Rapid Reservoir Modelling (RRM). In Chapter 3, the 3D application of the stratigraphic operators was demonstrated using RRM. Three case studies demonstrated the applicability of the stratigraphic operators to three different geological settings (deepwater slope systems, lacustrine carbonates and fluvial point-bar deposits) with three different data types (seismic, outcrop and wells) and with three different methods for creating three-dimensionality in the models (multiple cross-sections, plan-view contours and applied trajectories).

Case Study 3A demonstrated that multiple 3D models of deepwater slope system deposits can be quickly and easily produced using RRM by varying the correlation of basal surfaces. Deepwater slope system 3D models were created using the stratigraphic operators applied to surfaces across multiple parallel cross-sections. These models show that additional detail (e.g. interpretation of internal channel architecture) can be added to a model once it has been constructed and that geologically sound models can be created when sketching surfaces out of stratigraphic order.

Case Study 3B demonstrated how a pair of 3D prototype models representing different geological concepts can be created rapidly, including complex geometries. One prototype model includes mounded geometries with overhanging surfaces; this model would be difficult and time-consuming to create with standard reservoir modelling tools and workflows. However, these 3D mounded bioherm geometries were created rapidly in RRM using the technique of combining stratigraphic operators with sketched plan-view contours.

In Case Study 3C, models of two end-member scenarios were created to model the lateral extent of mudstone-prone intervals in point-bar deposits in a meander-belt sandbody. The prototype models were based on vertical well data and a seismically derived map, and 3D geometries were created by combining sketched cross-sections with plan-view surface trajectories. The prototype models were produced in minutes; other models could also be produced quickly with this approach. For example, the cross-sectional geometries of point-bar accretion surfaces, their plan-view trajectories, or the distribution and extent of mudstone-prone intervals could all be modified.

All case study prototype models serve as a starting point to investigate their implications for reservoir architecture and behaviour. The power of the stratigraphic operators implemented in RRM is the speed and simplicity with which the models were created and modified. Various prototype models of an area of interest can be made quickly, and the influence of variations between models can be tested.

After demonstrating the broad applicability of the operators to create stratigraphic models, it was demonstrated in Chapter 4 that the existing stratigraphic operators in RRM can be used to create a variety of structural models, provided that the sketching order of surfaces is determined prior to sketching. Case Study 4A demonstrated that a model of conjugate normal fault sets could be created in RRM by sketching faults oriented in 3D with plan-view trajectories. Case Study 4B demonstrated that output from a physical model could be sketched in RRM using multiple cross-sections to create 3D geometries of listric extensional faults along a salt detachment. However, the current RRM software prototype lacks the functionality to create all 'sketch-what-you-see' structural models.

To enable full representation of 'sketch-what-you-see' structural models in RRM, fault surfaces must be allowed to terminate within the model volume. The new operator Remove Between (RBW) would allow the insertion of a pair of surfaces to create a fault zone, to which specific rock properties could be assigned. Additional updates to future RRM software prototypes that would improve functionality for sketching structural surfaces include: (1) to implement sketching of non-monotonic surfaces; (2) to update existing stratigraphic surfaces within a model by inserting fault surfaces (when RBW is not employed to sketch fault zones); (3) to sketch stratigraphic surfaces onto fault planes; (4) to use the intersections of stratigraphic surfaces and fault surfaces to analyse fault displacement profiles and stratigraphic juxtaposition relationships; and (5) to leverage the metadata associated with structural surfaces to check and assign fault throw, sense and type.

6.2 Conclusions

Through the application of a small number of stratigraphic rules and operators, RRM can be used to create a wide variety of sketched stratigraphic and structural surface-based models. With the additional structural functionality outlined above, RRM will be able to capture even more structural complexity. The ability to quickly prototype a range of deterministic reservoir models is an opportunity that has not been previously available. RRM provides geologists with the opportunity to create models quickly that test conceptual interpretations, and the flexibility in the way surfaces can

be sketched and modified means that updating of existing models can also be carried out quickly. The beauty of this approach lies in its simplicity. All geology students are required to make maps and cross-sections and to create block diagrams in order to understand 3D geometries. RRM leverages this universal geological training to allow any geologist to pick up a stylus and create a 3D model. It has lowered the barrier of entry to geological modelling by opening it up to everyone with geological knowledge, without requiring specialist training as a reservoir modeller.

References

Allan, U.S. 1986. Model for hydrocarbon migration and entrapment. *AAPG Bulletin*, 73(7), 803-811.

Amorim, R., Brazil, E.V., Patel, D. and M.C. Sousa. 2012. Sketch modelling of seismic horizons from uncertainty. In: *Proceedings of the International Symposium on Sketch-Based Interfaces and Modelling*, Eurographics Association, Aire-la-Ville, Switzerland, SBIM 2012, 1-10.

Amorim, R., Vital Brazil, E., Samavati, F., and M.C. Sousa. 2014. 3D Geological modelling using sketches and annotations from geologic maps, ACM SIGGRAPH/EG 11th Intl. Symp. On Sketch-Based Interfaces and Modelling (SBIM '14), Vancouver, Canada, 17-25.

Arisoy, E.B., and L.B. Kara. 2014. Topology preserving digitization of physical prototypes using deformable subdivision models. ASME. International Design Engineering Technical Conferences and Computers and Information in Engineering Conference, *Volume 2B: 40th Design Automation Conference*, V02BT03A015. doi:10.1115/DETC2014-34390.

Bentley, M.R. and Smith, S. 2008. Scenario-based reservoir modelling: the need for more determinism and less anchoring, *in* Robinson, A., Griffiths, P., Price, S., Hegre, J. and Muggeridge, A., eds., The future of geological modelling in hydrocarbon development, *Geol. Soc. London Special Publication* **309**, 145-159.

Boersma, J. R., 1969, Internal structure of some tidal mega-ripples on a shoal in the Westerschelde estuary, the Netherlands: Geologie en Mijnbouw, v. 48, 409-414.

Bohacs, K.M., Lamb-Wozniak, K., Demko, T.M., Eleson, J., McLaughlin, O., Lash, C., Cleveland, D.M. and S. Kaczmarek. 2013. Vertical and lateral distribution of lacustrine carbonate lithofacies at the parasequence scale in the Miocene Hot Spring limestone, Idaho: An analog addressing reservoir presence and quality. *AAPG bulletin*, 97(11), 1967-1995.

Bryant, I.D. and S.S. Flint. 1993. Quantitative clastic reservoir geological modelling: problems and perspectives. *Spec. Pubs. In Ass. Sediment.*, **15**, 3-20.

Calgano, P., Chiles, J.P., Courrioux, G., and A. Guillen. 2008. Geological modelling from field data and geological knowledge: Part I. Modelling method coupling 3D potential-field interpolation and geological rules. *Physics of the Earth and Planetary Interiors* 171(1-4), 147-157.

Caumon, G., Collon-Drouaillet, P., Viseur, S. and J. Sausse. 2009. Surface-based 3D modelling of geological structures. *Mathematical Geosciences* **41**, 927-945.

Caumon, G. and P. Collon-Drouaillet. 2014. Special Issue on Three-Dimensional Structural Modeling, *Mathematical Geosciences*, 46, 905.

Caumon, G., Lepage, F., Sword, C.H., and J.L. Mallet. 2004. Building and editing a sealed geological model. *Mathematical Geology*, 36(4), 405-424.

Cherlin, J.J., Samavati, F., Sousa, M.C., and J.A. Jorge. 2005. Sketch-based modelling with few strokes. In: *Proceedings of the 21st Spring Conference on Computer Graphics*, ACM, New York, NY, USA, SCCG 2005, The Eurographics Association, 137-145.

Choi, K., Jackson, M.D., Hampson, G.J., Jones, A.D.W and A.D. Reynolds. 2011. Predicting the impact of sedimentological heterogeneity on gas-oil and water-oil displacements: fluvial-deltaic Pereriv Suite reservoir, ACG Oilfield, South Caspian Basin. *Petroleum Geoscience*, **17**, 143-163.

Colombera, L., Yan, N., McCormick-Cox, T. and N. P. Mountney. 2018. Seismic-driven geocellular modeling of fluvial meander-belt reservoirs using a rule-based method. *Marine and Petroleum Geology*, 93, 553-569.

Cross, T.A. (ed.). 1990. *Quantitative Dynamic Stratigraphy*, Prentice-Hall, Englewood Cliffs, New Jersey, 625 pp.

De Kemp, E.A. 1999. Visualization of complex geological structures using 3-D Bezier construction tools. *Computers and Geosciences,* 26 (5), 509-530.

de Kemp, E.A., and K.B. Sprague. 2003. Interpretive tools for 3D structural geological modeling part I: Bézier-based curves, ribbons and grip frames. *GeoInformatica,* 7(1), 55–71.

Denver, L.E. and D.C. Phillips. 1990. Stratigraphic geocellular modelling. *Geobyte*, **5**, 45-47.

Deutsch, C.V., Xie, Y. & Cullick, A.S. 2001. Surface geometry and trend modelling for integration of stratigraphic data in reservoir models. Society of Petroleum Engineers, SPE paper 68817.

Deveugle, P.K., Jackson, M., Hampson, G.J., Stewart, J., Clough, M.D., Ehighebolo, T., Farrell, M.E., Calvert, C.S. and J.K. Miller. 2014. A comparative study of reservoir modelling techniques and their impact on predicted performance of fluvial-dominated deltaic reservoirs. AAPG Bulletin. 98. 729-763. 10.1306/08281313035.

Dhont, D., Luxey, P., and J. Chorowicz. 2005. 3-D modeling of geologic maps from surface data. *AAPG Bulletin,* 89(11), 1465–1474.

Fagin, S. 1991. *Seismic Modeling of Geologic Structures: Applications to Exploration Problems*. Society of Exploration Geophysicists, Tulsa, OK, USA.

Fernández, O., Muñoz, J.A., Arbués, P., Falivene, O., and M. Marzo. 2004. Three-dimensional reconstruction of geological surfaces: an example of growth strata and turbidite systems from the Ainsa basin (Pyrenees, Spain). *AAPG Bulletin*, 88(8), 1049–1068.

Frank, T., Tertois, A.L., and J.L. Mallet. 2007. 3D-reconstruction of complex geological interfaces from irregularly distributed and noisy point data. *Computers and Geosciences*, 33(7), 932–943.

Fustic, M., Thurston, D., Al-Dliwe, A., Leckie, D.A., Cadiou, D. 2013. Reservoir modelling by constraining stochastic simulation to deterministically interpreted three-dimensional geobodies:

case study from Lower Cretaceous McMurray Formation, Long Lake steam-assisted gravity drainage project, Northeast Alberta, Canada, *in* Hein, F.J., Leckie, D., Larter, S., Suter, J.R., eds., Heavy-Oil and Oil-Sand Petroleum Systems in Alberta and Beyond: AAPG Studies in Geology **64**, 565-604.

Geiger, S., Matthäi, S.K., Niessner, J. and Helmig, R., 2009. Black-oil simulations for three-component, three-phase flow in fractured porous media. *Society of Petroleum Engineers Journal*, v. 14, p. 338-354.

Geiger, S. and S.K. Matthäi. 2012. What can we learn from high-resolution numerical simulations of single- and multi-phase fluid flow in fractured outcrop analogues? *Geological Society, London, Special Publications*, 374, 125-144.

Gjøystdal, H., Reinhardsen, JE, and K. Astebøl. 1985. Computer representation of complex three-dimensional geological structure using a new solid modeling technique. *Geophysical Prospecting*, v. 33, no. 8, 1195-1211.

Graham, G.H., Jackson, M.D., and G.J. Hampson. 2015. Three-dimensional modelling of clinoforms in shallow-marine reservoirs: Part 2. Impact on fluid flow and hydrocarbon recovery in fluvial-dominated deltaic reservoirs. *AAPG Bulletin*, v. 99, no. 6, p. 1049-1080.

Groshong, R.H. 2006. 3-D structural geology, 2nd edn. Springer, Berlin.

Hamilton, D.E. and T.A. Jones (eds). 1992. *Computer Modelling of Geologic Surfaces and Volumes*. American Association of Petroleum Geologists, Computer Applications in Geology, **1.**

Hjelle, Ø., and S.A. Petersen. 2011. A Hamilton–Jacobi framework for modeling folds in structural geology. *Mathematical Geosciences*, 43(7), 741.

Houlding, S. 1994. *3D Geoscience Modeling: Computer Techniques for Geological Characterization*. Springer-Verlag, Berlin Heidelberg, 311 p.

Hu, L.Y., Joseph, P. and O. Dubrule. 1994. Random genetic simulation of the internal geometry of deltaic sandstone bodies. *SPE Formation Evaluation*, **9**, 245-250.

Jackson, M.D. and A.H. Muggeridge. 2000. Effect of discontinuous shales on reservoir performance during horizontal waterflooding. *Society of Petroleum Engineers Journal*, **5**, 446-455.

Jackson, M.D., Yoshida, S., Muggeridge, A.H. and H.D. Johnson. 2005. Three-dimensional reservoir characterization and flow simulation of heterolithic tidal sandstones. *American Association of Petroleum Geologists Bulletin*, **89**: 507–528.

Jackson, M.D., Hampson, G.J., El-Sheikh, A., Sounders, J.H., Graham, G.H. and B.Y.G. Massart. 2013. Surface-based reservoir modelling for flow simulation, *in* Martinius, A.H., Howell, J.A. and T. Good, eds., Sediment Body Geometry and Heterogeneity: Analogue Studies for Modelling the Subsurface, *Geol. Soc. London Special Publication* 387, doi 10.1144/SP387.2.

Jackson, M.D., Hampson, G.J., **Rood, M.P**., Geiger-Boschung, S., Zhang, Z., Sousa, M.C., Amorim, R., Vital Brazil, E., Samavati, F.F., and L.N. Guimaraes. 2015a. Rapid Reservoir Modelling: Prototyping of reservoir models, well trajectories and development options using an intuitive, sketch-based interface. *Reservoir Simulation Symposium: SPE RSS 2015*. Richardson, Texas, Society of Petroleum Engineers, Vol. 1, 13 p. SPE-173237.

Jackson, M.D., Percival, J.R., Mostaghiml, P., Tollit, B.S., Pavlidid, D., Pain, C.C., Gomes, J.L.M.A., El-Sheikh, A.H., Salinas, P., Muggeridge, A.H., and M.J. Blunt. 2015b. Reservoir modelling for flow simulation by use of surfaces, adaptive unstructured meshes, and an overlapping-control-volume-finite-element method. *SPE Reservoir Evaluation and Engineering*, 18, 115-132.

Jacquemyn, C., Jackson, M.D., Hampson, G.J. 2019. Surface-based geological reservoir modelling using grid-free NURBS curves and surfaces. *Mathematical Geosciences*, **51**: 1-28. https://doi.org/10.1007/s11004-018-9764-8

Jacquemyn, C., Melnikova, Y., Jackson, M.D., Hampson, G.J. and C.M. John. 2016. Geologic modelling using parametric NURBS surfaces. *ECMOR XV – 15th European Conference on the Mathematics of Oil Recovery*, DOI: 10.3997/2214-4609.201601884.

Jones, A.D.W., Doyle, J.D., Jacobsen, T. and D. Kjønsvik. 1995. Which sub-seismic heterogeneities influence waterflood performance? A case study of low net-to-gross fluvial reservoir. *In:* De Haan H.J. (ed.) New Developments in Improved Oil Recovery. Geological Society, London, Special Publication **84**: 5-18.

Juanes, R., Spiteri, E.J., Orr Jr., F.M., and M.J. Blunt. 2006. Impact of relative permeability hysteresis on geological CO2 storage. *Water Resources Research*, **42**, W12418, doi:10.1029/2005WR004806.

Kaufman, O., and T. Martin. 2008. 3D geological modelling from boreholes, cross-sections and geological maps, application over former natural gas storages in coal mines. *Computers and Geosciences,* 34(3), 278–290.

Kjønsvik, D., Doyle, J.D., Jacobsen, T. and A.D.W. Jones. 1994. The effects of sedimentary heterogeneities on production from a shallow marine reservoir - what really matters? Society of Petroleum Engineers, SPE paper 28445.

Knipe, R.J. 1997. Juxtaposition and seal diagrams to help analyze fault seals in hydrocarbon reservoirs. *AAPG Bulletin*, 81(2), 187-195.

Kortekaas, T.F.M. 1985. Water/Oil Displacement Characteristics in Crossbedded Reservoir Zones. Society of Petroleum Engineers Journal, 25(6). doi:10.2118/12112-PA

Kosa, E., Warrlich, G.M.D. & Loftus, G. 2015. Wings, mushrooms, and Christmas trees: the carbonate seismic geomorphology of Central Luconia, Miocene–present, offshore Sarawak, northwest Borneo. *American Association of Petroleum Geologists Bulletin*, **99**: 2043-2075.

Kupfersberger, H., and C. V. Deutsch, 1999. Methodology for integrating analog geologic data in 3-D variogram modelling. *AAPG Bulletin*, **83**, 1262–1278.

Legler, B., Johnson, H.D., Hampson, G.J., Massart, B.Y.G., Jackson, C.A-L., Jackson, M.D., El-Barkooky, A. & Ravnas, R. 2013. Facies model of a fine-grained, tide-dominated delta: lower Dir Abu Lifa Member (Eocene), Western Desert, Egypt. *Sedimentology*, **60**, 1313-1356.

Lemon, A. and N. Jones. 2003. Building solid models from boreholes and user-defined cross-sections. *Computers & Geosciences* **29**, 547-555.

Lidal, E., Patel, D., Bendiksen, M., Langeland, T., and Viola, I. 2013. Rapid sketch-based 3d modelling of geology. In *Workshop on Visualisation in Environmental Sciences (EnvirVis)*, The Eurographics Association, 31--35.

MacDonald, A. C., and J. O. Aasen, 1994. A prototype procedure for stochastic modelling of facies tract distribution in shoreface reservoirs. *In:* J. M. Yarus and R. L. Chambers (eds), *Stochastic modelling and geostatistics: AAPG Computer Applications in Geology 3*, 91–108.

MacDonald, A.C., Fält, L.-M. and A.-L. Hektoen. 1998. Stochastic modelling of incised valley geometries. *American Association of Petroleum Geologists Bulletin*, **82**, 1156-1172.

Maerten, L., and F. Maerten. 2006. Chronologic modeling of faulted and fractured reservoirs using geomechanically based restoration; technique and industry applications. *AAPG Bulletin*, 90(8), 1201–1226.

Mallet, JL. 1992. GOCAD: A Computer-Aided design program for geological applications. *NATO-ASI Mathematics and Physical Sciences*, V. 354, 123-141.

Mallet, J.L. 2002. Geomodeling. Applied geostatistics. Oxford University Press, New York

Mallet, J.L. 2014. Elements of Mathematical Sedimentary Geology: The GeoChron Model. EAGE Publications.

Martinius, A.W., Fustic, M., Garner, D.L., Jablonski, B.V.J., Strobl, R.S., MacEachern, J.A. & Dashtgard, S.E. 2017. Reservoir characterization and multiscale heterogeneity modelling of inclined heterolithic strata for bitumen-production forecasting, McMurray Formation, Alberta, Canada. *Marine and Petroleum Geology*, **82**, 336-361.

Massart, B.Y.G., Jackson, M.D., Hampson, G.J., Johnson, H.D., Legler, B. & Jackson, C.A-L. 2016a. Effective flow properties of heterolithic, cross-bedded tidal sandstones, part 1: surface based modelling. *American Association of Petroleum Geologists Bulletin*, **100**, 697-721.

Massart, B.Y.G., Jackson, M.D., Hampson, G.J. & Johnson, H.D. 2016b. Effective flow properties of heterolithic, cross-bedded tidal sandstones, part 2: flow simulation. *American Association of Petroleum Geologists Bulletin*, **100**, 723-742.

Matthäi, S.K., Mezentsev, A., and Belayneh, M. 2007. Finite element-node-centered finite-volume two-phase-flow experiments with fractured rock represented by unstructured hybrid-element meshes. *Society of Petroleum Engineers Journal*, v. 10, p. 740-756.

Mayall, M., Jones, E. and Casey, M. 2006. Turbidite channel reservoirs—Key elements in facies prediction and effective development. *Marine and Petroleum Geology*, v. 23, p.821-841.

McHargue, T., Pyrcz, M.J., Sullivan, M.D., Clark, J.D., Fildani, A., Romans, B.W., Covault, J.A., Levy, M., Posamentier, H.W. and Drinkwater, N.J., 2011. Architecture of turbidite channel systems on the continental slope: patterns and predictions. *Marine and Petroleum Geology*, v. 28, pp. 728-743.

Melnikova, Y., Jacquemyn, C., Osman, H., Salinas, P., Gorman, G., Hampson, G.J. and M.D. Jackson. 2016. Reservoir modelling using parametric surfaces and dynamically adaptive fully unstructured

grids. *ECMOR XV – 15th European Conference on the Mathematics of Oil Recovery*, DOI: 10.3997/2214-4609.201601887.

Merriam, D.F. and J.C. Davis. 2001. *Geologic Modeling and Simulation: Sedimentary Systems*, Kluwer Academic/Plenum Publishers, New York, 352 p.

Ming, J., Pan, M., Qu, H., and Z. Ge. 2010. GSIS A 3D geological multi-body modeling system from netty cross-sections with topology. *Computers and Geosciences*, 36(6), 756-767.

Moczydlower, B., Salomao, M.C., Branco, C.C.M., Romeu, R.K., Homem, T.D.R., De Freitas, L.C. and Lima, H.A.T.S. 2012. Development of the Brazilian Pre-Salt Fields-When To Pay for Information and When To Pay for Flexibility. Society of Petroleum Engineers, SPE paper 152860.

Moretti, I. 2008. Working in complex areas: New restoration workflow based on quality control, 2D and 3D restorations. *Marine Petroleum Geology,* 25(3), 205–218.

Muniz, M.C. and Bosence, D.W.J. 2015. Pre-salt microbialites from the Campos Basin (offshore Brazil): image log facies, facies model and cyclicity in lacustrine carbonates, *in* Bosence, D.W.J., Gibbons, K.A., Le Heron, D.P., Morgan, W.A., Pritchard, T. and Vining, B. A., eds., Microbial Carbonates in Time and Space: Implications for Global Exploration and Production, *Geol. Soc. London Special Publication* **418**, 221-242.

Mutti, E. 1985. Turbidite systems and their relations to depositional sequences, *in* Zuffa, G.G., ed., Provenance of Arenites, Riedel Publishing, Dordrecht, 65–93.

Natali, 2012 - Mattia Natali, Ivan Viola and Daniel Patel. Rapid Visualization of Geological Concepts. In Proceedings of SIBGRAPI Conference on Graphics, Patterns and Images, 2012, pp. 150–157.

Natali, M., Klausen, T.G., and D. Patel. 2014a. Sketch-based modelling and visualization of geological deposition. *Computers and Geosciences*, **67**, 40-48.

Natali, M., Parulek, J., and D. Patel. 2014b. Rapid modelling of interactive geological illustrations with faults and compaction. *Spring conference on Computer graphics.* doi: 10.1145/2643188.2643201.

Nordahl, K. and P.S. Ringrose. 2008. Identifying the Representative Elementary Volume for Permeability in Heterolithic Deposits Using Numerical Rock Models. *Mathematical Geosciences*, **40**, 753-771.

Olsen, L., Samavati, F., Sousa, M.C., and J. Jorge. 2009. Sketch-Based Modelling: A Survey. *Computers & Graphics*, **33**, 85-103.

Olsen, L., Samavati, F., and J. Jorge. 2011. Naturasketch: Modelling from images and natural sketches. *Computer Graphics and Applications*, IEEE **31**, 24-34.

O'Sullivan, M.J., Pruess, K., and M.J. Lippmann. 2001. State of the art of geothermal reservoir simulation. *Geothermics*, **30**, issue 4, 395-429.

Paluszny, A., Matthäi, S.K., and M. Hohmeyer. 2007. Hybrid finite element-finite volume discretization of complex geological structures and a new simulation workflow demonstrated on fractured rocks. *Geofluids,* 7, 186-208.

Pereira, T., Brazil, E.V., Macêdo, I., Sousa, M.C., de Figuieredo, L.H., and L. Velho. 2011. Sketch-based warping of RGBN images. *Graphical Models*, **73**, 97-110.

Pollard, D., and R. Fletcher. 2005. Fundamentals of structural geology. Cambridge University Press, New York.

Posamentier, H.W. and V. Kolla. 2003. Seismic geomorphology and stratigraphy of depositional elements in deep-water settings. *Journal of Sedimentary Research*, v. 73, p. 367-388.

Posamentier, H.W. and Vail, P.R. 1988. Eustatic controls on clastic deposition II – sequence and systems tract models, *in* Wilgus, C.K., Hastings, B.S., Kendall, C.G.St.C., Posamentier, H.W., Ross, C.A.

and Van Wagoner, J.C., eds., Sea-Level Changes - An Integrated Approach*, SEPM Special Publication* **42**, 125-154.

Posamentier, H.W. and R.G. Walker. 2006. Deep-water turbidites and submarine fans. *In:* Posamentier, H.W. and Walker, R.G. (Eds.) *Facies models revisited*. Society for Sedimentary Geology (SEPM), Special Publication **84**, 399-520.

Price, N.J. and J.W. Cosgrove. 1990. *Analysis of geological structures*. Cambridge University Press.

Pyrcz, M.J., Catuneanu, O. and C.V. Deutsch. 2005. Stochastic surface-based modelling of turbidite lobes. *American Association of Petroleum Geologists Bulletin*, **89**, 177-191.

Pyrcz, M.J., Sech, R.P., Covault, J.A., Willis, B.J., Sylvester, Z. and Sun, T. 2015. Stratigraphic rule-based reservoir modelling. *Bulletin of Canadian Petroleum Geology*, **63**, 287-303.

Refsgaard, J.C., Christensen, S., Sonnenborg, T.O., Seifert, D., Højberg, A.L. and L. Troldborg. 2012. Review of strategies for handling geological uncertainty in groundwater flow and transport modelling. *Advances in Water Resources*, **36**, 36-50.

Ringrose, P.S., Nordhal, K. and Wen, R. 2005. Vertical permeability estimation of heterolithic tidal deltaic sandstones. *Petroleum Geoscience*, **11**, 29-36.

Ringrose, P.S., Martinius, A.W. and Alvestad, J. 2008. Multiscale geological reservoir modelling in practice, *in* Robinson, A., Griffiths, P., Price, S., Hegre, J. and Muggeridge, A., eds., The future of geological modelling in hydrocarbon development, *Geol. Soc. London Special Publication* **309**, 123-134.

Ringrose, P. and M. Bentley. 2015. *Reservoir Model Design: A Practitioner's Guide*. Springer Netherlands, 249 p., doi: 10.1007/978-94-007-5497-3.

Rouby, D., Xiao, H., and J. Suppe. 2000. 3-D restoration of complexly folded and faulted surfaces using multiple unfolding mechanisms. *AAPG Bulletin,* 84(6), 805–829.

Ruiu, J., Caumon, G., and S. Viseur. 2016. Modelling channel forms and related sedimentary objects using a boundary representation based on non-uniform rational B-splines. *Mathematical Geosciences* **48**, 259-284.

Salinas, P., Pavlidis, D., Xie, Z., Jacquemyn, C., Melnikova, Y., Jackson, M.D., and C.C. Pain. 2017. Improving the robustness of the control volume finite element method with application to multiphase porous media flow. *International Journal for Numerical Methods in Fluids*, 85, 235-246.

Salinas, P., Pavlidis, D., Xie, Z., Osman, H., Pain, C., and M. Jackson. 2018. A robust mesh optimisation method for multiphase porous media flows. *Computational Geosciences,* 22, 1389-1401.

Samson, P., and J.L. Mallet. 1997. Curvature analysis of triangulated surfaces in structural geology. *Mathematical Geology*, 29(3), 391–412.

Sech, R.P., Jackson, M.D. and G.J. Hampson. 2009. Three-dimensional modelling of a shoreface-shelf parasequence reservoir analog: Part 1. Surface-based modelling to capture high-resolution facies architecture. *American Association of Petroleum Geologists Bulletin* **93**: 1155-1181.

Shah, J.J., Vargas-Hernandez, N., Summers, J.D., and S. Kulkarni. 2001. Collaborative Sketching (c-sketch) – An idea generation technique for engineering design. *Journal of Creative Behavior*, **35**, 168-198.

Souche, L., Lepage, F., and G. Iskenova. 2013. Volume based modeling-automated construction of complex structural models. In *75th EAGE conference & exhibition incorporating SPE EUROPEC 2013*.

Sprague, K.B., and E.A. de Kemp. 2005. Interpretive tools for 3-D structural geological modelling part II: surface design from sparse spatial data. *GeoInformatica*, 9(1), 5–32.

Strebelle, S., Payrazran, K., and J. Caers, 2003. Modelling of a deepwater turbidite reservoir conditional to seismic data using multiple-point geostatistics. *Society of Petroleum Engineers Journal*, **8**, 227–235.

Strebelle, S., 2006. Sequential simulation for modelling geo-logical structures from training images. *In:* T. C. Coburn, J. M. Yarus, and R. L. Chambers (eds), *Stochastic modelling and geostatistics: Principles, methods and case studies—Volume II: AAPG Computer Applications in Geology 5*, 139–149.

Tetzlaff, D.M. and G. Priddy. 2001. Sedimentary Process Modeling: From Academia to Industry. In: *Geologic Modeling and Simulation, Sedimentary Systems* (Ed. by D.F. Merriam & J.C. Davis), Kluwer Academic/Plenum Publishers, New York, 352 pp.

Tetzlaff, D., Tveiten, J., Salomonsen, P., Christ, A.-B., Athmer, W., Borgos, H., Sonneland, L., Martinez, C., and F. Raggio. 2014. Geologic Process Modeling. IX Conference of Hydrocarbon Exploration and Development, Mendoza, Argentina.

Turner, A.K. 1992. Three-dimensional modeling with geoscientific information systems. *NATO-ASI Mathematics and Physical Sciences*, V. 354. Kluwer Academic, Dordrecht.

Walsh, J.J., Bailey, W.R., Childs, C., Nicol, A., and C.G. Bonson. 2003. Formation of segmented normal faults: a 3-D perspective. *Journal of Structural Geology,* 25(8), 1251–1262.

Weber, K.J. 1986. How heterogeneity affects oil recovery. *In:* Lake, L.W. and H.B. Carroll Jr. (eds) *Reservoir Characterization*. Academic Press, New York, 487-544.

Wellman, F. and G. Caumon. 2018. 3D structural geological models: concepts, methods, and uncertainties. *Advances in Geophysics,* 59, 1-122.

Wen, R., A. W. Martinius, A. Naess, and P. S. Ringrose, 1998. Three-dimensional simulation of small-scale heterogeneity in tidal deposits— A process-based stochastic method. *In:* A. Buccianti, G. Nardi, and R. Potenza (eds), *Proceedings of the 4th Annual Conference of the International Association of Mathematical Geology*, 129–134.

White, C.D. and Barton, M.D. 1999. Translating outcrop data to flow models, with applications to the Ferron sandstone. *SPE Reservoir Evaluation and Engineering Journal*, **2**, 341–350.

White, C.D., Willis, B.J., Dutton, S.P., Bhattacharya, J.P. and K. Narayanan. 2004. Sedimentology, statistics, and flow behavior for a tide-influenced deltaic sandstone, Frontier Formation, Wyoming, United States. In: Grammer, G.M., Harris, P.M. and Eberli, G.P. (eds) *Integration of outcrop and modern analogs in reservoir modelling*. American Association of Petroleum Geologists, Memoir **80**: 129-152.

Wycisk, P., Hubert, T., Gossel, W., and C. Neumann. 2009. High-resolution 3D spatial modelling of complex geological structures for an environmental risk assessment of abundant mining and industrial megasites. *Computers and Geosciences*, 35(1), 165–182.

Xu, Z.C., Ma, H.X., Fan, G.Z., Lu, F.L. and Ding, L.B. 2016. Deepwater depositional architecture, evolution and reservoir potential in the Rakhine Basin, offshore Myanmar. *78th EAGE Conference and Exhibition 2016* [extended abstract]

Yao, T., C. S. Calvert, G. Bishop, T. Jones, Y. Ma, and L. Foreman. 2004. Spectral component geologic model-ling: A new technology for integrating seismic information at the correct scale. *In:* O. Y. Leuangthong and C. V. Deutsch (eds), *Geostatistics Banff 2004: Quantitative geology and geostatistics 14*, Dordrecht, Netherlands, Springer, v. 1, p. 23–33.

Zhang, X., Pyrcz, M.J. and C.V. Deutsch. 2009. Stochastic surface modelling of deepwater depositional systems for improved reservoir models. *Journal of Petroleum Science & Engineering*, **68**, 118-134.

Zhang, Z., Geiger, S., **Rood, M.**, Jacquemyn, C., Jackson, M., Hampson, G., De Carvalho, F.M., Marques Machado Silva, C.C., Machado Silva, J.D., and M.C. Sousa. 2017a. A tracing algorithm for flow diagnostics on fully unstructured grids with multi-point flux approximation. *SPE Journal,* 22 (6), SPE-182635-PA.

Zhang, Z., Geiger, S., **Rood, M**., Jacquemyn, C., Jackson, M., Hampson, G., De Carvalho, F.M., Marques Machado Silva, C.C., Machado Silva, J.D., and M.C. Sousa. 2017b. Flow diagnostics on fully unstructured grids. *SPE Reservoir Simulation Conference 2017,* SPE-182635-MS.

Zhang, Z., Geiger, S., **Rood, M**., Jacquemyn, C., Jackson, M., Hampson, G., De Carvalho, F.M., Marques Machado Silva, C.C., Machado Silva, J.D., and M.C. Sousa. 2018. Fast flow computation methods on unstructured tetrahedral meshes for Rapid Reservoir Modelling. *ECMOR XVI - 16th European Conference on the Mathematics of Oil Recovery*, doi: 10.3997/2214-4609.201802241

Zhang, Z., Geiger, S., **Rood, M.**, Jacquemyn, C., Jackson, M., Hampson, G., De Carvalho, F.M., Marques Machado Silva, C.C., Machado Silva, J.D., and M.C. Sousa. 2019. Fast flow computation methods on unstructured tetrahedral meshes for Rapid Reservoir Modelling. *Computational Geosciences,* 1-21.

Appendix 1

This appendix contains descriptions of videos provided in the Supplemental Material. Each description includes the operators used to construct the model and timings for the accompanying video. All videos are created using the Rapid Reservoir Modelling prototype software. The top screen shows the sketching plane, the bottom left shows the 3D model of the surfaces, and the lower right shows the plan-view of the model. All videos are held online in the Figshare repository (figshare.com).

Video 1

https://doi.org/10.6084/m9.figshare.11902668.v1

This video demonstrates the flexibility in using the operators while constructing a blank screen model.

In this example, a simple model of strata is constructed with a channel form and internal channel deposits added later. All surfaces are extrapolated into 3D in this model; subsequent videos demonstrate the techniques for adding true three-dimensionality to the models. Each of the seven operators is demonstrated and the video is shown in real time; time of model construction is shown in brackets.

The model is constructed as follows:

1. No operator required
    a. Simple strata are sketched that do not intersect (0:01)
2. Using operator Remove Above Intersection
    a. A green channel form is inserted (0:32)
3. Using operator Remove Above
    a. A purple unconformity surface is inserted (0:45)
4. Using operator Remove Below
    a. A blue stratigraphic surface is inserted removing the lowermost surface (1:07)
5. Using operator Preserve Between

a. The channel form is selected (1:23)

b. Three lateral accretion surfaces are inserted into the channel (1:29)

c. A yellow basal mass-transport deposit top surface is inserted at the base of the channel fill (1:49)

6. Using operators Preserve Above (applied to the central stratigraphic surface) and Preserve Below (applied to the unconformity surface) (2:06)

    a. A turquoise stratigraphic surface is inserted on either side of the channel (2:16)

Video 2

https://doi.org/10.6084/m9.figshare.11902683.v1

This video demonstrates construction of the model described in Case Study 3A, Section 3.5, a seismic-scale prototype model of deepwater channel deposits using multiple parallel cross-sections based on the interpretation and data of Xu et al. (2016) (Figure 3.3A-C, 3.4A). The seismic cross-sections are loaded into the model and then used to guide sketching for model prototyping. Three parallel cross-sections are shown concurrently on the right side of the video, going from proximal (top) to medial to distal (bottom). The colored dots next to the 3D view (lower left) indicate the position of each cross-section: blue – proximal, green – medial, and red – distal. Each individual channel complex base surface is sketched in each cross-section before making the surface permanent, thus allowing the three-dimensionality of the surface to be created. This video shows the surfaces being added back to the model after construction. The operators required and individual steps of model construction are as follows:

1. No operator required

    a. Sketch lowermost channel complex base surface on proximal cross-section, then medial cross-section and distal cross-section (black)

2. Using operator Remove Above Intersection (RAI)

    a. Sketch next channel complex base surface on proximal to distal cross-sections (blue)

    b. Repeat with additional two channel complex base surfaces (green, yellow)

3. Using operator Preserve Above (PA)

    a. Select the top-most (youngest) channel complex base surface to PA

b. Sketch the top of the channel fill to close the model volume (orange)

c. Save Xu et al. (2016) interpretation Model

Video 3

https://doi.org/10.6084/m9.figshare.11902761.v1

This video demonstrates the addition of detail to the model shown in Supplemental Material Video 2 (Figure 3.5). The operators apply at all stratigraphic levels, thus they can be used to add detail to existing models. We select the lowermost channel complex to add architectural detail, adding channel element surfaces and a slump top surface. This could be repeated for additional channel complexes if desired. Only the distal cross-section is shown to simplify the visualization. The video is created in real time; times of model construction in the video are shown in brackets. The operators required and individual steps of model construction are as follows:

1. Using operator Preserve Between (PBW)
    a. Select the top channel complex (0:04)
2. Using operator Remove Above (RA)
    a. Sketch channel element surfaces (0:09)
3. Using operator Remove Below (RB)
    a. Sketch top of slump deposit (0:58)
    b. Save Model (1:17)

Video 4

https://doi.org/10.6084/m9.figshare.11902779.v1

This video demonstrates construction of the models described in Case Study 3B, Section 3.6, comparative outcrop-derived prototype models of lacustrine carbonates based on Bohacs et al. (2013). Interpretation A comprises continuous interbedded microbialite bioherms and skeletal grainstones whereas Interpretation B contains coeval mounded microbialite bioherms and skeletal grainstones (Figure 3.6A). The models are constructed over a blank screen, based on the interpretations of Bohacs et al. (2013). First, a model of interbedded microbialite bioherms and

skeletal grainstones is created (Interpretation A). Then this model is modified to create mounded geometries of the microbialite bioherms surrounded by coeval skeletal grainstones (Interpretation B). The mounded geometries are created by using the plan-view sketching window (lower left) to sketch contours to constrain their 3D geometry. In the video, contour surfaces appear angular but that is a visualization artefact; in 3D the mounds appear with rounded edges that match the way the contours are sketched. The video is created in real time; times of model construction in the video are shown in brackets. The operators required and individual steps of model construction are as follows:

To create the prototype model of Interpretation A (Figure 3.6B):

5. No operator required, work in length (xz or yz) cross-section
    a. Sketch top surfaces of microbialite bioherm layers (0:07)
    b. Sketch lowermost base surface of skeletal grainstone layer (0:24)
6. No operator required, work in length (xz or yz) cross-section
    a. Sketch top surfaces of skeletal grainstone layers in length cross-section (0:33)
    b. Save Model of Interpretation A (1:00)

To create the prototype model of Interpretation B (Figure 3.6C):

1. Open model of Interpretation A and remove the skeletal grainstone top surfaces (1:03)
2. Using operators Preserve Above and Preserve Below (PA and PB):
    a. Select the lower microbialite bioherm top surface to preserve above (1:36)
    b. Select the upper microbialite bioherm top surface to preserve below (1:40)
    c. Switch to sketching in Height view (1:46) and position the sketching plane at the top of the modelling area (2:13)
    d. Sketch contours in plan-view to represent the top of the mounded microbialite bioherms (2:32)
    e. Position the sketching plane at the base of the modelling area (3:22)
    f. Sketch contours in plan-view to represent the base of the mounded microbialite bioherms (3:31)

3. Using operators Preserve Above and Preserve Below (PA and PB), repeat the same process for lower mounded section:
    a. Select the lower skeletal grainstone base surface to preserve above (4:54)
    b. Select the lower microbialite bioherm top surface to preserve below (4:58)
    c. Position the sketching plane at the top of the modelling area (5:00)
    d. Sketch contours in plan-view to represent the top of the mounded microbialite bioherms (5:05)
    e. Position the sketching plane at the base of the modelling area (5:57)
    f. Sketch contours in plan-view to represent the base of the mounded microbialite bioherms (6:02)
    g. Save Model of Interpretation B (7:13)

Video 5

https://doi.org/10.6084/m9.figshare.11902827.v1

This video demonstrates construction of the models described in Case Study 3C, Section 3.7, comparative well-based prototype models of fluvial point-bar sandstones based on Colombera et al. (2018). The models are constructed over a correlation panel of facies logs containing sand-rich (yellow) and mud-rich (green) intervals with plan-view geometry based on a seismic time-slice map (Figures 3.7A-B) (Colombera et al., 2018). The correlation panel is loaded into the sketching window (centre top) and shown at 10x vertical exaggeration. In this example, three dimensionality is created by applying a trajectory to surfaces in the plan-view window (lower right). First, a common geometric framework model is constructed, then two alternative interpretations of the continuity of mudstones are prototyped. The video is created in real time; times of model construction in the video are shown in brackets. The operators required and individual steps of model construction are as follows:

To create the common geometric framework (Figure 3.7C):

4. No operator required
    a. Sketch top reservoir surface (0:01)
    b. Sketch base reservoir surface (0:36)

5. Using operator Preserve Between (PBW)
    a. Select volume defined by top and base reservoir surface (1:08)
    b. Sketch point-bar accretion surfaces across model (1:17), using cross-sections and plan-view trajectories to define surfaces in 3D (1:24)
    c. Save Common Geometric Framework Model (2:55)

To create prototype model of continuous mud-prone intervals (Figure 3.7D):

1. Open Common Geometric Framework Model
2. Using operator Preserve Between (PBW)
    a. Select entire reservoir volume
    b. Sketch top-shale surfaces, to define a continuous shale barrier in each point-bar deposit volume (3:20), using cross-sections and plan-view trajectories to define surfaces in 3D (3:32)
    c. Save Model (5:05)

To create prototype model of discontinuous mud-prone intervals (Figure 3.7E):

1. Open Common Geometric Framework Model or Undo previous surfaces (5:29)
2. Using operator Preserve Between (PBW)
    a. Select individual point-bar deposit volumes (5:41)
    b. Sketch top-shale surfaces, to define a discontinuous barrier that extends over only the upper 25-30% of each point-bar deposit volume (5:44), using cross-sections and plan-view trajectories to define surfaces in 3D (5:52)
    c. Save Model (7:45)

Video 6

This video series demonstrates construction of the model described in Case Study 4A, Section 4.4, a conjugate fault model based on a NURBS-created conjugate fault model (C. Jacquemyn, pers. comm.). The model is created from one cross-section loaded into the sketching window (centre top). In this model, three dimensionality is created by applying a surface trajectory to faults in the plan-

view window (lower right). This model is dimensionless. The video is created in real time in steps of model construction. The operators required and individual steps of model construction are as follows:

Fault Set 1 (Video 6A) - https://doi.org/10.6084/m9.figshare.11902836.v1

1. No operator required
    a. Sketch fault then sketch trajectory in plan-view window, apply trajectory
    b. Sketch second fault, re-use trajectory in plan-view window

Fault Set 2 (Video 6B) - https://doi.org/10.6084/m9.figshare.11902839.v1

2. Using operator Preserve Between (PBW)
    a. Select existing fault block that contains new fault
    b. Sketch fault, sketch trajectory in plan-view window
    c. Repeat for each fault block, selecting fault block then sketching fault, re-use trajectory

Stratigraphy (Video 6C) - https://doi.org/10.6084/m9.figshare.11902851.v1

3. Using operator Preserve Between (PBW)
    a. Select each fault block to PBW
    b. Sketch all strata within the fault block
    c. Select next fault block and repeat sketching of strata until strata are sketched in each block

Final Model (Video 6D) - https://doi.org/10.6084/m9.figshare.11902881.v1

4. Save model – colours of units changed to match original model

Video 7

https://doi.org/10.6084/m9.figshare.11902920.v1

This video demonstrates construction of the model described in Case Study 4B, Section 4.5, a 3D representation of a physical analogue model of a salt-influenced passive margin (S. Evans, pers. comm.). Three parallel analogue model time-slice cross-sections are loaded into RRM and then used to guide sketching for model prototyping. Each cross-section is the equivalent of ~39 km long, and cross-sections are spaced the equivalent of ~5 km apart. The coloured dots next to the 3D view (lower left) indicate the position of each cross-section within the model. Each individual surface is sketched in each cross-section before making the surface permanent, thus allowing the three-dimensionality of the surface to be created. This video is created in real time, times of model construction in the video are shown in brackets. The operators required and individual steps of model construction are as follows:

1. No operator required (Figure 4.8A)
    a. Sketch base of salt ramp and top of model (0:56)
2. Using operators Preserve Above (PA) and Preserve Below (PB) (Figure 4.8B)
    a. Select the salt ramp base surface to PA, select the top of the model surface to PB
    b. Sketch the top salt (3:36)
3. Using operator Preserve Between (PBW) (Figure 4.8C)
    a. Select the salt ramp base, top salt, and top of the model surfaces to PBW
    b. Sketch six basin-dipping synthetic fault surfaces (5:17)
4. Using operator Preserve Between (PBW) (Figure 4.8D)
    a. Select the top salt, top of the model and most basinward fault (fault 1) surfaces to PBW
    b. Sketch base of post-kinematic strata surface (12:29)
5. Using operator Preserve Between (PBW) (Figure 4.8E)
    a. Select the top salt, fault 1, and base of post-kinematic strata surfaces to PBW
    b. Sketch two antithetic fault surfaces (14:31)
    c. Save model (18:24) (Figure 4.8F)